



UNIVERSITAT DE
BARCELONA

Biopharmaceutical study of therapeutic efficacy of nanostructured formulations made from products of natural origin

Paola Bustos Salgado

ADVERTIMENT. La consulta d'aquesta tesi queda condicionada a l'acceptació de les següents condicions d'ús: La difusió d'aquesta tesi per mitjà del servei TDX (www.tdx.cat) i a través del Dipòsit Digital de la UB (diposit.ub.edu) ha estat autoritzada pels titulars dels drets de propietat intel·lectual únicament per a usos privats emmarcats en activitats d'investigació i docència. No s'autoritza la seva reproducció amb finalitats de lucre ni la seva difusió i posada a disposició des d'un lloc aliè al servei TDX ni al Dipòsit Digital de la UB. No s'autoritza la presentació del seu contingut en una finestra o marc aliè a TDX o al Dipòsit Digital de la UB (framing). Aquesta reserva de drets afecta tant al resum de presentació de la tesi com als seus continguts. En la utilització o cita de parts de la tesi és obligat indicar el nom de la persona autora.

ADVERTENCIA. La consulta de esta tesis queda condicionada a la aceptación de las siguientes condiciones de uso: La difusión de esta tesis por medio del servicio TDR (www.tdx.cat) y a través del Repositorio Digital de la UB (diposit.ub.edu) ha sido autorizada por los titulares de los derechos de propiedad intelectual únicamente para usos privados enmarcados en actividades de investigación y docencia. No se autoriza su reproducción con finalidades de lucro ni su difusión y puesta a disposición desde un sitio ajeno al servicio TDR o al Repositorio Digital de la UB. No se autoriza la presentación de su contenido en una ventana o marco ajeno a TDR o al Repositorio Digital de la UB (framing). Esta reserva de derechos afecta tanto al resumen de presentación de la tesis como a sus contenidos. En la utilización o cita de partes de la tesis es obligado indicar el nombre de la persona autora.

WARNING. On having consulted this thesis you're accepting the following use conditions: Spreading this thesis by the TDX (www.tdx.cat) service and by the UB Digital Repository (diposit.ub.edu) has been authorized by the titular of the intellectual property rights only for private uses placed in investigation and teaching activities. Reproduction with lucrative aims is not authorized nor its spreading and availability from a site foreign to the TDX service or to the UB Digital Repository. Introducing its content in a window or frame foreign to the TDX service or to the UB Digital Repository is not authorized (framing). Those rights affect to the presentation summary of the thesis as well as to its contents. In the using or citation of parts of the thesis it's obliged to indicate the name of the author.



UNIVERSITAT DE
BARCELONA

**“BIOPHARMACEUTICAL STUDY OF
THERAPEUTIC EFFICACY OF
NANOSTRUCTURED FORMULATIONS MADE
FROM PRODUCTS OF NATURAL ORIGIN”**

(ESTUDIO BIOFARMACEUTICO DE EFICACIA TERAPÉUTICA DE FORMULACIONES
NANOESTRUCTURADAS A PARTIR DE PRODUCTOS DE ORIGEN NATURAL)

Paola Bustos Salgado



UNIVERSITAT DE
BARCELONA

UNIVERSIDAD DE BARCELONA

FACULTAD DE FARMACIA Y CIENCIAS DE LA ALIMENTACIÓN

PROGRAMA DE DOCTORADO DE INVESTIGACIÓN, DESARROLLO Y
CONTROL DE MEDICAMENTOS

Paola Bustos Salgado

2021

UNIVERSIDAD DE BARCELONA

FACULTAD DE FARMACIA Y CIENCIAS DE LA ALIMENTACIÓN

PROGRAMA DE DOCTORADO DE INVESTIGACIÓN, DESARROLLO Y
CONTROL DE MEDICAMENTOS

**“BIOPHARMACEUTICAL STUDY OF THERAPEUTIC EFFICACY OF
NANOSTRUCTURED FORMULATIONS MADE FROM PRODUCTS OF
NATURAL ORIGIN”**

(ESTUDIO BIOFARMACEUTICO DE EFICACIA TERAPÉUTICA DE FORMULACIONES
NANOESTRUCTURADAS A PARTIR DE PRODUCTOS DE ORIGEN NATURAL)

Memoria presentada por Paola Bustos Salgado, para optar al título de doctor por la
Universidad de Barcelona



Ana Cristina Calpena Campmany

Directores de Tesis:



Ma. Luisa Garduño Ramírez

Doctoranda: Paola Bustos Salgado



Tutora: Ana Cristina Calpena Campmany

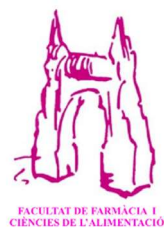
PAOLA BUSTOS SALGADO

2021

El presente trabajo de investigación se desarrolló en el Departamento de Farmacia y Tecnología Farmacéutica, y Fisicoquímica en la Unidad de Biofarmacia y Farmacocinética de la Facultad de Farmacia y Ciencias de la Alimentación de la Universidad de Barcelona así como también en el Laboratorio 325 de Química de Productos Naturales Básica y Aplicada del Centro de Investigaciones Químicas del Instituto de Investigación en Ciencias Básicas y Aplicadas de la Universidad Autónoma del Estado de Morelos, bajo la dirección de: Dra. Ana C. Calpena Campmany y Dra. María Luisa del Carmen Garduño Ramírez.

Este trabajo de investigación se llevó a cabo con base al Acuerdo de colaboración específica entre la Universidad de Barcelona y el Centro de Investigaciones Químicas de la Universidad Autónoma de Estado de Morelos firmado en el año 2011.

Agradecemos a CONACyT, México por su apoyo con la beca Doctoral otorgada No. de Becario: 709906.



CONTENTS

General Index	i
Abbreviations	v
Abstract	vii
Resumen (español)	ix

	Page
1. INTRODUCTION	1
1.1. Skin and Inflammation	3
1.2. Natural Products as Anti-inflammatory Agents	5
1.3. Molecular Design	9
1.4. Computational Studies (<i>In silico</i>)	12
1.5. Analytical Validation	16
1.5.1. Specificity	17
1.5.2. Linearity	17
1.5.3. Accuracy	17
1.5.4. Precision	18
1.5.5. Rank	19
1.5.6. Detection limits	19
1.5.7. Quantification limits	20
1.6. Dermal Administration	20
1.7. Nanostructured systems	22
1.7.1 Nanoemulsions	25
1.8. <i>In vitro</i> , <i>ex vivo</i> e <i>in vivo</i> formulation evaluation	31
1.8.1. <i>In vitro</i> Studies of Release Kinetics	31
1.8.2. <i>Ex vivo</i> Skin Permeation Studies	33
1.8.3. <i>In vivo</i> Studies to Evaluate Formulations Activities	34
1.8.4. Histological Studies	35
1.8.5. <i>In vitro</i> Studies of Cytokine Expression	35
2. OBJECTIVES	41
2.1. General Objective	43
2.2. Particulars Objectives	43
3. MATERIALS AND METHODS	45
3.1. General Considerations	47
3.2. Extraction and Isolation of Plant Material	47
3.3. Semi-synthesis from Natural Flavanone 1	47
3.4 <i>In silico</i> Analysis	49
3.5 Chromatographic Operating Conditions	50
3.6 Analytical Method Validation	50
3.6.1. Standard Solutions for Calibration Curves	50
3.6.2. Linearity	50

3.6.3. Limit of Detection and Limit of Quantification	51
3.6.4. Repeatability, Accuracy, and Precision	51
3.6.5. Specificity	51
3.7. <i>Ex Vivo</i> Human Skin Permeation (Intrinsic permeation)	52
3.7.1. Flavanone Extraction	52
3.7.2. Recovery from Human Skin Tissues and Flavanone Retained	52
3.8. Flavanone Solutions (FS)	53
3.9. Flavanone Formulations (FF)	53
3.10. Determination of FF physical parameters	54
3.10.1. Morphological studies	54
3.10.2. Rheology studies	54
3.10.3. Extensibility studies	54
3.10.4. Stability Studies	55
3.11. <i>In vitro</i> FF Studies	55
3.12. <i>Ex vivo</i> FF Studies	56
3.13. <i>In vivo</i> Studies: Anti-inflammatory Efficacy	58
3.13.1. TPA-Induced rat ear inflammation model	54
3.13.2. Arachidonic acid (AA)- induced rat ear inflammation model	59
3.14. Histological Analysis	60
3.15. Gene Expression Analysis by RT- <i>q</i> PCR	60
4. RESULTS	63
4.1. Computational Studies	65
4.2. Analytical Validation	66
4.3. <i>Ex Vivo</i> Human Skin Permeation (Intrinsic permeation)	67
4.4. FF Characterization	69
4.5. <i>In vitro</i> FF Studies	76
4.6. <i>Ex vivo</i> FF Studies	77
4.7. <i>In vivo</i> FF and FS Studies	78
4.7.1. Model of mice ear inflammation induced with TPA	78
4.7.2. <i>In vivo</i> rat Model and Anti-inflammatory Response after FS and FF treatment induced by AA	79
4.8. Histological Analysis	82
4.9. Gene Expression analysis by RT- <i>q</i> PCR	84
5. DISCUSION	87
6. CONCLUSIONS	97
7. REFERENCES	103
8. ANNEXED	119

8.1. Article 1: “Quantification of One Prenylated Flavanone from Eysenhardtia platycarpa and Four Derivatives in <i>Ex Vivo</i> Human Skin Permeation Samples Applying a Validated HPLC Method”.	121
8.2. Article 2: “Biopharmaceutic study and <i>in vivo</i> efficacy of natural and derivatives flavanones formulations”.	133
8.3. Proceeding from the 1st International Electronic Conference on Pharmaceutics (IECP 2020): “ <i>Ex Vivo</i> and <i>In Vivo</i> Anti-inflammatory Evaluations of Modulated Flavanones Solutions”	151

ABBREVIATIONS

Å	Angstroms
AA	Arachidonic acid
ABC	Avidin Biotin Peroxidase
AcN	Acetonitrile
ADME	Absorption, distribution, metabolism, and excretion
<i>ANOVA</i>	Variance analysis
AU	Arbitrary units
COX	Cyclooxygenase
CSF	Stimulating factors for colony formation
CV	Coefficient of variation
DLS	Dynamic light scattering spectroscopy
DNA	Deoxyribonucleic acid
E	Relative error
ELISA	Immunoenzymatic assay
EMA	European Medicines Agency
EtOH	Ethanol
FDA	Food and Drug Administration
FF	Nanostructured formulation of flavanones
FS	Flavanones solution
¹ H-NMR	Proton magnetic nuclear resonance
H ₂ O	Water
HPLC	High performance liquid chromatography
ICH	International harmonization conference
IFN	Interferon
IL	Interleukin
<i>J</i>	Active ingredient flux
<i>K_p</i>	Permeation constant
LD	Detection limit
<i>Log P</i>	Octanol-water partition coefficient
LOX	Lipoxygenase
LQ	Limit of quantification
M	Molar
MAPKs	Mitogen-activated protein kinases
ME	Microemulsions
MeOH	Methanol
MV	Molecular volume
NE	Nanoemulsion
nFF	Nanostructured formulation without flavanone
nFS	Solution without flavanone
NFκB	Nuclear factor κB
NIST	National Institute of Standards and Technology
NLC	Lipid nanostructured carriers

NP	Nanoparticle
nrotb	Number of rotating links
NSAID	Non-steroidal anti-inflammatory drugs
O/W	Oil in water emulsion
<i>Pa</i>	Probability of being active
PASS	Prediction of activity spectra for substance
PCK	Protein kinase C
PCR	Polymerase chain reaction technique
PFA	Paraffin-formalin
<i>Pi</i>	Probability of being inactive
PLA ₂	Phospholipase A ₂
PMN	Polymorphonuclear
PSA	Molecular polar surface area
ref	Reference drug
RNA	Ribonucleic acid
RSD	Relative standard deviation
SAID	Steroidal antiinflammatory drugs
SAR	Structure-activity relationship
SC	Stratum corneum
SCH	Stratum corneum hydration
SD	Standard deviation
SNC	Central Nervous System
TEM	Transmission electron microscopy
TGF	Transforming Growth Factor
<i>Tl</i>	Latency time
TLC	Thin layer chromatography
TNF- α	Tumor necrosis factor alpha
TPA	12- <i>O</i> -tetradecanoylphorbol-13-acetate
TPSA	topological polar surface area
W/O	water-in-oil emulsion
WDI	World Drug Index

ABSTRACT

This research work was aimed at the characterization *in vitro*, *ex vivo* and *in vivo* of nanostructured systems, which independently contain a natural flavanone extracted from *Eysenhardtia platycarpa* and another four flavanones obtained through semi-synthesis of the first flavanone with the objective of providing evidence of their efficaciousness as anti-inflammatory cutaneous agents. Initially the flavanone was isolated from its natural source, and following on from this, the derivatives were obtained through chemical reactions of acetylation, methylation, cyclization and vinyl cyclization. Calculations were made *in silico* using computational programs like *Molinspiration* and *PASS Online*. These gave the theoretical physio-chemical properties of the flavanones and estimated the profile of their probable anti-inflammatory activity. An analytical methodology was used for the quantification of the flavanones with High Performance Liquid Chromatography (HPLC) in samples that crossed human skin in an *ex vivo* study. The objective was to demonstrate that an analytical method had been selected that did not cause any interference from the biological components due to the tissue with which we worked. The results showed that the method was lineal, exact and precise in the assayed concentrations interval (1.56 - 200 µg/mL). Afterwards, nano-structured formulations were prepared individually: they contained each flavanone at 0.5 % and the excipients were: Labrasol[®], Labrafac[®] lipophile, Propylene glycol and Plurol Oleic[®]. These formulations were morphologically and physio-chemically characterized. The results obtained revealed that the flavanones formulations (FF) were suitable for topical administration. An *in vitro* assay was carried out of the liberation of the flavanones from their individual formulation, using a dialysis membrane with a system of Franz type cells to guarantee that the formulation liberated the flavanones and allowed there to be a sufficient quantity of each component susceptible to being permeated in human skin. Immediately afterwards, *ex*

vivo studies were realized using human skin with the objective of evaluating the permeation profile of the flavanones contained in dissolution individually and in the formulations. The study demonstrated that the quantity of flavanone permeated and retained in the skin was different, depending on the flavanone assayed. This was probably due to the different molecular interactions of the functional groups with the tissue components. The flavanones derived were retained in the skin in greater quantity than natural flavanone. Finally, an *in vivo* assay was carried out on the anti-inflammatory efficaciousness in a model of rat's auricular edema induced by arachidonic acid. The results demonstrated that the flavanones were capable of reducing the edema (swelling) and the formulation excipients did not influence in the biological activity. The formulations turned out to be more effective than the reference pharmaceutical drug used in this study (sodium diclofenac gel). It was shown that the structural modification of the natural flavanone improved the therapeutic activity in which the derived methylated and cyclized vinyl stood out. These results are in concordance with the results obtained in the evaluation of the cytokines expression (IL-1 β , IL-6 y TNF- α) carried out, and moreover allowed the advantage of the use of nano-structured systems in making the flavanones more effective to be shown in comparison with flavanones assayed in dissolution.

RESUMEN

El presente trabajo de investigación versa sobre la caracterización *in vitro*, *ex vivo* e *in vivo* de sistemas nanoestructurados que contienen de forma independiente una flavanona natural extraída de *Eysenhardtia platycarpa* y cuatro flavanonas obtenidas mediante semi-síntesis de la primera, con el objetivo de evidenciar su eficacia como agentes antiinflamatorios cutáneos. Inicialmente se aisló la flavanona de su fuente natural seguida de la obtención de los derivados mediante las reacciones químicas acetilación, metilación, ciclación y vinilo ciclación. Se realizaron cálculos *in silico* utilizando programas computacionales como *Molinspiration* y *PASS Online* para obtener las propiedades fisicoquímicas teóricas de las flavanonas y estimar su probable perfil de actividad antiinflamatoria. Se validó una metodología analítica para la cuantificación de las flavanonas por cromatografía líquida de alta eficacia (HPLC) en muestras que atravesaron piel humana en un estudio *ex vivo*. Lo anterior con el objeto de demostrar una selectividad del método analítico planteado sin que hubiese ninguna interferencia provocada por los componentes biológicos propios del tejido con el que se trabajaría. Los resultados mostraron que el método es lineal, exacto y preciso en el intervalo de concentraciones ensayadas (1.56 - 200 µg/mL). Posteriormente, se prepararon individualmente las formulaciones nanoestructuradas que contenían al 0.5 % cada flavanona y como excipientes: Labrasol[®], Labrafac[®], Propilenglicol y Plurol Oleico[®]. Dichas formulaciones fueron caracterizadas morfológica y fisicoquímicamente. Los resultados obtenidos revelaron que las formulaciones de las flavanonas (FF) eran adecuadas para su administración tópica. Se llevó a cabo un ensayo *in vitro* de liberación de las flavanonas desde su formulación individual, utilizando una membrana de diálisis en sistemas de celdas tipo Franz para garantizar que la formulación libera las flavanonas y permite disponer de cantidad suficiente de cada compuesto susceptible de ser permeado en piel humana. Seguidamente, se realizaron estudios *ex vivo* utilizando piel humana con el propósito de evaluar el perfil de permeación de las flavanonas contenidas en disolución de forma individual y en las formulaciones. El estudio demostró que la cantidad de flavanona permeada y retenida en la piel fue diferente dependiendo de la flavanona ensayada; probablemente debida a las diferentes interacciones molecular de sus grupos funcionales con los componentes del tejido. Las flavanonas derivadas se retuvieron en mayor cantidad en piel que la flavanona natural. Finalmente, se desarrolló un ensayo *in vivo* de eficacia antiinflamatoria en un modelo de edema auricular de rata inducido por

ácido araquidónico. Los resultados demostraron que las flavanonas fueron capaces de reducir el edema y los excipientes de las formulaciones no influyeron en la actividad biológica. Las formulaciones resultaron ser más efectivas que el fármaco de referencia usado en este estudio (gel de diclofenaco sódico). Se comprobó que la modificación estructural de la flavanona natural mejoró la actividad terapéutica destacando los derivados metilados y vinilo ciclizados. Estos resultados se encuentran en concordancia con los obtenidos de la evaluación de expresión de las citosinas (IL-1 β , IL-6 y TNF- α) realizado y además, permitió evidenciar la ventaja del uso de sistemas nanoestructurados para disponer las flavanonas, en comparación con las flavanonas ensayadas en disolución.

INTRODUCTION

1. INTRODUCTION

1.1. Skin and inflammation

The skin is the largest organ in the body and provides a barrier between the body and the environment, therefore it is a major target of injuries caused by physical, chemical and microbial agents that are capable of changing its structure [1].

Human skin is mainly made up of three histological layers: the epidermis, the dermis, and the subcutaneous fat layer (Figure 1). The epidermis is essentially made up of dead cells. The stratum corneum (SC) is the outermost layer of the epidermis and is composed of dead cells deposited in a keratin matrix. This results in a strong structure with no gaps between cells. This protects the body by preventing the loss of water and the entry of infectious organisms [2]. However, the sweat glands and hair follicles penetrate the SC. The dermis underlying the epidermis is made up of connective tissue containing various glands, hair roots, and blood vessels. In the diagram, below, we can see are the subcutaneous layer made up of fatty tissue [3].

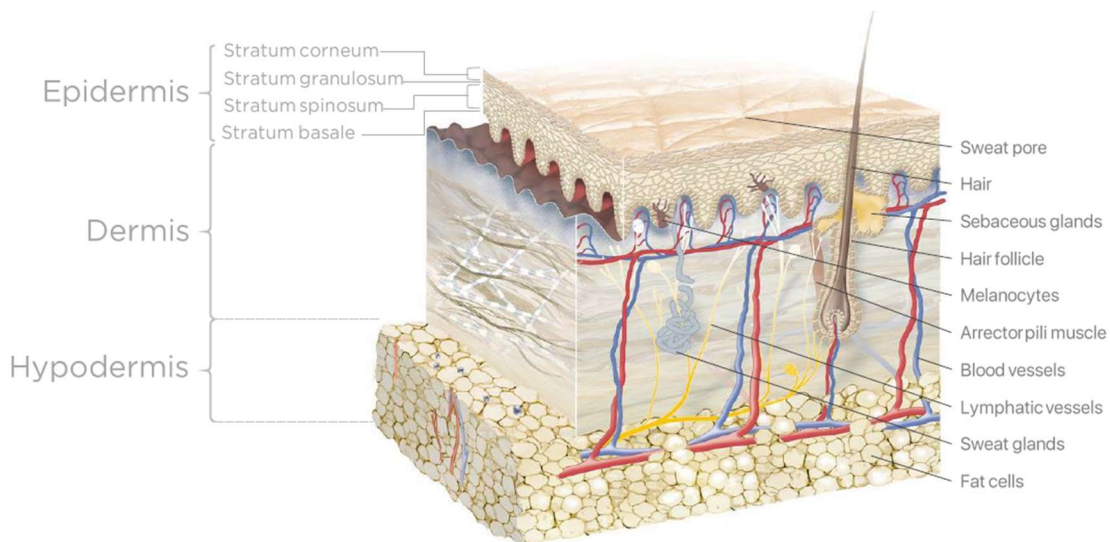


Figure 1. Structure of the skin [4].

The functional role of the skin is well known as a protective barrier. Now it is known that the skin is more than a container, it is a dynamic organ that has more functions such as endogenous homeostasis, metabolism, and sensory information. In addition, the skin actively participates in immune regulation processes and inflammatory responses [5].

Worldwide, skin conditions are the fourth leading cause of non-fatal morbidity. The main dermatological diseases that affect the general population are hyperpigmented diseases such as melasma, immune diseases such as urticaria and dermatitis, inflammatory diseases such as acne and psoriasis, infectious diseases caused by fungi, viruses and bacteria; as well as skin cancer [6]. Most skin disorders can be easily treated. But it is not so easy to successfully treat chronic inflammatory diseases, such as psoriasis and atopic dermatitis, partly due to a complex etiological origin and a not fully understood disease process [7].

Inflammation is known to be the human body's response to infection, tissue damage or invasion by microorganisms and its main objective is to eliminate the cause and promote the regeneration of any tissue that has been damaged [8]. Inflammation of the skin comprises a variety of organic actions, mainly including blood vessels and connective tissue; this is maintained through the interactions of local cells such as nerve terminals, keratinocytes, fibroblasts, mast cells, endothelial cells and macrophages; and in turn, the injured site also attracts granulocytes that migrate to the inflamed tissue [9]. The inflammatory process is characterized by the release of numerous mediators, including cytokines, prostaglandins, and vasoactive peptides, which culminates in changes in vascular permeability and cellular infiltration [10]. Under unfavorable conditions, such as the persistence of allergens or the failure of the resolution phase to reverse the process of tissue damage, acute inflammation can lead to chronic inflammatory diseases [11]. Specific therapies with non-steroidal drugs (NSAIDs) and steroids (SAIDs) to treat cases of inflammation show a variety of side effects with long-term use. These effects are such as gastric lesions and suppression of the immune system. SAIDs are the most powerful anti-inflammatory drugs. They act on inflammation by various mechanisms, among others the synthesis of proteins with an anti-inflammatory effect and the inhibition of the synthesis of numerous pro-inflammatory and growth factors. Dexamethasone, prednisone, prednisolone, methylprednisolone, cortisone, hydrocortisone, mometasone, among others are present in this group of drugs. However, its prolonged use can cause osteoporosis or block the regeneration of damaged tissue. The NSAIDs drugs are a group of agents whose primary effect is to inhibit the synthesis of prostaglandins through the inhibition of the COX enzyme. They are substances capable of suppressing the signs and symptoms of inflammation, and also some of them can exert antipyretic and analgesic

actions. We can mention examples of them: acetylsalicylic acid, paracetamol, indomethacin, diclofenac, ibuprofen, piroxicam, nimesulide, among others. In recent years, several investigations have revealed that the undesirable effects of NSAIDs, such as gastrointestinal and renal toxicity, were due in part to the inhibition of prostaglandin synthesis. In early 2000, more selective NSAIDs were introduced to the market, such as celecoxib, rofecoxib, etoricoxib, valdecoxib, meloxicam. However; selective cyclooxygenase (COX) inhibitors can lead to decreased inflammatory mediators, but they can also cause blood clotting disorders [9]. Therefore, it is important to consider the use of alternative treatments such as traditional medicine, and which gain particular interest mainly because they can lead to the development of new products derived from plants with the idea of obtaining new drugs with fewer unwanted side effects [12,13].

1.2. Natural Products as Anti-inflammatory Agents

Plants have been the basis of many medicinal systems throughout the world for thousands of years and continue to provide new remedies [14]. According to data from the World Health Organization, more than 80 % of the population of developing cities still depend on medicines from natural plants as their main source of medical care [8]. There are a large number of remedies in traditional medicine focused on relieving pain and inflammation, as well as being used for skin disorders. Since ancient times, many people who suffer from inflammation are treated with products derived from plants, which has been evident since the discovery of the first anti-inflammatory and analgesic product, the aspirin. Their discovery is consistent with the analgesic and antipyretic knowledge of willow bark since 400 BC by the Greeks and Romans. In 1899 acetylsalicylic acid (aspirin) was introduced as a potent drug for the treatment of rheumatic diseases [15].

Natural products offer therapeutic alternatives because of their ability to produce various bioactive metabolites that are difficult to synthesize. In fact, it is estimated that 40 % of approved drugs originate from or have been inspired by natural products [16]. A recent estimate indicates that by 2014 this percentage had increased to 50 % [17].

An important class of natural products corresponds to flavonoids; some plant species biosynthesize them. Flavonoids are polyphenolic compounds in which there are different

groups called: flavanones, flavones, flavonols, anthocyanins and isoflavonoids (Figure 2). In addition, to providing plants with phenotypic traits such as color, fragrance, flavor, resistance against radiation, pests and diseases. These advantages are compounded with others, such as it being antioxidant, antiviral, antitumor, antimicrobial, hormonal and anti-inflammatory activity [14].

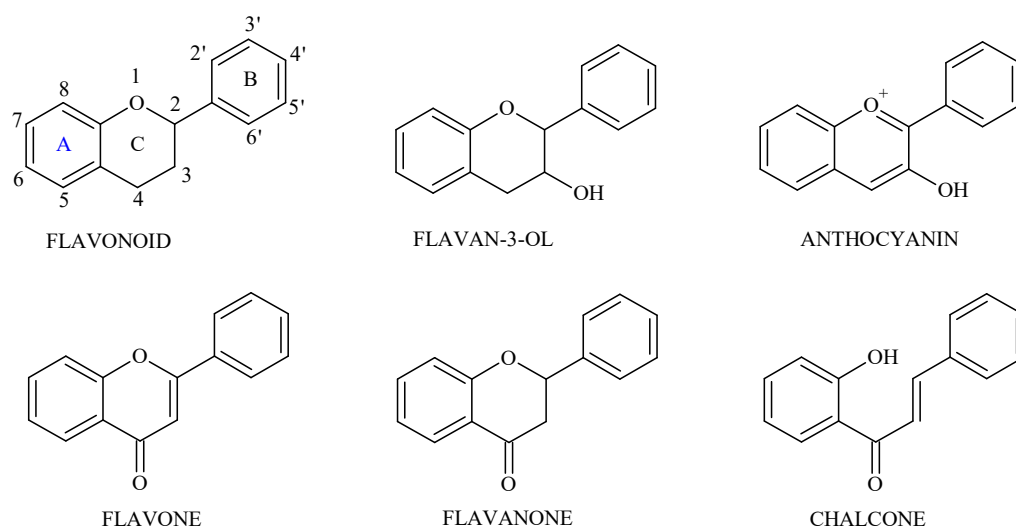


Figure 2. Structure of flavonoids and their derivatives.

Some natural flavonoids show anti-inflammatory activity *in vivo* after oral or dermal administration. Flavonoids can act in various inflammatory pathways and interact with mediators that involve the inflammatory response by directly modulating the enzymatic activities of phospholipase A₂, COX, and lipoxygenase (LOX). It was recently discovered that certain flavonoid derivatives modulate the expression level of several genes associated with inflammation. In addition, some derivatives of flavonoids inhibit the production of pro-inflammatory cytokines such as TNF- α [7]. This fact suggests that this type of compounds of natural origin may hold promise for a new therapy in the treatment of inflammation in the skin, and therefore it is of interest to find out more about plant species that produce flavonoids in their metabolism.

Eysenhardtia platycarpa it is a plant species of the angiosperm type. It is a small tree distributed in several regions of Mexico, where it is known by a variety of names among them; "Taray", "palo dulce", "cuate" and "palo azul" (Figure 3). Its bark is rough and

scaly with a dark coloration on the outside and reddish brown on the inside [18]. The genus *Eysenhardtia* (legume) comprises 14 species and some of these species have been used by local people as diuretics, antidiabetics and antiseptics [19]. It has shown to be an excellent source of secondary metabolites that includes in its composition flavonoids, flavones, isoflavones, flavonones, phenolic compounds, chalcones, dihydrochalcones, coumarins, sugars and fatty acids, among others.

The compound (2*S*)-5,7-dihydroxy-6-prenylflavanone **1** (Figure 4) corresponds to a flavanone belonging to a series of compounds obtained through the methanolic extraction of the leaves of *E. platycarpa*.



Figure 3. *Eysenhardtia platycarpa* tree [18].

Flavanones have been a potential source in the search for leading compounds and biologically active components and have been the focus of much research and development over the past 30 years [20]. Of the 58 drugs from natural products launched in the period of 1981-2011, 31 are structural analogues of those derived from the leading natural product [16].

Recently it was found that flavanone **1** (Figure 4) exhibits topical anti-inflammatory activity in *in vivo* models [21]. Anti-inflammatory efficacy was evaluated in CD-1 strain

male mouse ear using TPA (Tetradecanoyl-phorbol-acetate) as an inflammation-inducing agent, obtaining a 66.67 % inhibition of inflammation for a flavanone **1** solution in ethanol. This compound has been chemically characterized by interpreting its spectroscopic and spectrometric data. Considering that molecules of natural origin are currently an important source in the search for new drugs, molecular design has been used to optimize the biological properties of these types of compounds, taking them as the leading molecule.

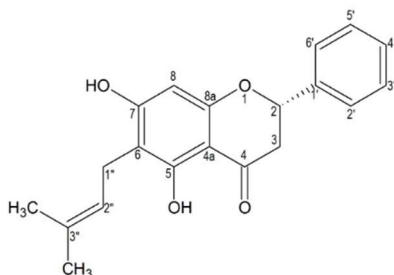


Figure 4. Structure of (2*S*)-5,7-dihydroxy-6-prenylflavanone **1**.

1.3. Molecular Design

Even though natural products have an innumerable capacity to present biological activities, there are problems associated with their nature. Typical limitations are the low solubility or chemical instability, which hinders the development of this type of molecules if they are to be used as drugs. In addition, their structures are complex and of high molecular weight that may not fit Lipinski's rules. Natural compounds can often be optimized through structural modifications to achieve a better candidate [16].

Structural modification begins with the identification of lead compounds that bind to a therapeutic target or that show biological activity in a specific assay, also known as a lead [22]. Subsequently, the design of analogs is carried out, thus allowing the systematic exploration of the so-called “lead compounds”. This design is known as molecular modification or pharmacomodulation. Molecular modification is proposed based on different objectives:

1. Preliminary study of the structure-activity relationships. Determination of the most suitable structural characteristics for a specific action.

2. Modification of the spectrum of action. To enhance the main action or mask certain side effects.
3. Modification of pharmacokinetics. Structural modifications that alter the rate of metabolism and / or excretion.
4. Modification of the distribution. Modulation of the distribution of the drug between the different tissues and organs to achieve a preferential location in those in which the action must take place. One of the ways to achieve this is the introduction of functional groups; but an alternative method consists of the use of transporter groups. A carrier group is a fragment that is covalently bound to the drug and allows drug distribution through selective transport mechanisms. Another technique consists of the binding of a drug to a protein that gives rise to the formation of intracellular vesicles that, by a process of lysosome hydrolysis, would release the drug inside the cell. The control of the distribution of a drug can be carried out by applying biophysical techniques.
5. Increased chemical stability. Look for chemical stability in the acidic medium so that its administration by oral route is possible.
6. Development of substitutes and therapeutic copies. It is used as a faster option to find any new patentable molecule by pharmaceutical companies.

The first advantage, inherent in the pharmacomodulation itself, is the greater probability of improving the pharmacological properties in the congeners of the lead compound, taking into account the close relationship between the resulting compounds [23].

There are three main types of techniques to perform the pharmacomodulation of a compound:

1. Disjunctive approaches. They are based on the reduction of the structure of the seeded head until it only retains the essential fragment for the action or pharmacophore, no more. It is applied to complex structure models, especially natural products.

2. Modulative approximations. They make small changes to the seed trying to preserve the essential structural aspects. However, these changes can affect the overall physicochemical properties of the molecule. For example, a change of a chlorine atom for a hydroxyl group (-OH) affects the polarity of the molecule. The resulting alcohol is much more hydrophilic than the halide, which will affect its solubility and its elimination via the kidneys. On the other hand, the ability to form hydrogen bonds with related groups at the site of action appears, which can drastically influence their binding mechanisms with the receptor or with plasma proteins. Other modulative approaches could be the opening, formation, rearrangement, or variation of the size of rings; homology (homologues are those molecules that differ from each other by a methylene group); vinylogy; isomerization; alkylation or dealkylation; double bond saturation and bioisostere. These variations can change the polarity of the molecule and influence its lipophilicity, until they substantially alter the activity of the seeded head.
3. Conjunctive approximations. These consist of the union by means of covalent bonds the structural elements of several compounds with the idea of obtaining a new one that presents pharmacological properties common with those of the prototypes. They can come from the combination of two identical molecules (molecular duplication) or from two different molecules (hybrid or molecular combination) [24].

Taking into account the modulative technique of pharmacomodulation; the modulated ester (acetylated) was synthesized (2*S*)-5,7-diacetyl-6-prenylflavanone **1a**; alkylated ((2*S*)-5-hydroxy-7-methoxy-6-prenylflavanone) **1b**; cyclized (pyranized) (8*S*)-5-hydroxy-2,2-dimethyl-3,4-dihydropyran- [4a,10a:6.7] flavanone **1c** and cyclized vinylogy (8*S*)-5-hydroxy-2,2-dimethyl-3,4-dehydropyran- [4a,10a:6.7] flavanone **1d** (Figure 5) [25]. Prenylated flavanones showed activity against *Artemia salina* and therefore these compounds were evaluated to establish their cytotoxic potential [25]. In this bioassay, it was found that flavanone **1** did not show significant cytotoxic activity, since a concentration of 100 ppm only caused 11.5 % mortality of *Artemia salina* nauplii. At the minimum concentration tested (10 ppm), null toxicity was obtained. However, when evaluating **1a-1d** changes in biological activity were obtained due to the structural modifications made. It is observed that **1a** and **1c** have a mortality percentage of 36.7 and

50 % at a concentration of 10 ppm, respectively. For cases **1a** and **1c**, it is possible to identify that the mortality percentages are at their effectiveness threshold, since even when increasing the concentration, the effect is not modified. For the cases of **1b** and **1d**, it is possible to consider perhaps that a significant structural change limited the effect shown by flavanone **1**, which corroborates that in the cytotoxic activity observed for flavanone **1**, the presence of the hydroxyl group in position 7. As well as the free disposition of the prenyl group in position 6, are required for the observed cytotoxic action and this recognize that the double bond involvement of both the prenyl group and the **1d** modulated double bond have no correlation since the final cytotoxicity response is different. For the transformation from **1** to **1a**, the increase in lipophilia may be the explanation for the increase in cytotoxic potential against *Artemia salina*. This permits a greater bioavailability in the case of the modification of **1** to **1c** as the molecule is modified, liberating it of a pair of π electrons. Maybe this gives it lipophilia and allows the compound greater movement through the biological membranes as well as making some pharmacological receptor selective.

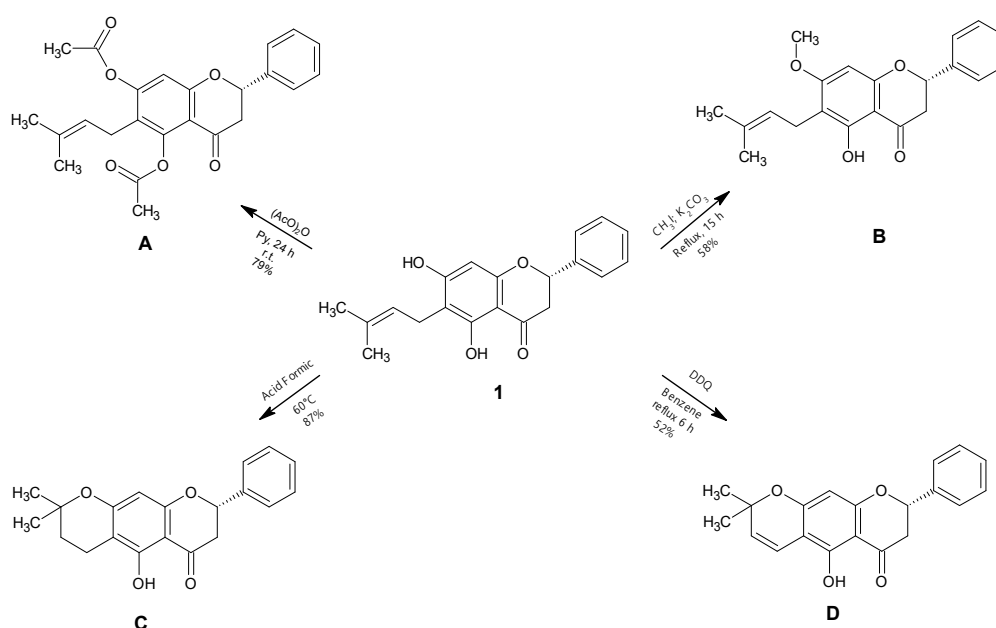


Figure 5. Pharmacomodulation of (2S)-5,7-dihydroxy-6-prenylflavanone **1**.

In the results obtained when evaluating compounds **1**, **1a-1d** with the MiaPaCa-2 cell line (Pancreatic cancer cells), compounds **1b** and **1d** were observed to decrease cell viability

in a concentration range of 10-50 μM and 25-50 μM , respectively. Once again, methylation has been the best strategy used to enhance the cytotoxic effect of flavanone **1**, as well as the rigidity of the molecule as occurs in compound **1d**. Although most processes in pharmaceutical research fall predominantly into the category of experimental work in the laboratory, computational work has been increasing in recent years [26].

Through the presented tests, it is possible to recognize a pharmacological interaction of flavanones without being highly specific on their possible biological properties. This is why, *in silico* studies represent an important tool to identify, through information libraries, the possible therapeutic targets that could be addressed with this new group of pharmacomodulated compounds.

1.4. Computational Studies (*In silico*)

In silico studies are based on the construction of recreation models of complex structures using computers. It has been given this name referring to the internal structure of computers as it is mostly made of silica materials (90 %) [27]. The investigation of new pharmacologically active compounds involves multiple criteria, since in addition to having a specific biological activity, the compounds must present as few side effects and toxic properties as possible. Experimental evidence of tens of millions of organic compounds for thousands of biological activities is obviously unattainable. This leads us to resort to computational methods for the search and optimization of new pharmacologically active compounds [28]. Computational approaches are designed to search for compounds in databases and select a limited number of candidate molecules to be evaluated as new entities that possess a desired biological activity [29,30].

Current computational studies for drug discovery are divided into design based on the structure of the therapeutic target and design based on the ligand. Despite advances in computational methods based on the structure of the therapeutic target, their use is limited due to several factors such as the need for 3D information on the structure of the macromolecule of the therapeutic target, which is far from being available to all proteins of interest. Also, the fact that there are changes in the structure of proteins during their function and after the formation of the protein-ligand complex. In addition to the

difficulty of determining the biologically active conformation for the ligands, the design of virtual compound libraries (*in silico*) offers the option of reducing the number of compounds that must be evaluated [28]. The goal is to select compounds from an existing library of compounds or to design compounds with three dimensions for the therapeutic target to be bound. When the lead molecules have been identified, they must be optimized in terms of potency, selectivity, pharmacokinetics [absorption, distribution, metabolism and excretion (ADME)] and toxicology, and then they can become candidates for drug development. *In silico* approaches to predict ADME pharmacokinetic parameters were pioneered by Lipinski et al. When studying the physicochemical properties of more than 200 drugs from the WDI (World Drug Index), it is assumed that, as they are made up of data derived from clinical trials in humans, they have properties like those of drugs. The so-called "rule of five" was derived to predict oral bioavailability (intestinal adsorption) in a compound that can be regarded as the main target of drug development. *In silico* approaches contribute significantly to early pharmaceutical research and are important in the discovery of potential compounds. This type of contribution will increase soon. The so-called "rule of five" was derived to predict oral bioavailability (intestinal adsorption) in a compound that can be regarded as the main target of drug development. *In silico* approaches contribute significantly to early pharmaceutical research and are important in the discovery of potential compounds [26].

The computer program called *PASS Online* (Prediction of Activity Spectra for Substances), makes possible the prediction of about 3300 types of biological activities of substances based on their structural formula including pharmacological effects, molecular mechanisms of action, specific toxicity, and biotransformation. The average prediction accuracy is around 94 %. The main purpose of the *PASS Online* program is to predict the spectrum of biological activity in new substances [31]. This program uses the description of the compound obtaining in response the probability of being active "*Pa*" or inactive "*Pi*" and it varies from one to zero. The possibility of having an experimental activity increases as the value of *Pa* increases and that of *Pi* decreases. The probability *Pa* mainly reflects the similarity of the structure of the test compound's structure of the most typical active compounds for a given biological activity.

Since 2000, the *PASS Online* program has been operating as an open access resource for predicting spectra of biological activity. The user of this program can make the prediction by selecting the structural formula of an organic compound in a file with Molfile format or directly indicating the structure of the formula using the Marvin program. *PASS Online* provides predictions for over 4,000 types of biological activity with an average accuracy of 95 %.

On the other hand, the *Molinspiration* Company focuses on the development and application of chemical-computer techniques offering a wide range of tools for the calculation of molecular properties necessary in the design of drugs. The software developed by this company offers free online service for the calculation of important molecular properties such as LogP, polar surface area (PSA), number of hydrogen bond donors and acceptors and others. In addition, it supports the prediction of bioactivity for the most important drug targets such as GPCR ligands, kinase inhibitors, ion channel modulators and nuclear receptors [32].

The molecular polar surface area (PSA) is a parameter that can be used to predict drug transport properties. It is defined as the sum of the surfaces of the polar atoms (generally oxygen, nitrogen and hydrogen atoms attached) in a molecule. PSA has been shown to correlate very well with human intestinal absorption, permeability of Caco-2 monolayers, and penetration of the blood-brain barrier. However, the calculation of PSA in the classical way is time consuming, due to the need of generating a reasonable 3D molecular geometry and determining the surface itself. In addition, the calculations require specialized software to generate the 3D molecular structures and determine the surface. However, *Molinspiration* allows the estimation of the topological polar surface area (TPSA) based on the sum of the tabulated surface contributions of the polar fragments (atoms with respect to their surroundings). These fragment contributions were determined by least squares fit to the single conformer 3D PSA for 34,810 drugs from the World Drug Index. The topological polar surface area provides results of nearly the same quality as classic 3D PSA. However, calculations are two of the order of two to three times faster [33].

The octanol-water partition coefficient ($\text{Log } P$) is used in QSAR studies and in drug design as a measure of molecular lipophilicity. Lipophilicity affects drug absorption, bioavailability, hydrophobic drug-receptor interactions, metabolism of molecules, as well as their toxicity. The method for predicting $\text{Log } P$ developed in *Molinspiration* (*miLogP* 2.2 - November 2005) is based on group contributions. These have been obtained by fitting calculated LogP values with experimental $\text{Log } P$ values for more than twelve thousand drug-like molecules. In this way, lipophilicity values have been obtained for 35 small simple "basic" fragments, as well as values for 185 larger fragments, characterizing the contribution of intramolecular hydrogen bonding to $\text{Log } P$ and charge interactions. For 50.5 % of the molecules, $\text{Log } P$ is predicted with an error <0.25 , for 80.2 % with an error <0.5 and for 96.5 % with an error <1.0 . Only for 3.5 % of the structures LogP is predicted with an error > 1.0 . These data make *Molinspiration* one of the best available methods for predicting $\text{Log } P$.

Molecular volume (MV) determines the transport characteristics of molecules, such as intestinal absorption and penetration of the blood-brain barrier. Therefore, volume is often used in QSAR studies to model molecular properties and biological activity. The method for calculating the volume of molecules developed in *Molinspiration* is based on group contributions. These have been obtained by adjusting the sum of the contributions of the fragments to the "real" 3D volume for a set of approximately twelve thousand mostly drug-like molecules. The 3D molecular geometries were optimized using the AM1 semi-empirical method. The calculated volume is expressed in cubic Angstroms (\AA^3).

Similarity to drugs can be defined as a complex balance of various molecular properties and structure characteristics that determine whether a particular molecule is similar to known drugs. These properties, mainly hydrophobicity, electronic distribution, hydrogen bonding characteristics, size and flexibility of the molecule and, of course, the presence of several pharmacophoric characteristics influence the behavior of the molecule in a living organism, including bioavailability, transport properties protein affinity, reactivity, toxicity, metabolism, stability and many others.

The so-called "rule of 5" is a set of simple molecular descriptors used by Lipinski in which it is established that the majority of "drug-like" molecules have $\text{Log } P \leq 5$, molecular weight ≤ 500 , number of hydrogen bond acceptors ≤ 10 and number of hydrogen bond donors ≤ 5 . Molecules that violate more than one of these rules can have problems with bioavailability. The rule is called the "Rule of 5" because the key values are 5, 500, 2 * 5, and 5.

The number of rotating links (nrotb) is a topological parameter of the molecular flexibility measure. It has been shown to be a very good descriptor of the oral bioavailability of drugs. Rotating bond is defined as any single non-ring bond attached to a non-terminal heavy atom (i.e., not hydrogen).

In the last 20 years, there has been a rapid increase in the number of databases and collections of information on natural products that favor studies of this nature [17].

When multidisciplinary work is developed based on the discovery of new drugs and in which these will be tested in experimental models, the use of analytical instruments will undoubtedly be essential in the quantification of some important parameters and for this reason it is essential that the equipment is validated to guarantee the reproducibility of the assays.

1.5. Analytical validation

Validation is the process by which an analytical method is proven acceptable for its intended purpose. For pharmaceutical products, the guidelines to be followed are those established by the International Conference on Harmonization (ICH), the Food and Drug Administration (FDA), which provide a framework to carry out such validations. In general, the method should include studies of specificity, linearity, accuracy, precision, range, detection limits, quantification limits, and robustness once it is challenged by an analyte [34].

1.5.1. Specificity

Specificity is the ability of the method to accurately measure the response of each of the analytes in the presence of all sample components. The signal of the analyte in the study samples that contain the analyte and all the components (excipients, degradation products, impurities, among others) is compared with the response of a solution that contains only the analyte. Once an acceptable resolution for the analyte and the main components of the sample has been obtained, parameters such as column type, mobile phase composition, flow rate and detection mode are established. An example of a specificity criterion is that the analyte peak has a chromatographic resolution of at least 1.5 of all other components of the sample [35].

1.5.2. Linearity

Linearity verifies that the sample is in a concentration range in which the analyte response is linearly proportional to the concentration. Standard solutions are generally prepared at five concentration levels, from 50 to 150 % analyte concentration. These levels are necessary to allow detection of the curvature of the plotted data. Standards must be prepared and analyzed a minimum of three times. The linearity data are accepted by analyzing the correlation coefficients and the intercept of the linear regression line given by the response versus the concentration. A correlation coefficient > 0.999 is considered acceptable [34].

1.5.3. Accuracy

The accuracy of the method is defined as the closeness of the measured value to the actual value. It is generally determined in four ways: in the first, a sample of known concentration is analyzed and compared with the mean value of the true value. Reference standards from the National Institute of Standards and Technology (NIST) are used. However, standards are not always available for the substance to be evaluated. The second way to assess accuracy is to compare the results obtained with the results of an alternative method in which its accuracy is known. Again, it may happen that there is no alternative method for the analyte we are studying.

The third and fourth approximations are based on the recovery of known amounts of analyte contained in a matrix. The third approach is the most used for recovery studies. It is developed by adding analyte to the blank matrices. Samples are prepared in triplicate at three concentration levels ranging from 50 % to 150 % of the usual working concentration. The fourth approach is the standard addition technique.

It shows the systematic error of the method because it is a constant or proportional to the amount of substance (relative error, E). Mathematically it is expressed (Equation 1):

$$E(\%) = \frac{X - X_r}{X_r} (100) \quad (1)$$

Where:

X_r is the theoretical concentration of each solution of the drugs tested.

X is the experimental mean concentration.

Accuracy should be calculated using a minimum of three concentrations (low, medium, and high). Accuracy or relative error values should not exceed 15 % in all determinations, except for concentrations close to the limit of quantification. In all cases, it may be associated with a relative error close to 20 %.

1.5.4. Precision

The precision of an analytical method is defined as the amount of data dispersion obtained in multiple analyzes of the sample. One of the precision studies is based on evaluating the precision of the instrument or repeatability of the injection. A minimum of 10 injections of the sample to be tested are run to test the performance of the chromatographic instrument. Another precision study is the intra-assay one obtained by analyzing aliquots of the analyte on the same day. The precision criterion for this type of test is < 10 % relative standard deviation (RSD). Precision is expressed in terms of repeatability (in one day) and reproducibility (in successive days) by means of the mean values of the determinations made (X_{mean}), the standard deviation (SD) and the coefficient of variation

(CV). The standard deviation is a measure of the data dispersion obtained and is calculated using the following equation 2:

$$SD = \left(\frac{X_{mean} - X_{real}}{n-1} \right)^{\frac{1}{2}} \quad (2)$$

Being X_{mean} the average value of the repetitions and X_{real} the real value.

The coefficient of variation (CV) is a statistical parameter that indicates the dispersion of a series of data with respect to a mean value and is calculated using the following equation. The precision of the analytical methods is checked by the following equation 3:

$$CV(\%) = \frac{SD}{X} (100) \quad (3)$$

Where:

SD = Standard deviation of the samples for each concentration.

X = Average experimental concentration.

1.5.5. Rank

The range of an analytical method is the range of concentrations over which it achieves acceptable accuracy, linearity, and precision. In practice, the range is determined using data from linearity and accuracy studies. Therefore, it is considered as an acceptable criterion of range when a precision value of relative standard deviation (RSD) of < 3 % [34].

1.5.6. Detection limits

The method's detection limits refer to the lowest analyte concentration that can produce a detectable response above the system noise level, typically three times the noise level. It is calculated using the following equation 4:

$$LD = 3.3 \frac{SD}{p} \quad (4)$$

Where:

SD is the standard deviation of the ordinate to the origin.

p the slope of the calibration line.

1.5.7. Quantification limits

The limits of quantification refer to the lowest level of analyte that can be measured with precision and accuracy. One of the acceptance criteria for the limit of quantification is defined by an RSD < 20 % obtained from the intra-assay precision study (Equation 5).

$$LQ = 10 \left(\frac{SD}{p} \right) \quad (5)$$

The validation of the analytical method must be carried out by preparing and evaluating at least six calibration lines on different days (interday validation), to detect the maximum variability of the method.

To analyze the results, a statistical study such as the so-called ANOVA (Analysis of Variance) global comparison method is used. A one-way analysis of variance must be generated for a quantitative dependent variable relative to a single independent variable. This analysis is used to test the hypothesis that several means are equal. There are no statistical differences when $p > 0.05$ for all tests applying Tukey's correction.

Once a validated analytical method is in place, it will be possible to quantify the number of compounds in pharmacological studies regardless of the route of administration to the body.

1.6. Dermal administration

The nature, structure, characteristics and behavior of the skin have led to its choice as a route of drug administration. Dermal treatments for skin conditions provide benefits including avoidance of first-pass metabolism, ease of application, less fluctuation in drug levels, improvements in efficacy with a decrease in total daily dose, drug discontinuation if necessary, the ability to be more specific with drug delivery, better adherence, and avoiding risks associated with oral or intravenous administration. Though, dermal administration is most used when the skin is intended to be the site of action. However, the use of this route of administration also has some drawbacks, such as, for example, drugs that require high doses cannot be used, drugs can undergo cutaneous metabolism, the drug and / or formulation may cause skin irritation or sensitization. The passage of drugs through the skin is a passive diffusion process that can occur in two main ways:

1. Transepidermal: by diffusion through the SC.
 - a. Intercellular pathway (between corneocytes)
 - b. Intracellular route (passing through corneocytes and extracellular spaces).
2. Transpendicular: it can be transfollicular (by hair follicles and sebaceous glands) or transudoriparous (by ducts and sweat glands).

The penetration of the substances turns out to be a slow process, followed by a rapid diffusion through the viable epidermis and the papillary dermis. The first stage of the penetration process is the dissolution of the drug and its release from the formulation, this being the limiting step of the process. Once the active principle is released, the drug is distributed in the stratum corneum, where it reaches equilibrium. Penetration from the formulation to the systemic circulation or local tissues involves multiple processes:

1. Dissolution of the drug and its release from the formulation.
2. Distribution of the drug in the stratum corneum.
3. Diffusion through the stratum corneum, mainly intercellularly.
4. Distribution of the drug between the stratum corneum and the living epidermis.
5. Diffusion, through the epidermis, to the dermis.
6. Move to the local capillary network, through the wall of the blood vessel and, eventually the drug, passes into the systemic circulation.

Topical agents used as anti-inflammatories could inhibit the expression of cytokines, growth factors, adhesion molecules, nuclear factor κ B (NF κ B), nitric oxide, prostanoids and other autacoids, in addition to acting by modulating the level of activation and capacity, and response of target cells such as monocytes, T cells and platelets. Taking into account that commercial NSAIDs generate some adverse effects, plant-related compounds and their extracts represent alternatives for the development of new drugs that can be used for the treatment of topical inflammatory diseases, especially those that are associated with acute and chronic disorders of the disease. the skin [36,37].

For years, research has been carried out on obtaining formulations of phytopharmaceuticals from whole extracts of some plant species or, from isolated natural products for application on the skin that allow a slow flow to be achieved for anti-inflammatory treatment. This considers the transdermal route as an alternative to the oral route. Thus, part of the research in galenic development is aimed at finding; novel forms of administration, such as nanostructured systems.

1.7. Nanostructured systems

Various strategies are used to optimize the bioavailability of natural products, including the development of semi-synthetic analogs, the production of prodrugs, and the technological approach to the production of formulations. The last strategy refers to the development of drug delivery systems, those of nanometric size, generally between 50 and 300 nm down to 1 μm . The low solubility in water, the low lipophilicity, and the inadequate size of many natural compounds; as well as its structural instability in biological media, rapid clearance and high metabolic rate, have all limited its clinical use. Thus, the use of nanostructured systems represents an excellent tool to increase the bioavailability and activity of natural products. There are different nanostructured systems made either based on polymer or lipid constituents that give rise to a classification of this type of system. Each nanosystem has its own advantages, disadvantages and characteristics[38–40].

1. Polymeric systems. Natural, semi-synthetic or synthetic polymer compounds. Natural polymers are obtained from bacteria, fungi, animals, or plants and are mainly represented by polysaccharides (pectins, cellulose, starch, acacia, among others) and proteins. Among the synthetic polymers are polyvinyl alcohol, polyglycolic acid, polylactic acid, among others. These types of systems include (Figure 6):

1.1. Nanoparticles: include nanospheres and nanocapsules. Their production is based on chemical polymerization reactions:

1.1.1. Nanospheres: these are systems in which the drug is uniformly dispersed

1.1.2. Nanocapsules: these are systems in which the drug is confined in a cavity surrounded by a polymeric membrane.

- 1.2. Polymeric micelles: they are nanostructures (20-200 nm) composed of amphiphilic polymers and copolymers of hydrophobic and hydrophilic units that associate in aqueous solution to form a micelle. Generally, the hydrophilic polymer is on the outside and the core is made up of the hydrophobic polymer. Their main advantages are high safety and stability to physiological environments. Their small particle size prolongs the residence time in the circulatory system bypassing the filtration of the liver and spleen.
- 1.3. Dendrimers: they are hyperbranched polymers that form globular structures. Their diameters are generally less than 10 nm. They are characterized by a central nucleus surrounded by branches of repeating units. The drugs are usually bound to the middle of the surface or in the interior cavities.

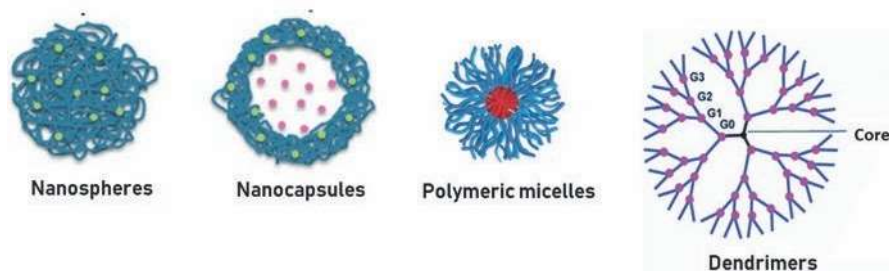


Figure 6. Polymeric systems[40].

2. Lipid systems (see Figure 7):

- a. Solid lipid nanoparticles: they are colloidal systems with a diameter of between 50 and 1000 nm made with a solid lipid matrix at physiological temperature stabilized in an aqueous solution by one or more surfactants. Their core is made up of glycerides, fatty acids, fatty alcohols, and waxes since they are solid at room temperature. Surfactants can be phospholipids, polysorbates, polaxamers, polyoxyethylene ethers, polyvinyl alcohols, etc. They can be obtained by different methods including homogenization by ultrasound, high pressure, by heat and by emulsification / evaporation of solvents. They can be administered topically, nasal, orally, ocularly, and parentally. They have a high biocompatibility, biodegradability and low

toxicity, as well as a high stability with respect to polymeric nanoparticles and vesicles.

- b. Nanostructured lipid particles: contains a liquid lipid at room temperature. They are made with the same methods as nanostructured lipid systems. Solid, liquid lipids, emulsifiers and water are used. The lipids are mixed to form the matrix, obtaining a high level of drug capture due to the structural differences of the lipids that compose it, since they form imperfections that result in a greater space to accommodate the drugs in their molecular structure. The most used lipids are triglycerides and oleic acid.
- c. Vesicles: they are characterized by the presence of amphiphilic molecules composed of natural or synthetic phospholipids or non-ionic surfactants, called liposomes. They have innumerable advantages because both hydrophobic and hydrophilic drugs can be easily encapsulated due to their aqueous and lipophilic compartment. It improves the bioavailability of drugs, delays the elimination of highly metabolizable drugs, prolongs the useful life of drug circulation, greater stability, and decreased toxicity. Their disadvantages are premature drug release, poor encapsulation efficiency of hydrophilic drugs. Their structure is spherical with a size ranging from 20 nm to several μm .
- d. Nanoscale emulsions: formulated with an oil phase, an aqueous phase, a surfactant, and a co-surfactant.
 - i. Microemulsions: homogeneous dispersions of two immiscible liquids stabilized by surfactants, thermodynamically stable and transparent. They have a droplet size greater than 100-500 nm and require very little energy for their formation since they form spontaneously when the aqueous, oily, and amphiphilic components are put in contact. They are characterized in three systems: oil in water, water in oil and a two-phase system called bicontinuous system. They are much more sensitive than nanoemulsions to environmental changes such as temperature

- ii. Nanoemulsions: are systems with a tendency to spontaneously separate into their constituent phases. They use lower amounts of surfactants than microemulsions. There is no agreement on the size range, which distinguishes a nanoemulsion. According to the literature, the droplet size can vary from 20 nm to 100, 200, 300 or 500 nm, and up to the present day it is still a controversial issue as to their classification as nanoemulsions.

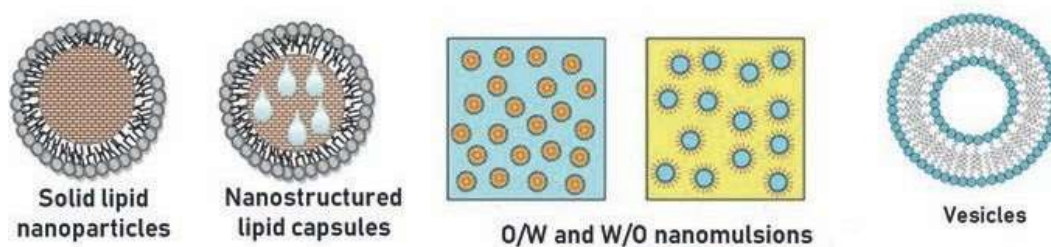


Figure 7. Lipid systems [40].

1.7.1. Nanoemulsions

In order to achieve a successful topical application and the release of active ingredients, nanoemulsions are ideal systems for drug delivery due to their ability to penetrate the deepest layers of the skin (Figure 8) [6].

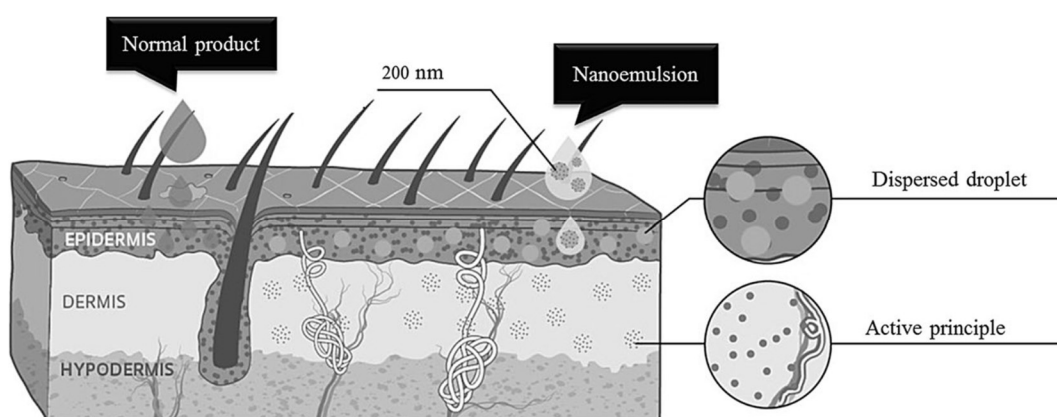


Figure 8. Permeation of a product with a normal formulation versus a product formulated in a nanoemulsion [6].

Nanoemulsions are nanoscale colloidal dispersions. They are thermodynamically unstable isotropic systems in which two immiscible liquids are mixed to form a single

phase by means of an emulsifying agent, for example, a surfactant. Most of them are optically transparent systems. They are kinetically stable systems due to the Brownian movement of the droplets that overcomes the force of gravity and prevents sedimentation and coalescence of the droplets. When the continuous phase is an aqueous solution and the dispersed phase is an oil, the emulsion is called an oil-in-water (O / W) emulsion. On the other hand, when the dispersed phase is an aqueous solution and the continuous phase consists of an oil, the emulsion is called a water-in-oil (W / O) emulsion. In both cases, an emulsifying agent or surfactant is needed to reduce the interfacial tension between the dispersed and continuous phases for there to be a stable system. The use of nonionic or polymeric surfactants causes steric repulsion between the droplets and contributes to the stability of the system.

The development of nanoemulsions requires an exact selection of components such as, surfactants, and oils, as well as a method for its preparation being carefully chosen. It takes a minimum of energy for its formation. Generally, nanoemulsions require a high content of surfactants, about 10-15 % by weight to stabilize the system. Surfactants are molecules whose structure consists of two parts with opposite affinities, one is hydrophilic and the other is hydrophobic. Both parts must be in equilibrium in the surfactant molecule, achieving the so-called the hydrophilic-lipophilic balance.

Surfactants can be divided into ionic (anionic or cationic), nonionic, amphoteric or zwitterionic [40]. Co-surfactants are added to obtain systems with a lower concentration of surfactant (Figure 9). Short to medium chain alcohols (C3-C8) are commonly used as co-surfactants, which reduce the interfacial tension and increase the fluidity of the interface. They also increase the mobility of the hydrocarbon chain and allow better penetration of the oil phase within this region. Alcohols can increase the miscibility of the aqueous and oil phases due to their fractionation between these phases. Therefore, ethanol, isopropyl alcohol, 1-butanol, and propylene glycol are selected as good co-surfactants [41].

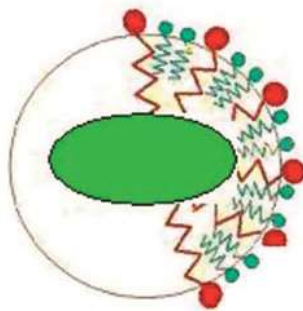


Figure 9. The co-surfactant (green) reduces the interfacial tension and therefore provides flexibility to the interfacial layers; while surfactant (red) forms the interfacial layer [42].

The production of nanoemulsions is thermodynamically unfavorable and the process is not spontaneous. Nanoemulsion manufacturing methods can be classified into two groups: low energy methods and high energy methods. High-energy ones require the input of a substantial amount of mechanical energy. They mainly include microfluidization, high pressure homogenization and ultrasound-assisted emulsifying methods. Several low-energy techniques have been developed to form nanoemulsions, including compositional phase inversion, temperature, spontaneous emulsification, and emulsion point inversion methods [43]

In general, nanoemulsions tend to be more stable to gravitational separation, flocculation, and coalescence and more susceptible to Ostwald ripening (Figure 10). Ostwald ripening is the process whereby the largest particles grow from the smallest droplets by continuous phase molecular diffusion due to their greater solubility [40].

The most important advantages of NEs as drug delivery systems include their ease of manufacture, increased drug encapsulation, increased solubility and consequently increased bioavailability of drugs that are poorly soluble in water, increased stability and permeation, reduced patient variability, controlled drug release, drug protection against enzymatic and chemical degradation [44].

Nanostructured systems show promise in effectiveness for the transcutaneous delivery of lipophilic compounds at the target site of inflamed muscles, thus avoiding the side effects

of anti-inflammatory drugs currently used in conventional pharmaceutical presentations such as ibuprofen, paracetamol, among others. Within the field of pharmaceutical technology, in particular galenic development, the American company Pharmos has developed a topical diclofenac nanoemulsion as a treatment to relieve the pain of osteoarthritis [45]. This type of system, being solvent-free and low-irritating, gives you advantages when looking for a formulation for drugs. On the other hand, in vivo studies in an animal leg edema model carried out by Shah et al. showed that both diclofenac and ketoprofen contained in nanostructures showed better anti-inflammatory efficacy compared to their classic commercial formulations. In addition, it was observed that the nanostructured formulation showed 4 to 6 times lower drug concentration in plasma, but 60 to 80 times more drug in muscle compared to oral administration. These results are very promising in terms of achieving an increase in the transcutaneous penetration of lipophilic drugs.

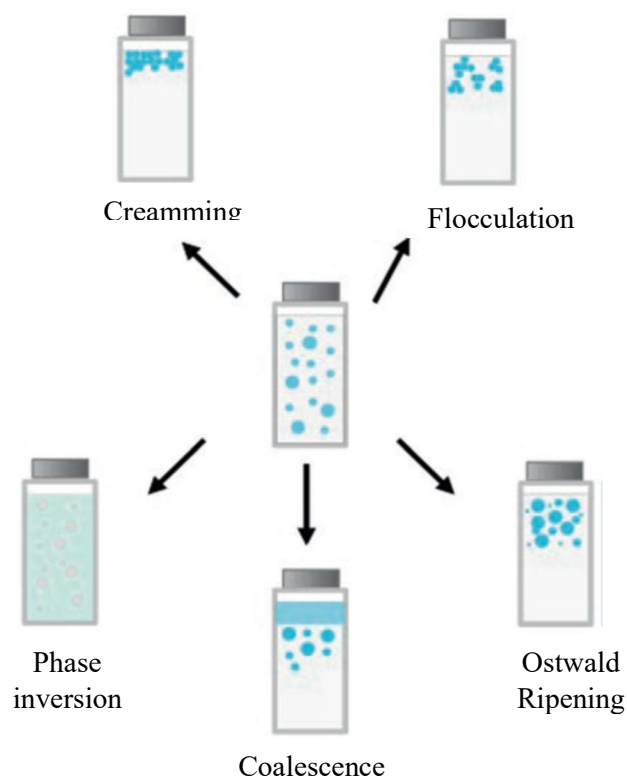


Figure 10. Instability phenomena in emulsions [40].

Anti-inflammatory drugs that are on the market with active ingredients such as piroxicam, diclofenac, and ketoprofen come in pharmaceutical presentations such as: gels, creams or lotions. However, new forms of administration are being sought in which lower doses are

used, the frequency of dosing is decreased, and higher concentrations are reached at the site of action. That is why the application of all knowledge can be applied to the design of new formulations from active ingredients of natural origin. However, it is known that one of the main problems with natural products is their low stability, bioavailability and solubility once conventionally formulated [46–48].

Simion and colleagues in 2016 manufactured lipid nanoemulsions containing dexamethasone to reduce vascular inflammation. The formulations were characterized by physicochemical tests. In its *in vitro* and *in vivo* study, the nanostructured formulation was found to have anti-inflammatory activity. Some other examples of nanostructured formulations are Norvir (Ritonavir), Restasis, Gengraf (Cyclosporin), Etomidat-Lipuro (Etomidate), Ropion (Flurbiprofen axtli), diprivan, Troypofol (popofol), limethason (dexamethasone) and liple (alprostadil pamitate) [49].

Hesperetin, a flavonoid with anti-inflammatory action, UV protective and antioxidant effect formulated in a microemulsion showed high permeation *in vitro* compared to the aqueous suspension and with hesperetin isopropyl myristate [50].

Previous studies showed that the permeation rates of nanostructured formulations were much higher compared to their conventional formulations [51–54]. Considering all, Domínguez-Villegas et al formulated some natural flavanones isolated from the leaves of *E. platycarpa*, including flavanone **1**. The development contemplated the formulation of a nanoemulsion (NE) and a nanoparticle (NP) that independently contained flavanone **1**. From the *in vivo* evaluation carried out in a mouse ear model of TPA-induced edema, it was observed that the percentage of inhibition of inflammation for NE**1** was 82.91 ± 0.95 and for NP**1** of 80.97 ± 1.48 [55].

The characterization of nanostructured formulations is based on the description of their properties such as droplet size, morphology, size distribution, viscosity, refractive index, physical and chemical stability, among others [56]. Various analytical methodologies are required to characterize nanoemulsions, such as their droplet size, rheology, and stability.

Droplet size distribution is an important physical characteristic of nanoemulsions and can influence their solubility, release profile, and bioavailability. In general, when nanoemulsions are produced, a range of different droplet sizes are distributed throughout the system, hence the droplet size is reported as the mean of the droplet size and its polydispersity index. Polydispersity indices less than 0.3 indicate a small size distribution, while values close to 1.0 are indicative of high heterogeneity in the system. Dynamic light scattering spectroscopy (DLS, from its acronym in English) or transmission electron microscopy (TEM). The latter allows the visualization of the size and distribution of the droplets in the nanoemulsion. This technique allows the observation of the morphological spherical shape of the droplets [40]. The samples are examined with a voltage booster, usually 20 kV, at different magnifications. Image analysis software is used to obtain the result of the shape and morphology of the surface. With the TEM technique, higher resolution images of the dispersed phase are obtained. The sample is negatively stained with a 2 % uralin acetate solution on a 200 μm mesh size Pioloform coated copper screen or with a carbon coated microscopic screen using a micropipette. The sample is examined under the transmission electron microscope at 80 kV [50].

The rheological behavior of nanoemulsions can affect the application of nanoemulsions, particularly for some routes of administration such as topical and dermal. The viscosity of nanoemulsions increases with increasing droplets and when their dispersed phase is more concentrated. As droplet concentration increases, both viscosity and viscoelastic behavior can increase [40]. The viscosity of the emulsions increases as the droplet size decreases [57]. Viscosity is a function of surfactants, oily and aqueous components, and their concentrations. Increasing the water content lowers the viscosity, while decreasing the amount of surfactant and co-surfactant increases the interfacial tension between water and oil and consequently results in greater viscosity, which is very important for the stability and efficiency of drug release. Viscosity changes are a method of evaluating the stability of liquid preparations including nanoemulsions [50].

Stability studies of nanostructured systems are carried out by storing them in the refrigerator and at room temperature for a defined time period. Viscosity, refractive index, and droplet size are determined during this storage period. Negligible changes in these

parameters indicate stability. The amount of the drug degraded and maintained in the nanostructure is also determined [50].

In the same way, the characterization of nanostructured systems is based on the calculations obtained by their permeation in artificial membranes and human skin, as well as in vivo studies on their anti-inflammatory efficacy [56]. *In vitro* skin permeation studies using Franz diffusion cells are carried out to obtain the drug release profile of the nanoemulsion formulation in the case of a transdermal application [50].

1.8. *In vitro*, *ex vivo* and *in vivo* Formulations Evaluations

1.8.1. *In vitro* Studies of Release Kinetics

During the initial phase of the development of new formulations, artificial membranes are used to evaluate the transfer capacity of the active principle of formulations. The results obtained are used to determine the kinetics that best explains the transfer process in each formulation. The functions of order zero, order one, Higuchi, Weibull and Korsmeyer-peppas are the most used [58]. The mathematical expressions of these functions are as follows (equation 6-10):

$$\text{Zero order function: } Q_t = K_d(t - t_0) \quad (6)$$

Where:

Q_t = amount of active ingredient dissolved at time t (μg)

K_d = rate constant of the transfer ($\mu\text{g} / \text{h}$)

t_0 = latency period (h)

t = time (h)

$$\text{One order function: } Q_t = Q_\infty(1 - e^{-K_d(t-t_0)}) \quad (7)$$

Where:

Q_∞ = is the maximum quantity that can be transferred (μg)

K_d = speed constant (1 / h)

$$\text{Higuchi function: } Q_t = A + K(t)^{\frac{1}{2}} \quad (8)$$

Where:

A = ordered to the origin (μg)

K = rate constant of the transfer ($\mu\text{g h}^{-2}$)

$$\text{Weibull function: } Q_t = Q_\infty \left[1 - e^{-\left(\frac{t}{t_d}\right)^\beta} \right] \quad (9)$$

Where:

t_d = the time it takes to release 63.2 % of the maximum amount of the active ingredient that can be released (h).

β = dimensionless parameter of shape.

$$\text{Korsmeyer-peppas function: } Q = At^n \quad (10)$$

Where:

A = is a kinetic constant ($\mu\text{g/h}^n$)

n = exponent of diffusion or release

t = time (h)

For this type of evaluation, Franz cells are one of the most used systems (Figure 11). The Franz diffusion cell is a system composed of two chambers, a donor and a recipient, separated by either an artificial membrane or skin. The diffusion cells are kept at 32-35 °C [4].



Figure 11. Franz diffusion cells.

1.8.2. Ex vivo Skin Permeation Studies

The phenomenon of permeation of a substance through the skin is a complex process influenced by many factors. This phenomenon is limited by the diffusion of the active principle through the stratum corneum since this acts as a passive diffusion medium according to Fick's diffusion laws. In transdermal permeation studies, the variation in the concentration of the active principle is related as a function of time. The resulting curve allows one to obtain the parameters that reflect the penetration, such as, flow of the active principle (J) and constant of permeation (K_p). The slope of the line that relates the amount of the active principle permeated as a function of time is equivalent to the flow J ($\text{mg} \cdot \text{h}^{-1} \cdot \text{cm}^2$). The characteristics of the active principle that mainly influence the rate of permeation are its distribution (K) and its diffusion (D) through the membrane. The product of the two coefficients that quantify these properties (K and D) per unit of space traveled (L) of the membrane is defined as the coefficient or constant of permeability (K_p). The direct calculation of K_p as a function of D , K and L is very difficult to carry out, but with some substitutions and knowing the value of the flow, the value of the permeability constant K_p can be estimated knowing the concentration of the active principle in the donor compartment (C_0) using the equation 11:

$$J = K_p C_0 \quad (11)$$

If the representative line of permeation in steady state is extrapolated to the abscissa axis, the value of the accumulated asset quantity is zero and the time in which this is fulfilled

is equal to the latency time (T_l) (point of intersection of the line with the abscissa axis). Consequently, the latency time indicates the time it takes, from beginning of the experience, to reach the steady state of equilibrium.

The resolution of the equations that describe the drug permeation model by means of Laplace lead to equations that describe the accumulation of solute in the receptor compartment. New variables appear in these equations, and therefore, for these to be operational, they are expressed using the following parameters (Equations 12-15):

$$P_1 = (K)(L) \quad (12)$$

$$P_2 = \frac{D}{L^2} \quad (13)$$

Hence:

$$K_p = (P_1)(P_2) \quad (14)$$

$$Tl = \frac{1}{6}(P_2) \quad (15)$$

1.8.3. *In vivo Studies to Evaluate Formulations Activities*

As has been seen, in addition to in vitro and ex vivo studies, there are in vivo models, which are used for dermal applications and to evaluate anti-inflammatory activity. Several models are available, such as that of mouse edema induced by TPA or by arachidonic acid (AA) (Figure 12). Nanostructured systems have been tested in these models: ear edema has been widely used as a useful pharmacological model to evaluate the anti-inflammatory activity of therapeutic agents. TPA can induce inflammation of the skin manifesting itself in the formation of edema, epidermal hyperplasia, and overproduction of inflammatory mediators. In addition, the AA is capable of generating inflammation in the skin through the release of inflammatory eicosanoids (prostaglandin E2 and leukotrienes) and histamine, thus generating erythema, edema, vascular permeability and accumulation neutrophilic [59]. Cytokines are local protein mediators and are currently known to be involved in almost all biological processes, including cell growth and activation, inflammation, immunity, and differentiation [60]. Among the supporting evidence of the anti-inflammatory effect in the previous models is precisely the histological study.



Figure 12. Treatment application in *in vivo* test.

1.9. Histological studies

Histology is the microscopic study of animal and plant cells and tissues by sectioning, staining, and examination under a microscope [61]. Histological analysis is the gold standard for examining tissues, whether for research or diagnosis, for both qualitative and quantitative measurements. This analysis is used, for example, to study inflammatory processes that have taken place in a tissue. Different stains are used to identify the possible changes that have occurred in the tissue, its cells, and structures. The most common staining method is called Hematoxylin-eosin, in which the cytoplasm of the cells is shown in pink and the nucleus in blue [62].

Histological staining includes a series of technical processes that are carried out to prepare tissue samples and subsequently microscopic analysis can be performed. The process has several stages which include, fixation, processing, embedding, sectioning, and staining. Fixation refers to the use of chemicals to preserve the natural structure of the tissue and keep the cellular structure from degradation. In general, a formaldehyde buffer is used when an optical microscope is to be used to carry out the study. The fixation phase retains the chemical composition of the tissues, hardens the cells and tissues to section them, and delays degradation. These fixatives are administered by immersing the tissue in a formalin buffer substance that stabilizes amino acids in proteins and offers good preservation of tissue and cell structure. Paraffin-formalin (PFA) is effective in immunostaining but requires fresh preparation to improve its effectiveness. In the inlay, the material has to be sufficiently firmness when cut, and therefore dehydration process is used so that the water contained in the fabric is replaced by a substance that gives it

rigidity and prevents it from deforming. Dehydration is the step of which the objective is to remove the water from the selected tissue to solidify it and facilitate the cutting of thin sections and placing them on a slide. The water is removed by dehydration with ethanol. The process is repeated through a hydrophobic cleaning substance such as xylene to remove the alcohol and paraffin. In the embedding stage, paraffin wax is used to improve the extraction of cell structures. Once the material is embedded, the cut is carried out using special equipment, which has a blade that cuts "flakes" of the material. Steel blades are used for optical microscopy and the equipment is called a microtome. The samples should be approximately 5-8 μm thick. The sections for observation under the light microscope are mounted on a glass slide. For electron microscopy, they are mounted on small metal grids that have perforations which allow the passage of the electron beam. For the study of sections under a bright field optical microscope, it is necessary to previously color the sample with different chemical compounds (dyes), which can react with the various components of cell structures. It is at this stage at which Hematoxylin-eosin is used [61]. As a result, images like the one shown in figure 13 are obtained.

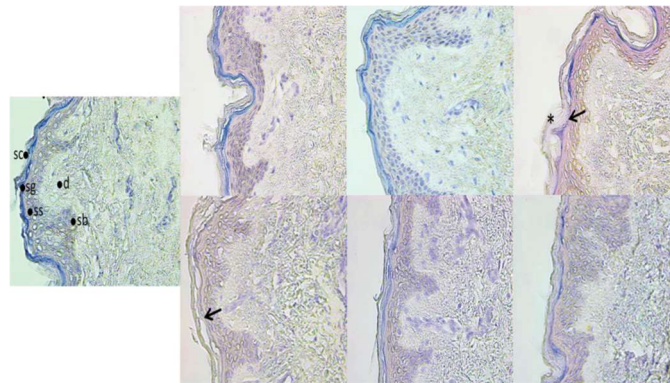


Figure 13. Example of image obtained from histological study [63].

1.10. *In vitro* Studies of Cytokine Expression

Cytokines (from the Greek "kyto" cell and "ina" substance) are molecules of low molecular weight (from 10 to 40 kD) and are made up of about 120 to 180 amino acids, which can modulate the function of cells and tissues, They are produced mainly by leukocytes, although some of them can also be secreted by other types of cells. Under physiological conditions, cytokines are not produced in significant quantities, the activation of cells being necessary for them to be produced in sufficient quantities to exert their biological effects. Most of them are secreted into the extracellular space in

glycosylated form, which increases their stability and solubility. However, some cytokines can accumulate inside the cell or adhere to the cell membrane [22].

In the generic name of cytokines, the nomenclature of interleukin or interleukin (IL) was used for those molecules that served as communication signals between different types of leukocytes, being numbered as they were discovered, thus they can be found from IL-1 to IL-43. However, some of the cytokines were identified by *in vitro* tests, which is why they were given the name of the biological function they develop, such as Interferon (IFN), Tumor Necrosis Factor (TNF), Stimulating Factors of Formation Colonies (CSF) or Transforming Growth Factor (TGF). Cytokines, in addition to having a fundamental role in the inflammatory and immune response, are be involved in numerous biological processes such as hematopoiesis, embryogenesis and angiogenesis. As well as in different cellular processes such as mitosis, differentiation, migration or even cell death. The two main functional characteristics of cytokines are pleiotropism, a condition in which the mutation in a single gene affects multiple phenotypic characteristics since the same cytosine can exert different biological effects by acting on different cell types, and redundancy, since several cytokines can contribute to the development of the same effect in a cell. Furthermore, cytokines can act in what are known as amplification cascades, stimulating the consecutive production of other cytokines as they amplify the biological effects, or they can set in motion an antagonist effect thereby regulating the original response and/ or intensity thereof.

Hence, we are dealing with a complex system, where the effect of a molecule is closely regulated, positively or negatively, by other molecules of the same system and that, in addition, when a cytosine is missing, its functions can be totally or partially replaced by others [64].

The expression and activity of cytokines can be measured in various ways by using: bioassays, on cell lines, immuno-assays, such as the enzyme-linked immunosorbent assay (ELISA), which makes it possible to quantify their concentration in different biological fluids. Another method is, the ELISPOT, which derives from the technique above, and which allows the number of cells to be determined. Flow cytometry makes, it is possible

not only to quantify, but also to characterize the producer cells. Polymerase Chain Reaction (PCR) techniques, allow the measurement of the levels of messenger RNA that encode the production of a certain cytosine. Immunohistochemical techniques, such as Avidin Biotin Peroxidase (ABC), allows cytokines to be detected in tissues and organs [65].

In the inflammatory response, cytokines can act in two totally opposite ways, since while some (pro-inflammatory cytokines) will favor its development, the so-called immunosuppressive cytokines, will have a marked suppressive effect on inflammation. Cytokines with pro-inflammatory activity are: IL-1, IL-6, TNF- α , TNF- β , IFN- γ and the cytokines with immunosuppressive activity are: IL-4, IL-10, IL-13 and TGF [66].

Cytokines with pro-inflammatory activity are molecules produced mainly by monocytes and macrophages, activated after contact with a pathogen, although they can also be synthesized by other cells such as endothelial cells or dendritic cells, among others [22].

Interleukin 1 (IL-1), of which there are two forms, alpha (α) and beta (β), which, although only 25 % homologous, share the same receptor and exert similar biological effects; It is known that it is the main endogenous pyrogen, inducing fever, thanks to the production of prostaglandins, and it acts on the CNS, causing sleep and anorexia that are associated with infectious processes. In addition, this cytosine induces the release of histamine, responsible for vasodilation and increased vascular permeability at the site of inflammation. It, is a chemotactic factor of leukocytes [67].

As for the Tumor Necrosis Factor (TNF), two molecules, α and β , have been described. They have a high homology and they are closely related. TNF- α is produced by monocytes, macrophages, T and B lymphocytes, natural killer cells, fibroblasts, and mast cells. It is involved, along with IL-1, in the development of fever, cachexia and sleep patterns that are established in infectious processes, being a powerful activator of monocytes and neutrophil polymorphonuclear cells. In addition, it induces the expression of adhesion molecules and stimulates the production of other cytokines, such as IL-8, by

the vascular endothelial cells, which contributes to the extravasation of lymphocytes, neutrophils and monocytes, and the production of proteins in the acute phase by stimulating IL-6. On the other hand, TNF- β , is produced, exclusively by activated T lymphocytes, although it binds to the same receptors as TNF- α and induces similar functions. In addition, Tumor Necrosis Factor has the ability to induce necrosis of some types of tumor cells, as well as initiate apoptosis phenomena, or programmed cell death, in some cells, by binding to surface receptors that initiate the cascade of the extrinsic pathway. This, is the way in which an extracellular stimulus can induce a cell to die without causing an inflammatory response [22].

Interleukin 6 (IL-6) is responsible for the production by the liver of acute phase proteins, which have a protective and regulatory function of the inflammatory process through their anti-protease activity. In addition, this cytokine induces the production of neutrophil, monocyte and megakaryocyte precursor cells in the bone marrow and promotes the differentiation of B lymphocytes into plasma cells, inducing the production of immunoglobulins. However, this cytokine is also capable of exerting an immunosuppressive function since it induces the synthesis of antagonists of the IL-1 β receptors, and therefore this cytokine does not find receptors to bind to and cannot develop its pro-inflammatory function [67].

To finish with this group of cytokines, we will mention interferon (IFN), initially described as a protein produced by cells infected by some viruses. These molecules are classified into two types: Type I, which includes IFN- α and IFN- β , with antiviral and anti-proliferative properties, and Type II, which includes IFN- γ , which has an immunomodulatory effect. While IFN- α is secreted by fibroblasts and some epithelial cells, IFN- γ is produced mainly by monocytes and macrophages, being considered the main activator of macrophages and a trigger of the cellular immune response, by stimulating the differentiation of cells. T lymphocytes to Th1. However, type I interferons (α and β) can also be considered immunosuppressive cytokines due to their regulatory effect on cytosine production and their anti-proliferative capacity. This effect means that it also has an antitumor activity [67].

OBJECTIVES

2. OBJECTIVES

2.1. **General objective:** To carry out a biopharmaceutical and pharmacological study of solution and nanostructured formulations containing natural flavanone **1** and derived flavanones **1a-1d** (Figure 14) to demonstrate their transdermal permeation capacity in human skin and thus to show that they can be applied through the skin to treat pathological skin conditions which present inflammation.

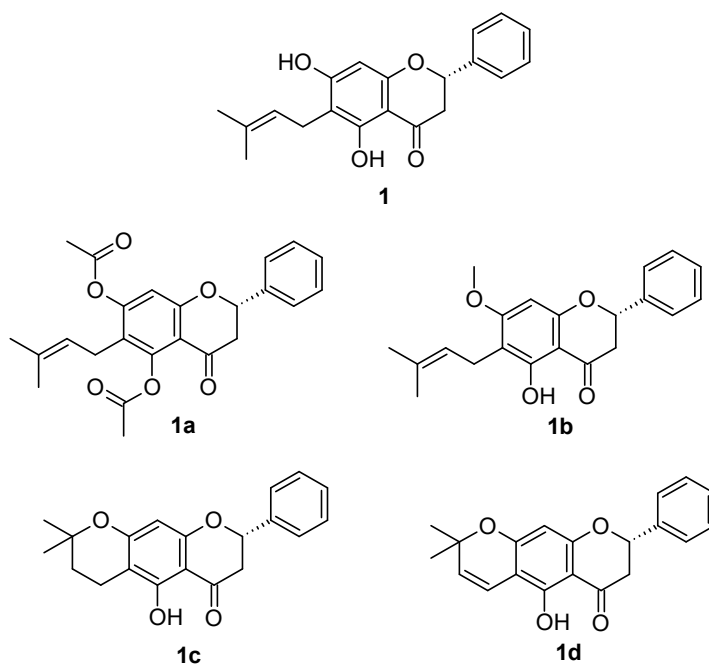


Figure 14. Chemical structure of flavanones for study.

2.2. Particular objectives:

- To prepare and identify flavanones derived **1a-1d** from flavanone **1**.
- To analyze the physicochemical properties and predict the possible bioactivity of flavanones using an *in silico* study.
- To validate the analytical methodology used to quantify the amounts of flavanones in the study released from their formulations, permeated and extracted during the human skin test, by using flavanones in solution.
- To prepare stable nanostructured formulations containing natural flavanone **1** and derivatives **1a-1d**.

- To carry out the physical-chemical characterization study of the formulations, as well as of their stability.
- To achieve the biopharmaceutical study of the release of flavanones from the formulations. In addition, the objective is to find out their release kinetics and the parameters that explain them.
- To complete the *ex vivo* permeation study in human skin, looking at the flavanones in both solutions and nanostructures; to find out the transdermal penetration and the amounts withheld from them in the body.
- To evaluate the anti-inflammatory efficacy and safety of the formulations through *in vivo* studies.
- To carry out an *in vitro* study of cytokines expressed or reduced by the effect of the flavanones arranged in the formulations, using tissues from an *in vivo* study with induced inflammation.

MATERIALS AND METHODS

3. MATERIALS AND METHODS

3.1. General Considerations

The purified water used in all experiments was obtained from the MilliQ[®] Plus System (Millipore Corporation, MA, USA) lab supply. The solvents were appropriately filtered through a 0.45 µm Millipore membrane filter (Merck, Darmstadt, Germany) and degassed in an ultrasonic bath for 20 min.

Polyglyceryl-6-dioleate (Plurol[®] oleique), triglycerides medium-chain EP/NF/JPE (Labrafac[®] lipophile), and caprylocaproyl macrogol-polyoxyl-8-glyceride (Labrasol[®]) were gifted by Gattefossé (Gennevilliers, France). Propylene glycol, ethanol, HPLC-grade Acetonitrile, DMSO and, all other chemicals and reagents used in the study were acquired from Sigma-Aldrich (Madrid, Spain). Dialysis cellulose membrane molecular weight cutoff (MWCO) 12 kDa was purchased from Iberlabo (Madrid, Spain).

3.2. Extraction and Isolation of Plant Material

E. platycarpa leaves were collected in Tetipac, Guerrero, Mexico, and identified by Prof. Ramiro Cruz (Registration Number: Ramiro Cruz 1325 from the Sciences Faculty Herbarium Facilities of the Autonomous University of the State of Morelos). The leaves were dried at room temperature, then pulverized and extracted by three consecutive macerations with methanol at room temperature (100g of dried vegetal material per 1000 mL methanol). The extraction solvent was removed under reduced pressure. Next, the prenylated flavanone **1** was isolated by column chromatography at reduced pressure. Finally, it was purified and characterized by direct thin-layer chromatography (TLC) comparison with original samples available in the laboratory. The product was a yellow powder precipitate with a melting point of 200.2 °C. The compound obtained was characterized by comparison with previously published melting point data and with ¹H-NMR results [19].

3.3. Semi-synthesis from Natural Flavanone 1

Each prenylated flavanone was prepared following the method as previously reported by Andrade-Carrera *et al.* [68]. The esterification was performed with acetic anhydride over pyridine to obtain the esterified derivate **1a** (Figure 15). First, 50 mg of natural flavanone

1 was stirred with 2 ml of a previously prepared system of pyridine: acetic anhydride (1: 2), for 24 h at room temperature. Upon completion of stirring, the reaction mixture was dissolved with ice. The extraction separation process then was carried out.

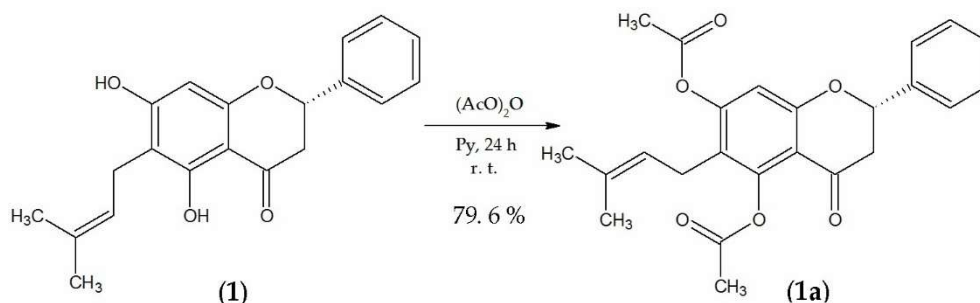


Figure 15. Esterification reaction of (2*S*)-5,7-dihydroxy-6-(3-methyl-2-buten-1-yl)-2-phenyl-2,3-dihydro-4*H*-1-Benzopyran-4-one (**1**) to obtain (2*S*)-5,7-bis(acetyloxy)-6-(3-methyl-2-buten-1-yl)-2-phenyl-2,3-dihydro-4*H*-1-Benzopyran-4-one (**1a**).

Diazomethane was used as the alkylating agent for the methylation reaction to obtain the corresponding modulated ether **1b** (Figure 16). 50 mg of natural flavanone **1** were placed and 10 ml of a solution of diazomethane in diethyl ether were added to it. The resulting solution was allowed to stand for 5 hours and then the solvent was removed under reduced pressure to obtain flavanone **1b**.

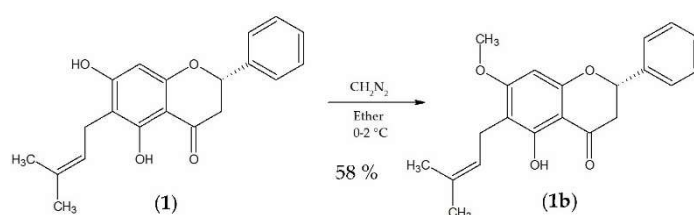


Figure 16. Methylation reaction of (2*S*)-5,7-dihydroxy-6-(3-methyl-2-buten-1-yl)-2-phenyl-2,3-dihydro-4*H*-1-Benzopyran-4-one (**1**) to produce (2*S*)-5-hydroxy-7-methoxy-6-(3-methyl-2-buten-1-yl)-2-phenyl-2,3-dihydro-4*H*-1-Benzopyran-4-one (**1b**).

To obtaining modulated compound **1c** (Figure 17) a mixture of 50 mg of flavanone **1** with 20 ml of formic acid were heated at 60 ° C for 2 hours in a water bath. Subsequently, the

mixture was left to stand for 6 h at room temperature for subsequent recrystallization in an ice bath. The flavanone **1c** was finally obtained by organic extraction.

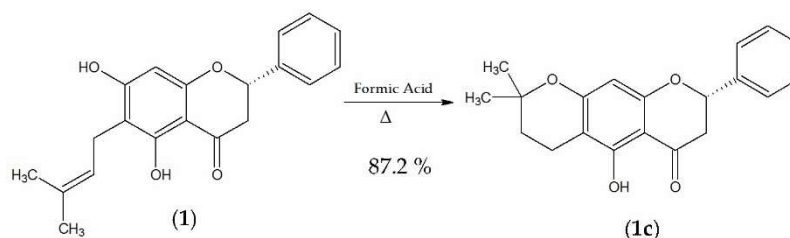


Figure 17. Cyclization reaction of (2S)-5,7-dihydroxy-6-(3-methyl-2-buten-1-yl)-2-phenyl-2,3-dihydro-4H-1-Benzopyran-4-one (**1**) to form (8S)-5-hydroxy-2,2-dimethyl-8-prenyl-3,4,7,8-tetrahydro-2H,6H-benzo[1,2-b:5,4-b']dipyran-6-one (**1c**).

The intramolecular cyclization of flavanone **1** to form compound **1d** was done by the reaction of 50 mg of flavanone **1**, 40 mg of 2,3-dichloro-5,6-dicyanobenzoquinone (DDQ) and 10 ml of dry benzene in a three-neck flask. The mixture was refluxed at 78 °C for 5 h. After the reaction, the mixture was filtered hot and washed with CH₂Cl₂, obtaining the derivative flavanone **1d** under anhydrous conditions is schematized in the Figure 18.

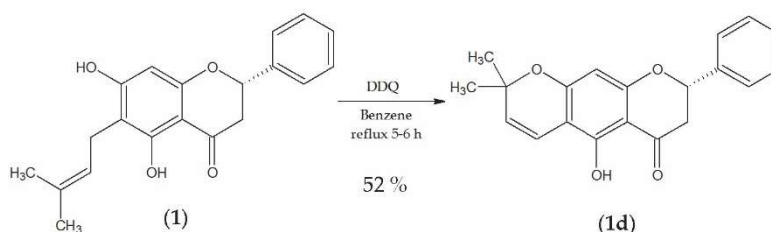


Figure 18. Reaction of vinyllogous-cyclization of (2S)-5,7-dihydroxy-6-(3-methyl-2-buten-1-yl)-2-phenyl-2,3-dihydro-4H-1-Benzopyran-4-one (**1**) gives (8S)-5-hydroxy-2,2-dimethyl-8-phenyl-7,8-dihydro-2H,6H-benzo[1,2-b:5,4-b']dipyran-6-one (**1d**).

3.4. *In silico* Analysis

The computational methods (*in silico*) are one of the well-known approaches that has been used regularly to produce the 3D models to identify physicochemical properties and to predict biological activities [69]. Molinspiration[®] server and PASS Online (Prediction of Activity Spectra for substance) were used to predict the flavanones **1**, **1a-d** bioactivity [28,70].

3.5. Chromatographic Operating Conditions

The HPLC system consisted of a Waters 515 HPLC pump, a 717 Plus autosampler, and a dual λ absorbance UV-vis 2487 detector (Waters, Milford, MA, USA). The analytical column was Atlantis[®] C18 5 μ m 250 mm \times 4.6 mm, Waters. The analyte separation was performed with 10 μ L sample injection volume. The separations were done in isocratic mode at room temperature. The mobile phase with a flow rate of 1 mL/min comprised of W-water and AcN-acetonitrile (%W: %AcN) with a different composition for each prenylated flavanone studied: **1** (30:70), **1a** (20:80), **1b** (40:60), **1c** (20:80) and **1d** (10:90). The detection wavelengths determined by spectrum scan were 300 nm for **1**, **1b**, **1c**, **1d**, and 320 nm for **1a**. The Peak area was used to quantify each analyte.

3.6. Analytical Method Validation

The method was validated according to the International Conference on Harmonization guidelines (ICH) [71,72] for linearity, the limit of detection (LOD), the limit of quantification (LOQ), accuracy, and precision. Calibration curves were analyzed in two ranges; from 200 to 12.5 μ g/mL in a high concentration level, and from 12.5 to 1.56 μ g/mL in a low concentration level.

3.6.1. Standard Solutions for Calibration Curves

Standard stock solutions of each compound (**1**, **1a**, **1b**, **1c**, and **1d**) were prepared daily by dissolving the appropriate amount of each analyte in ethanol: water (7:3; v/v) to obtain a final concentration of (200 μ g/mL). The working solutions were elaborated by the dilution of appropriate aliquots of the stock solutions with the diluting solvent to reach the concentration ranges 1.56, 3.12, 6.25, 12.5, 25, 50, 100 μ g/mL.

3.6.2. Linearity

The linearity was evaluated by a one-way analysis of variance (ANOVA) test to compare peak areas versus nominal concentrations of each standard [73]. Differences were considered statistically significant when $p < 0.05$. The least-square linear regression analysis and mathematical determinations were performed by Prism, V 5.0 software (Graph Pad Software Inc., San Diego, CA, USA).

3.6.3. Limit of Detection and Limit of Quantification

The limit of detection (LOD) and the limit of quantitation (LOQ) for each analyte (**1**, **1a**, **1b**, **1c**, and **1d**) were calculated based on the standard deviation of the response and the slope of the calibration curve, generated from six replicate analysis applying the equation 16 [74].

$$LOD \text{ or } LOQ = k \frac{SD_{Sa}}{S_b} \quad (16)$$

where k is the factor related to the level of confidence ($k = 3.3$ and 10 for LOD and LOQ respectively), SD_{Sa} is the standard deviation of the intercept, and S_b is the slope.

3.6.4. Repeatability, Accuracy, and Precision

The instrumental repeatability was assayed by analyzing the concentration sample of 200 $\mu\text{g/mL}$ for each flavanone (**1**, **1a**, **1b**, **1c**, and **1d**) repeatedly seven times, consecutively. The accuracy and precision were investigated by measuring samples in three concentrations 1.56, 12.5, and 200 $\mu\text{g/mL}$ [75]. The inter-day test was conducted by analyzing each analyte (**1**, **1a**, **1b**, **1c**, and **1d**) with each of the three concentration levels mentioned before, once a day for six consecutive days. The accuracy was expressed as a relative error (RE %). The precision was defined as the relative standard deviation (RSD %) of the measurement. The method is considered accurate and precise if RE % and RSD %, respectively, are within ± 15 %.

3.6.5. Specificity

Specificity is defined as the ability of the method to distinguish the analyte from all other substances present in the sample. This can be proven by comparing the analyte chromatographic retention time in extracted matrix samples and with its retention time in at least one reference solution [76]. To test the specificity of the analytical method, *the ex vivo* human permeation procedure described in Section 6.7 was followed. The blank sample peaks should not appear at the same retention times of the prenylated flavanones.

3.7. *Ex Vivo* Human Skin Permeation (Intrinsic permeation)

A blank sample (ethanol: water; 70:30; v/v) was used as a negative control and the samples of flavanones (**1**, **1a**, **1b**, **1c**, and **1d**) with a concentration of 200 µg/mL were permeated through human skin membrane in the receptor compartment of the Franz diffusion cells (FDC 400, Crown Glass, Somerville, NY, USA), with a diffusion area of 2.54 cm². Human skin from abdominal plastic surgery of healthy patients was used as a permeation membrane. The skin was cut into 400 µm thickness and placed between the donor, and the receptor compartment of the Franz diffusion cells, avoiding the formation of bubbles [18]. The flavanone samples **1**, **1a**, **1b**, **1c**, and **1d** (300 µL) were applied to the donor compartment and the receptor compartment was filled with ethanol: water (70:30) solution. The receptor compartment was kept at 32 ± 1 °C. Twenty-four h after the application of the tests, 300 µL aliquots were collected from the receptor side. Sink conditions were always followed. The flavanones amount permeated (Q) through human skin were determined by HPLC analysis described in Section 6.5.

3.7.1. *Flavanone Extraction*

At the end of the *ex vivo* human skin permeation study, the flavanones amounts remaining in the skin were quantified by calculating the flavanone amount extracted from the skin to the flavanone amount added. For this purpose, the skin was removed from the Franz cells, cleaned with gauze soaked in a 0.05% solution of dodecyl sulfate and washed with distilled water. The permeated areas of the skin were then excised and weighed. The flavanone contained in the skin was extracted with ethanol: water (70:30) mixture under sonication (20 min) in an ultrasonic bath. The resulting solutions were measured with HPLC, quantifying the flavanone amount retained in the skin in micrograms of prenylated flavanone per grams of skin and per area unit µg/g_{skin}.cm²).

3.7.2. *Recovery from Human Skin Tissues and Flavanone Retained*

The accuracy of the extraction was evaluated by adding 1 mL of each flavanone solution (200 µg/mL) to their corresponding vials containing approximately 100 mg of human skin. These vials remained for 24 h at 32 °C to simulate the permeation conditions experiments. This experiment was conducted in triplicate. After the time of the study, the skin was submitted to drug extraction, as described in Section 6.7.1. The initial solutions

and the eluates from each assay were collected and analyzed with HPLC. The differences obtained between the initial flavanone amount in the solution and the final flavanone amount in the collected solutions after 24 h were considered to be the value of the respective flavanone amount bound to tissue. Recovery percentage was calculated comparing the corresponding drug extraction results with the flavanone amount bound to the tissue [77]. A comparison of the amount of prenylated flavanone extracted and the recovery percentage was made in order to find out the real amount of flavanone retained in the skin.

3.8. Flavanone Solutions (FS)

The flavanone solutions (FS1, FS1a-FS1d) were prepared by dissolving 5.0 mg of the respective flavanone (**1**, **1a**, **1b**, **1c** and **1d**) with 1 mL of the mixture of EtOH/H₂O (7:3). Non-Flavanone solution (nFS) consists of a mixture of EtOH/H₂O (7:3). The purity and chemical stability of dissolutions were examined after 5 days of their preparation storage at 4 ± 1 °C using the validated analytic method described before in Section 6.6 in terms of linearity, accuracy and precision [78].

3.9. Flavanone Formulations (FF)

The flavanone formulations (FF) were elaborated by an ultrasonic homogenization method as described by Domínguez-Villegas *et al.*[55]. To sum up, the flavanones **1**, **1a**, **1b**, **1c** and **1d** (0.5 % w/w) were dissolved with Labrasol[®] (53.475 % w/w, Surfactant), Plurol oleique[®] (13.275 % w/w, Co-surfactant), Labrafac lipophile[®] (14.875 % w/w, lipophilic phase) and Propylene glycol (17.875 % w/w, hydrophilic phase) by sonication of the components in an Elma Transonic Digital S T490 DH ultrasonic bath (Elma, Singen, Germany) for 30 min at 32 °C. In the next step, the resulting solutions were cooled at -20 °C for 24 h to yield FF1, FF1a, FF1b, FF1c and FF1d. Non-Flavanone formulation (nFF) was prepared with the same procedure described before but without adding any flavanone.

3.10. Determination of FF physical parameters

3.10.1. Morphological studies

The transmission electron microscopy (TEM) was used for the morphological and structural examination of FF. First, one drop of each FF was adsorbed into carbon-coated copper grids (EMS, London, UK) for 1 min and filter papers were used to remove the excess. Then, they were stained with Uranylless (EMS) for 1 min. The excess of liquid was manually blotted from the edge of the grids. The sample was observed in a Tecnai™ Spirit microscope (EM; FEI, Maastricht, The Netherlands) equipped with a tungsten filament, at the Cryomicroscopy Unit from the CCiTUB. Finally, images were acquired at 120 kV and at room temperature with a 1376 × 1024 pixel CCD Mega view camera [79].

3.10.2. Rheology studies

The FF (**n**, **1**, **1a**, **1b**, **1c** and **1d**) viscosity was measured at 25 ± 2 °C in triplicate with a Haake Rheo Stress 1 rheometer (Thermo Fisher Scientific, Karlsruhe, Germany) with a cone rotor C60/2-Ti (60 mm diameter, 2° angle, 0.105 mm gap between cone-plate). The rheometer executed the tests and run the analyses connected to a thermostatic circulator Thermo Haake Phoenix II + Haake C25P and to a computer (Haake Rheowin® Job Manager and Data Manager v3.3 software; Thermo Electron Corporation, Karlsruhe, Germany). As described by Sunér *et al.*: Ramp-up from 0 to 100/s in 3 min, a constant shear rate of 100/s during 1 min and Ramp-down from 100 to 0/s in 3 min [80,81].

3.10.3. Extensibility studies

A volume of 50 µl of FF (**n**, **1**, **1a**, **1b**, **1c** and **1d**) was placed on a steel plate circle (10 cm diameter) then a glass plate was placed over it. Increasing standard weight pieces (1, 2, 5, 10, 20, 50, 100 and 200 g) were replaced and allowed to rest on the upper glass plate for 1 min. The increase in the diameter due to the formulation spreading was noted. Each formulation was tested in triplicate at room temperature. The increase in surface area (mm²) of the FF was plotted as a function of the increasing weights applied [82]. The two-site binding hyperbola model described as equation 17 was the best fitted to formulations.

$$y = \frac{B_{max1} \cdot x}{K_{d1} + x} + \frac{B_{max2} \cdot x}{K_{d2} + x} \quad (17)$$

where B_{max1} and B_{max2} are the maximal surfaces, and K_{d1} and K_{d2} are the weights required to reach the half-maximal surfaces.

3.10.4. Stability Studies

To assess physical stability, aliquots of 1 ml of the FF (**n**, **1**, **1a**, **1b**, **1c** and **1d**) were deposited in glass vials. The samples were stored for 180 days and kept at $4 \pm 1^\circ\text{C}$. The FF macroscopic characteristics were studied to detect any instability by visual observation over the storage period. Their physical appearance was captured by high-resolution digital camera (Panasonic DMC-FZ20). The clarity, the precipitation appearance, phase separation and any other macroscopic changes were compared with the initial formulations [83,84]. The pH of FF was measured at room temperature using a calibrated digital pH meter GLP 22 (Crison Instruments S.A., Barcelona, Spain), once FF had been elaborated and after 180 days of storage. Measurements were done in triplicate and mean and standard deviation (SD) values were reported.

The chemical stability was evaluated by measuring the quantity of flavanone present in the FF (**1**, **1a**, **1b**, **1c** and **1d**) to verify if potential changes occurred during the storage at $4 \pm 1^\circ\text{C}$ for 30, 60 and 180 days. For this purpose, an exact volume of 100 μl of each formulation was dissolved in 5 ml of DMSO by stirring for 10 min in an ultrasonic bath[85]. The amount of flavanone extracted was determined by HPLC described in Section 6.5. If the flavanones profiles had variations of more than 10 %, they were indicated as unstable formulations.

3.11. *In vitro* FF Studies

The release study of flavanones (**1**, **1a**, **1b**, **1c** and **1d**) was performed using dialysis membrane (12 kDa, Dialysis Tubing Visking, Medicell International Ltd, London, UK) hydrated for 24 h before being fixed in the Franz diffusion cell with an effective diffusional area of 2.54 cm^2 . The experiment was performed under “sink conditions”. The receptor phase was filled with 12 ml of ethanol: water (7:3) maintained at $32 \pm 1^\circ\text{C}$ under continuous stirring. Afterward, 0.3 ml of FF samples were placed into the donor

compartment. Moreover, aliquots of 0.3 ml were taken from the receptor compartment at fixed times for 120 h and replaced with the same volume of receptor medium. The concentration of each sample was quantified by HPLC with an UV detector [78]. Data were expressed as mean \pm SD ($n = 3$). Different kinetic models (first order, hyperbola, Korsmeyer–Peppas and Weibull, Equations 18–21) were evaluated to find out the flavanones release profile from FF. Coefficients of determination (r^2) were used as discrimination criteria.

$$Q_t = K_d(t - t_0) \quad \text{Zero Order} \quad (18)$$

$$Q_t = Q_\infty(1 - e^{-K_d(t-t_0)}) \quad \text{First Order} \quad (19)$$

$$Q = At^n \quad \text{Korsmeyer-Peppas} \quad (20)$$

$$Q_t = Q_\infty \left[1 - e^{-\left(\frac{t}{t_d}\right)^\beta} \right] \quad \text{Weibull} \quad (21)$$

where Q_t is the drug amount released at time t (μg), K_d is the release rate constant ($\mu\text{g/h}$), Q_∞ is the maximum amount susceptible to release (μg), t_0 is the latency period (h), A is a kinetic constant ($\mu\text{g/h}^n$), n is the diffusion release exponent; t_d is the time in which the 63.2 % of the drug is released, and β is the sigmoidicity.

Analysis of variance and t -test were calculated to evaluate the significant differences between release profiles of all the formulations. Data were considered statistically significant at $p < 0.05$.

3.12. *Ex vivo* FF Studies

The permeation studies were carried out with vertical Franz diffusion cells of 0.64 cm² and dermatome human skin from the abdominal region (0.4 mm) for a unique donor as membrane. All provided from the plastic surgery unit (Hospital de Barcelona, SCIAS, Barcelona, Spain), with written informed consent. Three parallel determinations were addressed. The receptor phase was filled with 5 ml of ethanol: water (70:30), under the temperature of $32 \pm 1^\circ\text{C}$ kept by a circulating-water jacket and stirred at 700 r.p.m. with teflon[®] coated magnetic stirring bars. The donor side was filled with 0.1 ml of each FF (**1a**, **1b**, **1c** and **1d**) covered with parafilm[®] in order to avoid evaporation. Samples were

withdrawn at different points in time over 29 h and quantified by means of a validated HPLC method with 1 ml/min flow rate and Machery Nagel® C18 5mm, 25 × 4.6 cm column (Section 6.5). At the end, the experimental data were analyzed using the Prism®, V.5 software (GraphPad Software Inc., CA, USA). The cumulative amount of flavanones permeated through the human skin membrane were plotted as a function of time. The estimated permeation parameters such as the flux across the skin J ($\mu\text{g}/\text{cm}^2/\text{h}$) were calculated from the slope of the linear portion of cumulative amounts of each flavanone permeated through human skin per unit surface area Q ($\mu\text{g}/\text{cm}^2$), set out on a time plot. The intercept with X-axis (time) of this plot is equal to lag time T_l (h). The transdermal permeability coefficient K_p (cm/h) resulted by dividing the flux (J) by the initial concentration of the flavanones studied (C_o) in the donor compartment [86]. The partition coefficient P_1 (1/h) (Equation 23) and the diffusion coefficient P_2 (Equation 22) were also estimated as followed:

$$P_2 = \frac{1}{6T_l} \quad (22)$$

$$P_1 = \frac{J}{(A * C_o * P_2)} \quad (23)$$

where T_l is the lag time; J is the flux across the skin, A is the membrane area, C_o is the concentration of the flavanones at time zero in the donor compartment.

Once the experiment had finalized, the amount of flavanone retained (skin retention, Q_r , $\mu\text{g}/\text{g}$ skin/ cm^2) in the human skin membrane was determined. For that purpose, the flavanones skin extraction was carried out as followed: the skin was removed from the Franz cells at the end of the permeation studies, and then it was cleaned with 0.05 % solution of dodecylsulphate and was washed with distilled water. The permeation areas of the skin were cut and weighed. The flavanone contained was extracted with ethanol: water (70:30) mixture under sonication (20 min) in an ultrasonic bath. Finally, the solutions were quantified by HPLC as described in Section 6.5, yielding the amount of each flavanone that could be extracted Q_{ext} ($\mu\text{g}/\text{g}$) by this method from the skin study.

The recovery percentage (R %) was obtained as described in section 6.9 in accordance with a mass balance calculation. Briefly, 1 ml of each flavanone solution (200 $\mu\text{g}/\text{ml}$) was added to vials with 100 mg of human skin ($n = 3$). These vials remained for 24 h in a water bath at 32°C. Once 24 h had passed, the skin was extracted with ethanol: water

(70:30) mixture under sonication (20 min) in an ultrasonic bath. Finally, the initial solutions and the eluates were analyzed by HPLC (see Section 6.5). The R % of each flavanone (**1**, **1a**, **1b**, **1c** and **1d**) was calculated comparing the corresponding drug extraction results, with the flavanone amount bound to the tissue (difference between initial flavanone amount and flavanone amount in the eluates at 24 h). The amount of flavanone retained in tissue (Q_r) was calculated at the end by the comparison of the amount of flavanone extracted (Q_{ext}) and the recovery percentage as described above and in accordance with the equation 24:

$$Q_r = \frac{Q_{ext}}{R\%} * 100 \quad (24)$$

where Q_{ext} is the amount of flavanone extracted and R % is the percentage of recovery of flavanones [75].

The statistical analysis and data comparisons were achieved using the nonparametric statistical Mann–Whitney U test with significant statistical differences when $p < 0.05$.

3.13. *In vivo* Studies: Anti-inflammatory Efficacy

3.13.1. TPA-Induced rat ear inflammation model

TPA-induced mouse ear edema was carried out using male Wistar CD-1 mice ($n = 3$ for each of the flavanones **1a–1d**, 20 to 25 g) based on the protocol previously described [63]. Edema was induced by the topical application of 2.5 μg of TPA (12-O-tetradecanoylphorbol-13-acetate) dissolved in 20 μL ethanol per ear (10 μL each ear side). The standard drug indomethacin was used as a reference. It was dissolved in acetone and put simultaneously on both sides of the right ear (1 mg/ear) with TPA. In the same way, 1 mg of each flavanone (**1a–1d**) was dissolved in acetone and applied on both sides of the right ear with TPA at once. Similarly, acetone was put on both sides of the left ear. Four hours after the flavanone solutions were put on, the animals were sacrificed by dislocation of their necks. Subsequently, the left and right ears were perforated by punching bear (7 mm diameter), and the resulting tissues were accurately weighed. The percent of inhibition of edema formation was assessed according to the following equation 25:

$$\text{Inhibition (\%)} = \frac{\text{difference in weight of ear,control} - \text{difference in weight of ear,treated}}{\text{difference in weight of ear,control}} \times 100 \quad (25)$$

The studies were conducted under a protocol in accordance with the Mexican Official Norm for Animal Care and Handling (NOM-062-ZOO-1999) and with the approval of the Academic Committee of Ethics of the Vivarium of the Autonomous University of Morelos State, Mexico, with number 0122013.

3.13.2. Arachidonic acid (AA)- induced rat ear inflammation model

Adult male SpragueDawley[®] rats (200–240 g) were brought from the Bellvitge animal facility services and approved by the Ethics Committee of Animal Experimentation of the University of Barcelona. Prior to the experiments, they were fed with standard food and water *ad libitum*. The experiments reported in this study were carried out following the guidelines stated in the protocol “Principles of Laboratory Animal Care” publication 214/97 of 30 July).

The anti-inflammatory effects of the FS1, FS1a-FS1d and FF1, FF1a-FF1d were assessed using the AA-induced rat ear edema model. The experiment was carried out using a slight modification of the procedure described by Espinoza, *et al.* [87]. Adult male Sprague Dawley rats were used with a weight ranging from 200 to 240 g ($n = 5$ for each treatment). An irritant solution was prepared by dissolving AA (5 mg/ml) in phosphate buffered saline. The inflammatory process was induced by one topical application of 60 μ l of AA solution on both sides of the ears; and left for 20 min of exposure, except the negative control group (Control -). The animals in the positive control (Control +) were treated only with AA solution. Moreover, one animal group was treated only with the mixture EtOH/H₂O (7:3) without any flavanone, i.e. only excipients (nFS). Similarly, another animal group was assayed with 50 μ L of the formulation without flavanones only excipients (nFF). The other groups were treated with 50 μ L of the respective flavanone solution (FS1, FS1a, FS1b, FS1c and FS1d) and flavanone formulation (FF1, FF1a, FF1b, FF1c and FF1d). A solution of diclofenac sodium (5 mg/mL) in EtOH/H₂O (7:3) was used as a reference drug solution (RS) and the commercial gel diclofenac sodium 10 mg/g (0.5 mg, ATC Code: M02AA15) as the reference drug formulations (Rd). All groups, except the negative and positive control, were treated with the respective formulation 20 min after AA exposition and the treatment was kept for 20 min.

The measurements of stratum corneum hydration (SCH) were done before and after the AA application and treatments using a corneometer CM825 (Courage & Khazaka electronics GmbH, Köln-Germany). Values (arbitrary units) reported as the mean of five replications \pm SD. In the same way, ear thicknesses were recorded before and after the AA and the different treatments with a digital micrometer (Wisamic Digital Thickness Gauge 0–12.7 mm). The anti-inflammatory activity was expressed by means of the following equation 26 [55]:

$$\Delta \text{Inhibition inflammation} = \frac{\text{difference in thickness, positive control} - \text{difference in thickness after treatment}}{\text{difference in thickness, positive control}} \quad (26)$$

Finally, at the end of the experiment, the rats were sacrificed using carbon dioxide, following the recommendations for euthanasia of experimental animals from the European Commission [88]. Then, the ears were cutoff and stored to assess histological assay with left ears (section 6.16) and gene expression analysis by RT-qPCR with right ears (section 6.17)

3.14. Histological Analysis

After the *in vivo* study, the rats' ears were immediately removed from the treated animals. The positive and negative control groups were used to study the anti-inflammatory effect. First, the tissues were rinsed with PBS pH 7.4, and set overnight in 4 % buffered formaldehyde and finally embedded in paraffin wax. Transversal sections (5 μ m) were stained with hematoxylin and eosin and viewed for the evaluation of the ear inflammation under a light microscope (Olympus BX41 and camera Olympus XC50) on blind coded samples. Ears from the non treated animals were used as the control condition.

3.15. Gene Expression Analysis by RT-qPCR

Sections of right ear rat tissue from each animal group were homogenized in 1 mL of ice-cold TRI Reagent[®] (Sigma Aldrich) for 3 min using the Polytron[™] Homogenizer PT1200E (Thermo Fisher Scientific). Total RNA was isolated using TRIZol method (Thermo Fisher Scientific) following the manufacturer's protocol. Purity and RNA concentration were measured with Thermo Scientific Nano Drop TM 2000/2000c Spectrophotometer (Thermo Fisher Scientific)

Total RNA (1 µg) was reversed transcribed to cDNA using High Capacity cDNA Reverse Transcription kit (Applied Biosystems) in a final volume of 20 µL following the manufacturer's recommendations. qPCR was performed using the StepOne Plus PCR cyclers (Applied Biosystems) by using SYBR[®] Green PCR Master Mix (Applied Biosystems) and specific oligonucleotides for interleukin-6 (IL-6), interleukin-1β (IL-1β), tumor necrosis factor-α (TNF-α), and the housekeeping β-actin (Table x). The standard PCR program used was: one denaturation cycle for 10 minutes at 95 °C followed by 40 cycles of 15 s at 95 °C and 1 minute at 60 °C. Relative gene expression of each gene was normalized to β-actin and the $2^{-\Delta\Delta C_t}$ formula was used to calculate fold-change. In the end, the experimental data were analyzed using the GraphPad Prism[®] software (version 5, GraphPad Software, San Diego, CA) to perform an *ANOVA* statistical analysis followed by the Tukey's multiple-comparison *post hoc* test. Statistical significance was set at $p < 0.05$.

Table 1. Primer sequences used for quantitative RT-qPCR in Sprague Dawley[®] rats.

Gene (Rat)	Primer sequences (5' - 3')	Gene accession number
IL-6	FW: AGAAAAGAGTTGTGCAATGGCA RV: GGCAAATTTCTGGTTATATCC	NM_012589.2
TNF-α	FW: AAATGGGCTCCCTCTCATCAGTTC RV: TCTGCTTGGTGGTTTGCTACGAC	NM_012675.3
IL-1β	FW: CACCTCTCAAGCAGAGCACAG RV: GGGTTCCATGGTGAAGTCAAC	NM_031512.2
β-actin	FW: AAGTCCCTCACCTCCCAAAA RV: AAGCAATGCTGTACCTTCCC	V01217.1

RESULTS

4. RESULTS

4.1. Computational Studies

Modern drug discovery is based on high data screening of small molecules against macromolecular disease targets, as there is high demand that molecular screening libraries contain drug-like compounds [89]. The freely accessible web resource PASS Online, designed for the prediction of the biological activity spectra of organic compounds based on their structural formulas [28], was used to evaluate the flavanones **1**, **1a-d** before *in vivo* assays. The output information of flavanones ‘potential activity as anti-inflammatory agents “*Pa*” is given in Table 2.

Table 2. Predicted Activity Anti-inflammatory Spectrum and Molinspiration[®] bioactivity score data for chemical structure flavanones **1**, **1a-d**.

DATA	FLAVANONE					Diclofenac	Indomethacin
	1	1a	1b	1c	1d		
Antiinflammatory (<i>Pa</i>)	0.66	0.72	0.61	0.74	0.62	0.79	0.71
miLog <i>P</i>	4.49	3.82	4.56	4.22	4.07	4.57	3.99
TPSA	66.76	78.92	55.77	55.77	55.77	49.33	68.54
natoms	23.23	29	24	24	24	19	25
MW	310.35	394.42	324.38	324.38	322.36	296.15	357.79
nON	4.4	6	4	4	4	3	5
nOHNH	2.2	0	1	1	1	2	1
nviolations	0	0	0	0	0	0	0
nrotb	2.2	6	3	1	1	4	4
volume	282.78	355.81	300.31	295.6	289.41	238.73	303.24
GPCR ligand	0.04	-0.05	0.02	0.31	0.19	0.14	0.24
Ion channel modulator	-0.25	-0.26	-0.27	0.06	-1.19	0.20	-0.31
Kinase inhibitor	-0.18	-0.23	-0.18	-0.29	-0.18	0.17	-0.11
Nuclear receptor ligand	0.41	0.29	0.34	0.71	0.67	0.09	0.42
Protease inhibitor	-0.03	-0.04	-0.05	0.28	0.18	-0.10	-0.11
Enzyme inhibitor	0.31	0.18	0.26	0.38	0.46	0.25	0.30

Pa: probability to be active; *P*: octanol–water partition coefficient, TPSA: Topological Polar Surface Area; natoms: number of atoms; MW: molecular weight; nON: number of N-O bonds; nOHNH: number of OH-NH bonds; nviolations: number of violations to Lipinski’s rules; nrotb: number of rotatable bonds GPCR: G protein-coupled receptors.

Molecular properties (lipophilicity, molecule size, flexibility, and so on) influence the behavior of compounds in a living organism, including bioavailability, transport properties, affinity to proteins, reactivity, and many others [90]. Accordingly, the activity of the natural **1** and derivatives flavanones **1a-d** was analyzed under Molinspiration[®] bioactivity criteria of known successful activity in the areas of GPCR ligand activity, ion channel modulation, Kinase inhibition activity, and nuclear receptor ligand activity. Results are shown in Table 2 by means of numerical assignment.

4.2. Analytical Validation

The linearity of the analytical method is the capability over a range of data to obtain proportional results. The applied HPLC method for the flavanone's quantification (**1**, **1a**, **1b**, **1c**, and **1d**) showed satisfactory linearity in the tested concentrations. In order to have a better mathematical analysis, the linearity was evaluated in two concentration ranges: from 200 to 12.5 µg/mL and from 12.5 to 1.56 µg/mL. Two linear calibration curves were fitted for each flavanone. The R² value for each analyte was found above 0.999 for all studied flavanones, indicating the linear relationship between the analyte concentration and the peak area. No statistical differences were found ($p > 0.05$) after the *ANOVA* test of the calibration curves of each flavanone **1**, **1a**, **1b**, **1c**, and **1d** with p values for each two levels of 0.12 and 0.08, 0.93 and 0.08, 0.38 and 0.47, 0.63 and 0.56, and 0.53 and 0.46, respectively (see Table 3).

LODs and LOQs for all the investigated flavanones were calculated using the response standard deviation and the calibration curve slope of 12.5 to 1.56 µg/mL for each flavanone, described in Materials and Methods Section 3.6.3. The values of LODs and LOQs for each flavanone are listed in Table 3. These results indicate that the method is sensitive enough for flavanones determination in the range of 1.56 to 200 µg/mL.

Precision and accuracy values were obtained from sample analyses of the 1.56, 12.5, and 200 µg/mL flavanones concentrations (**1**, **1a**, **1b**, **1c**, and **1d**). The inter-day precision and accuracy were calculated after analyzing the samples on six different days. The results are reported in Table 3. Both parameters were lower than the 15 % limit value in EMA (European Medicines Agency) guidelines. These results suggest that the proposed method

has satisfactory accuracy and precision. Repeatability studies of the instrumental system showed RSD % not greater than 0.6% for all flavanones.

Table 3. Linearity (expressed in R^2 and p with two ranges, one by row), Precision, Accuracy (calculated at maximum, medium, and minimum concentration values), and Repeatability of the HPLC Method for the determination of flavanones.

COMPOUND	LINEARITY		LOD	LOQ	ACCURACY	PRECISION	R.I.S ¹
	R ²	P value			RE (%)	RSD (%)	RSD (%)
	200-12,5 (µg/mL)		Mean (µg /mL)		200 (µg /mL)		200 (µg /mL)
	12,5-1,56 (µg /mL)		SD (µg /mL)		12,5 (µg /mL)		
					1,56 (µg /mL)		
1	0.9998	0.12	0.51	1.53	-0.23	0.20	0.36
	0.9991	0.08	0.13	0.38	0.59	0.24	
					11.02	2.63	
1a	0.9997	0.93	0.28	0.84	-0.09	0.09	0.54
	0.9997	0.08	0.10	0.29	0.63	0.21	
					1.48	0.81	
1b	0.9998	0.38	0.49	1.48	0.46	0.27	0.43
	0.9990	0.47	0.12	0.36	-0.13	0.36	
					-7.91	2.92	
1c	0.9999	0.63	0.48	1.45	-0.19	0.29	0.37
	0.9996	0.56	0.43	1.30	0.38	0.07	
					4.15	1.12	
1d	0.9999	0.53	0.30	0.91	-0.01	0.21	0.32
	0.9997	0.46	0.08	0.24	0.17	0.27	
					3.74	0.42	

¹ R.I.S = REPEATABILITY OF INSTRUMENTAL SYSTEM

4.3. *Ex Vivo* Human Skin Permeation (Intrinsic permeation)

The analytical methodology was implemented for the flavanone's quantitation (**1**, **1a**, **1b**, **1c**, and **1d**) in skin permeation studies. In order to show the specificity, 300 µL of the flavanones at 200 µg/mL concentration was permeated into human skin using Franz cells. The amount of each flavanone normalized by the surface (Q) in the receptor compartment

during percutaneous permeation experiments ($n = 3$) is indicated in Table 4. Percentages of permeation were calculated, accounting for the experimental flavanone content of each assay. At the end of each experiment, skin samples were removed from the diffusion cell, flavanones amount retained (Q_{ret}) were quantified as previously described and expressed in micrograms of prenylated flavanone per grams of skin and per area unit ($\mu\text{g}/\text{g}_{\text{skin}}\cdot\text{cm}^2$) in Table 4. As shown in Table 4, the prenylated flavanone **1** is the one which most permeates, followed by **1d** and **1c**. In the case of **1a** and **1b**, Q was detectable but not quantifiable because their values were below LOQ determinate before (see Table 3). On the contrary, **1a** and **1b** were found retained in the skin in a greater amount, so we can infer that it is possible that these molecules have greater interactions with the different skin components due to their physicochemical characteristics. Therefore, they have prevented permeation as **1**, **1c**, and **1d** did too.

Table 4. Results of permeation studies expressed by mean and SD ($n = 3$).

COMPOUND	24 h PERMEATED AMOUNT	DEGREE OF PERMEATION	RECOVERY	SKIN RETENTION
	Q ($\mu\text{g}/\text{cm}^2$)	(%)	(%)	Q_{ret} ($\mu\text{g}/\text{g}\cdot\text{cm}^2$)
1	1.29 ± 0.12	2.15	46.20 ± 6.46	50.22 ± 7.51
1a	NQ	NQ	0.38 ± 0.05	321.52 ± 45.23
1b	NQ	NQ	3.43 ± 0.5	381.75 ± 57.26
1c	0.75 ± 0.07	1.26	NQ	NQ
1d	0.91 ± 0.08	1.52	38.1 ± 5.23	116.14 ± 17.24

¹ NQ = non quantifiable; value below LOQ

The chromatograms showed the absence of interference of any other peak corresponding to each flavanone (Figure 19: 1a, 1b; Aa, Ab; Ba, Bb; Ca, Cb; Da, Db). Furthermore, no interference from the human skin components assays were observed during the analysis in the *ex vivo* permeation studies (Figure 19: 1c, 1d; Ac, Ad; Bc, Bd; Cc, Cd; Dc, Dd).

Flavanone extraction was done, as described in Section 3.7.1. Recovery was calculated comparing the corresponding extraction result with the amount of flavanone bound to the skin. The results were reported as the mean value of the percentage between the amount of flavanone in each sample and the weight of the skin sample (see in Table 4). The

aforementioned results show the real quantity for each prenylated flavanone that can be recovered using the extraction method previously described. Thus, the exact quantity of flavanone retained can be known, and this quantity is responsible for the exercising of the biological effect.

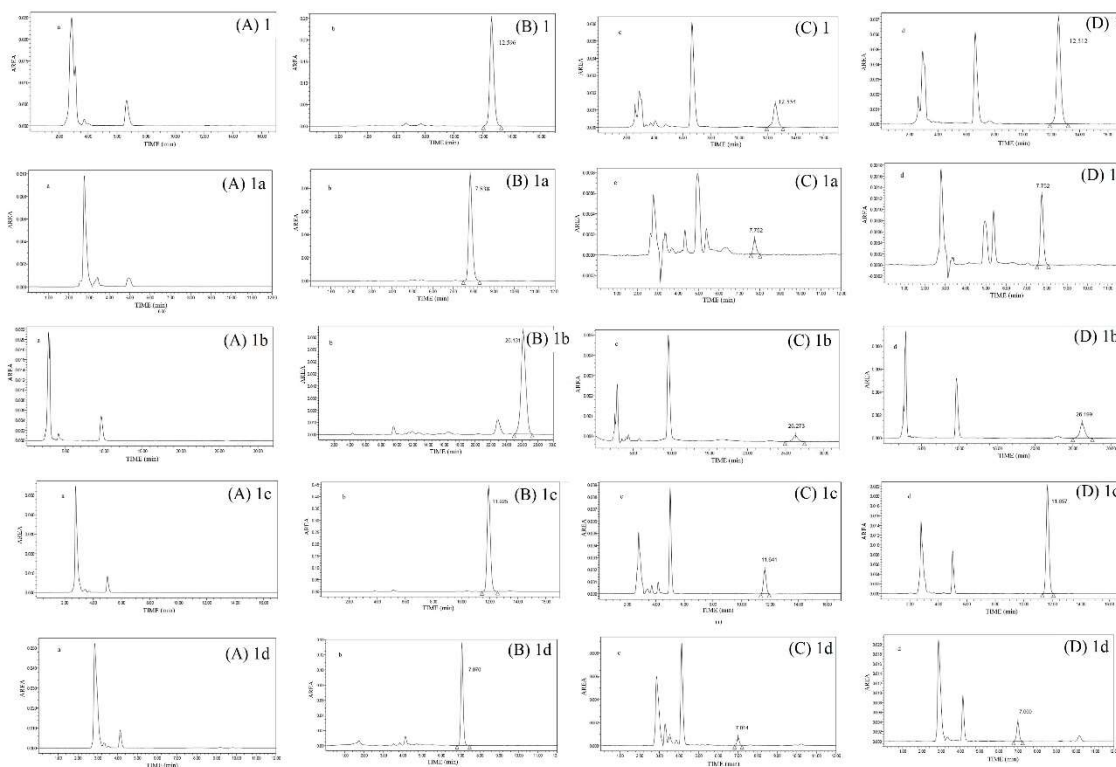


Figure 19. HPLC chromatograms of prenylated flavanones **1**, **1a–1d**. (A) correspond to: Blank sample (ethanol: water, 70:30) permeated at chromatographic conditions of each prenylated flavanone; (B) correspond to prenylated flavanone standard; (C) correspond to prenylated flavanone from receptor compartment Franz diffusion cells; and, (D) correspond to prenylated flavanone extracted from human skin after permeation study.

4.4. FF Characterization

Flavanones formulations FF1, FF1a, FF1b, FF1c and FF1d and nFF were qualitatively and quantitatively assayed in terms of appearance, droplet and particle size. The FF obtained were isotropic, transparent and slightly viscous. TEM imaging is the most powerful and accurate technique to determine a sample’s morphology, purity and particle size distribution [85]. As shown in Figure 20, the droplets were distributed uniformly in FF1a, FF1b and FF1c.

In addition, the droplets were spherical and no aggregation process was observed. The mean size from all the formulations is listed in Table 5. The formulation without flavanone **nFF** exhibited the size of 155.31 ± 27.64 nm and **FF1c** showed the least droplet, sized 12.56 ± 1.77 nm.

Table 5. Droplet size of FF formulations. Values are reported as mean \pm SD ($n = 3$).

FF	DROPLET SIZE
nFF	155.31 ± 27.64 nm
FF1	218.40 ± 89.71 nm
FF1a	38.28 ± 4.50 nm
FF1b	305.77 ± 11.18 nm
FF1c	12.56 ± 1.77 nm
FF1d	370.64 ± 142.09 nm

The viscosity measurements are used to determine if the material is characterized by linear-viscous (Newtonian) behavior (shear-stress exponent $n = 1$) in the investigated shear rate range or if it shows power-law behavior ($n \neq 1$) [27]. The potential dependence of the FF viscosity on the shear rate is shown in Figure 21. The viscosity graph (η) for all FF is a line, thus the behavior was Newtonian. Therefore, the viscosity values at 100 s^{-1} were 80.01 ± 0.04 , 80.64 ± 0.04 , 81.29 ± 0.05 , 82.77 ± 0.03 , 85.2 ± 0.03 and 86.83 ± 0.03 mPa·s for **nFF**, **FF1**, **FF1a**, **FF1b**, **FF1c** and **FF1d**, respectively, at t_0 .

All the formulations were in accordance with the two-site binding hyperbola model (see Figure 22 and Table 6). Extensibility values increases with loading weight. These results are in accordance with that obtained in the rheological characterization of FF. The **nFF** and **FF1** were the most extensible with $B_{\max 1}$ of 16.39 ± 4.05 and 17.84 ± 14.37 mm², respectively. Otherwise, the least extensible were **FF1a**, **FF1b**, **FF1c** and **FF1d** with $B_{\max 1}$ of 13.11 ± 3.08 , 9.61 ± 2.65 , 10.79 ± 1.19 and 3.19 ± 2.15 mm², respectively. The parametric analysis of the t -test showed no significant influence of the FF composition FF except in **nFF** with **FF1d**.

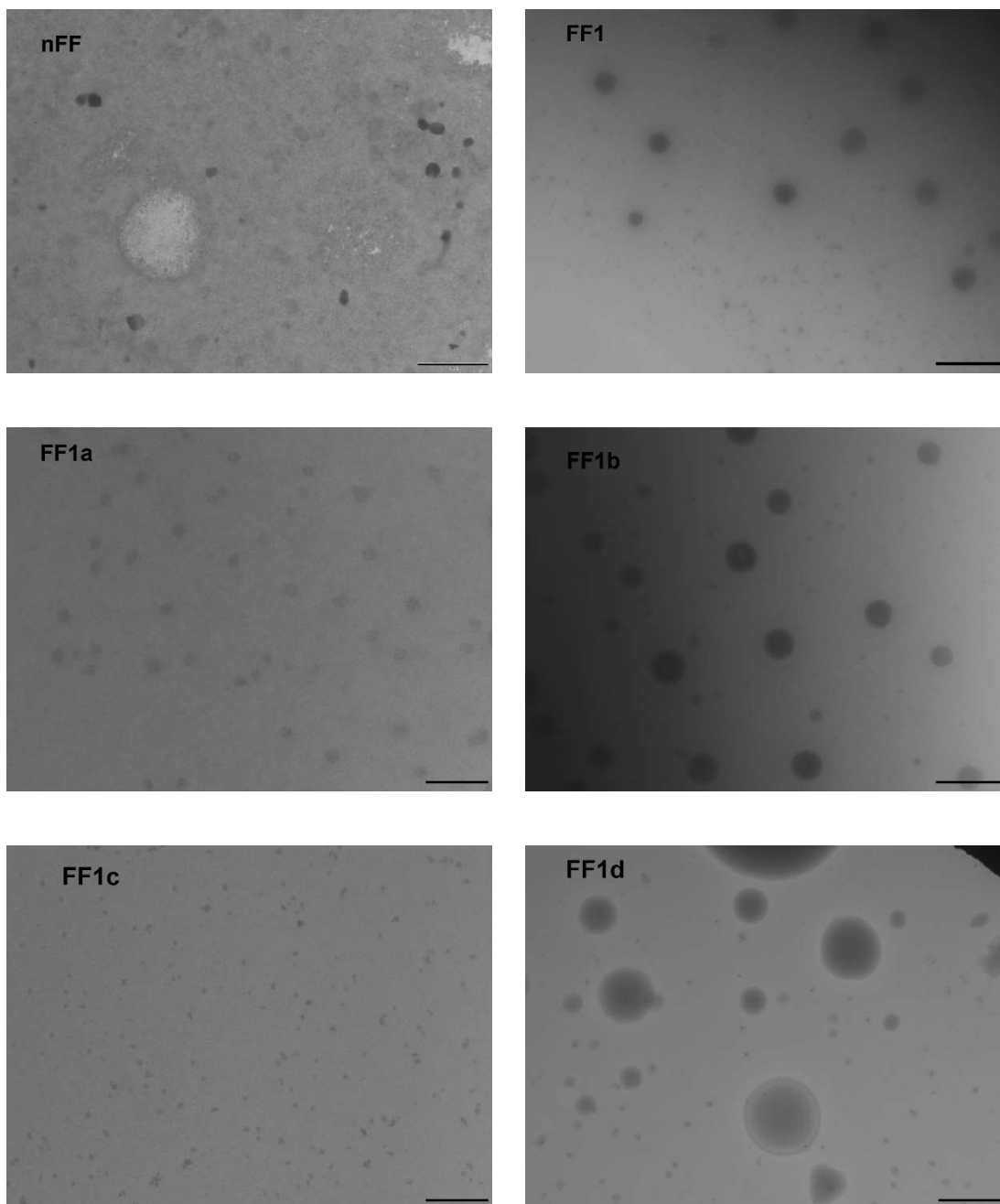


Figure 20. Transmission electron microscopy images of the flavanones formulations. Bar length 200 nm for FF1a and FF1c; 1 μm for nFF, FF1, FF1b and FF1d.

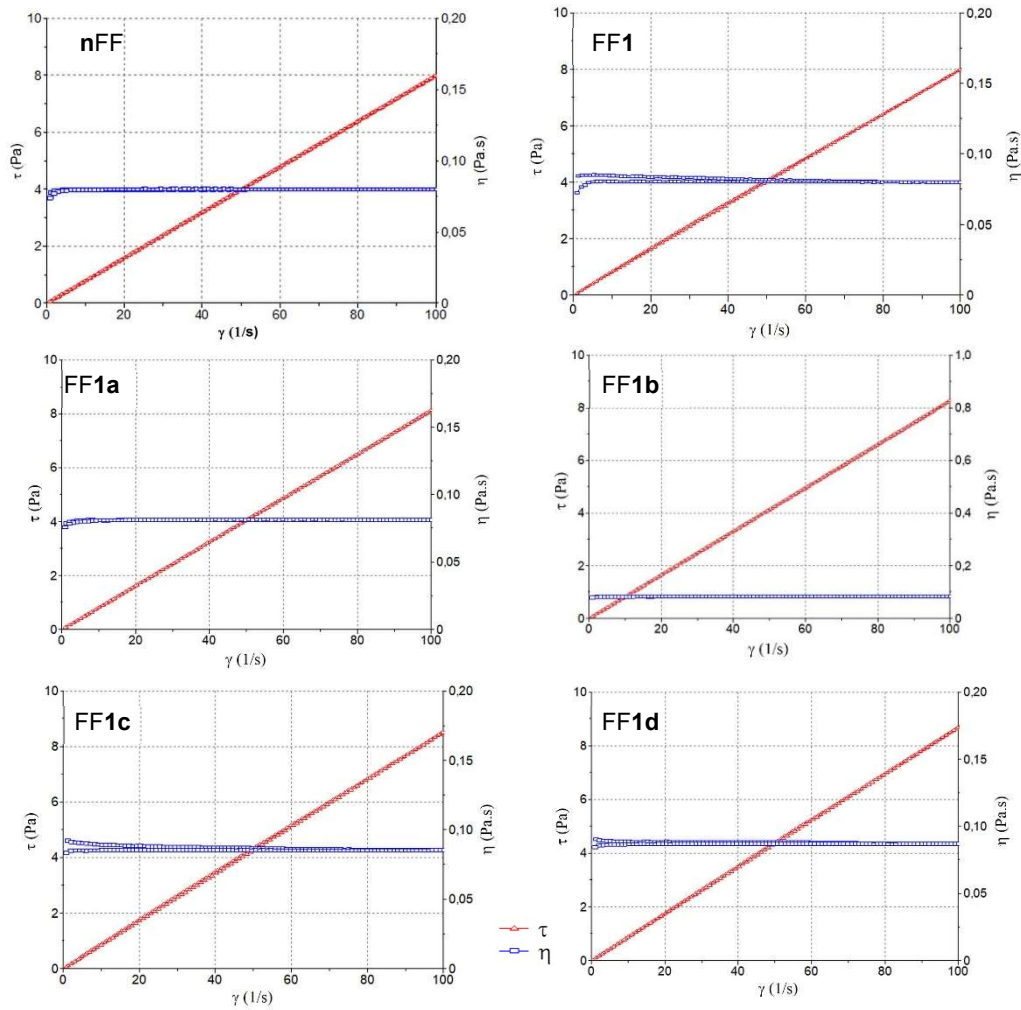


Figure 21. Rheograms of the tested formulations: **nFF**, **FF1**, **FF1a**, **FF1b**, **FF1c** and **FF1d**. The flow curve represents in red the shear stress (Pa) versus shear rate (s^{-1}), and the viscosity curve represents viscosity ($\text{Pa}\cdot\text{s}$) versus shear rate (s^{-1}), which is in blue.

Table 6. Parameters of two-site binding hyperbola model (Mean \pm Std. Error).

	nFF	FF1	FF1a	FF1b	FF1c	FF1d
B_{max1}	16.39 \pm 4.05	17.84 \pm 14.37	13.11 \pm 3.08	9.61 \pm 2.65	10.79 \pm 1.19	3.19 \pm 2.15
K_{D1}	0.92 \pm 0.45	1.95 \pm 1.87	0.45 \pm 0.27	0.36 \pm 0.24	0.50 \pm 0.15	0.12 \pm 0.26
B_{max2}	19.78 \pm 3.36	18.44 \pm 13.11	15.50 \pm 2.71	11.23 \pm 2.44	11.63 \pm 0.98	17.60 \pm 1.96
K_{D2}	23.25 \pm 12.06	19.11 \pm 23.34	14.23 \pm 6.84	8.78 \pm 4.05	23.38 \pm 7.45	5.49 \pm 1.67
r²	0.998	0.996	0.997	0.998	0.999	0.997

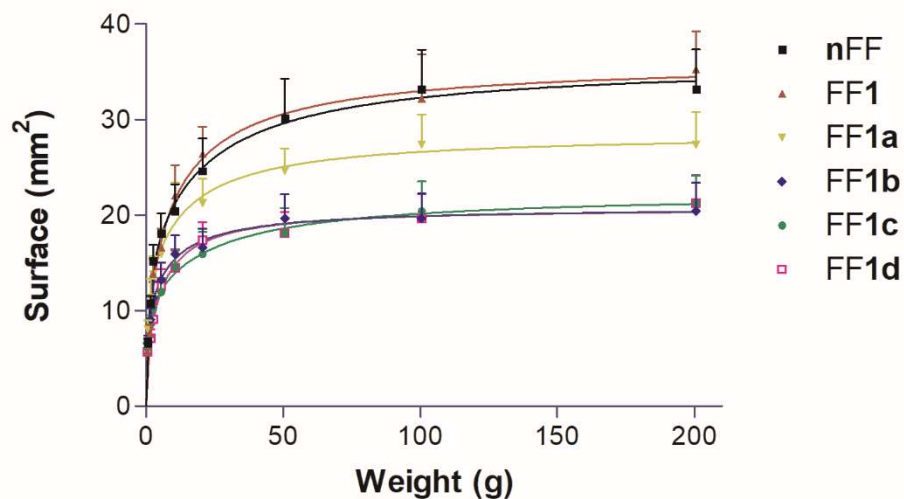


Figure 22. Extensibility of nFF, FF1, FF1a, FF1b, FF1c and FF1d (Mean \pm SD).

Flavanone formulations were considered stable if the physical appearance did not change. As seen in, Figure 23, there was no sign of creaming action, phase separation or sedimentation even after 180 days of storage.

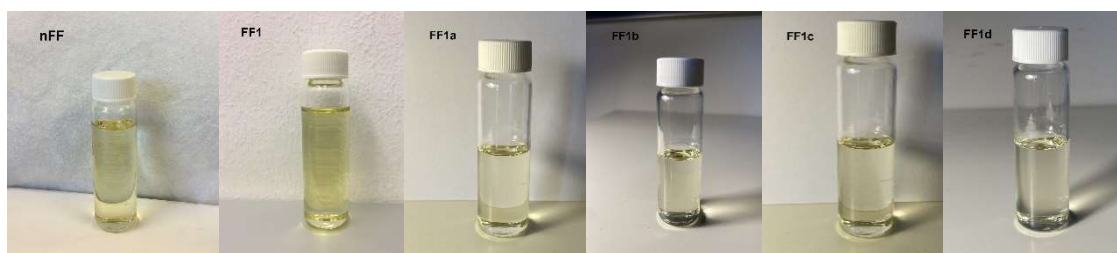


Figure 23. Physical appearance of flavanone formulations obtained with Labrasol[®], Labrafac lipophile[®], Plurol Oleique[®] and Propylene glycol. Flavanone ratio (w/w): 0.5 % after 180 storage days.

Additionally, as mentioned in Table 7, there were no significant changes in pH values of FF at 180 storage days except in FF1a and FF1d where the pH were a little bit lower. Therefore, the data indicated that the examined FF were physically stable. Moreover, the pH of FF after 180 days slightly decreased, being these values within the physiological range accepted for dermal and transdermal preparations (4.5–7) [91].

Table 7. FF pH values (mean \pm SD) at basal time and after storage at 4 °C for a period of 180 days.

Storage Time (days)	pH values (mean \pm SD)					
	nFF	FF1	FF1a	FF1b	FF1c	FF1d
0	6.95 \pm 0.04	7.11 \pm 0.03	7.25 \pm 0.02	7.12 \pm 0.02	6.96 \pm 0.03	7.15 \pm 0.03
180	6.93 \pm 0.03	7.09 \pm 0.03	6.99 \pm 0.02	7.09 \pm 0.03	6.95 \pm 0.02	6.97 \pm 0.04

On the other hand, the results on chemical degradation of flavanones during storage showed that in all the FF except FF1a the flavanone content remained above 90 % of the original amount of flavanone (see Table 8) after 60 storage days. While after 180 storage days, only FF1, FF1b and FF1d showed the same stability tendency with percentages that could be considered stable.

Table 8. Chemical Stability Study of flavanone formulations (FF) after 180 days of storage at 4 °C. (Mean \pm SD).

SAMPLE	FLAVANONE REMAINED (%)			
	0 DAYS	30 DAYS	60 DAYS	180 DAYS
FF1	99.10 \pm 0.80	95.14 \pm 0.71	94.84 \pm 1.10	94.12 \pm 1.89
FF1a	98.90 \pm 1.22	71.25 \pm 1.45	60.18 \pm 1.01	57.78 \pm 1.97
FF1b	99.32 \pm 0.51	98.43 \pm 0.70	96.31 \pm 0.99	95.50 \pm 1.35
FF1c	98.84 \pm 1.42	92.67 \pm 1.20	95.49 \pm 0.89	60.02 \pm 1.40
FF1d	99.18 \pm 1.00	95.46 \pm 0.53	97.14 \pm 1.21	88.75 \pm 1.30

4.5. *In vitro* FF Studies

Figure 24 shows the different release profiles of FF. The release process can be described in two phases. In the cases of FF1, FF1a, FF1b and FF1d, the initial phase displays a rush release, followed by a slower sustained release phase of the flavanone loaded FF. The cumulative release curve of FF1c presents a sigmoidal profile, which is in agreement with the fact that the experiments were developed with a finite dose and thus the donor compartment reaches a stage of flavanone depletion. The mathematical modeling to describe drug release profiles offers several advantages. It allows the simplifying of the process elucidating the drug release mechanisms and it can be used to guide formulation development efforts [55,92]. Besides, the release model is useful for assessing the excipients effect on the drug release and for simulating different situations not assayed. The modeling is also used in quality control studies because the drug release parameters can detect changes in the formulation over time [93].

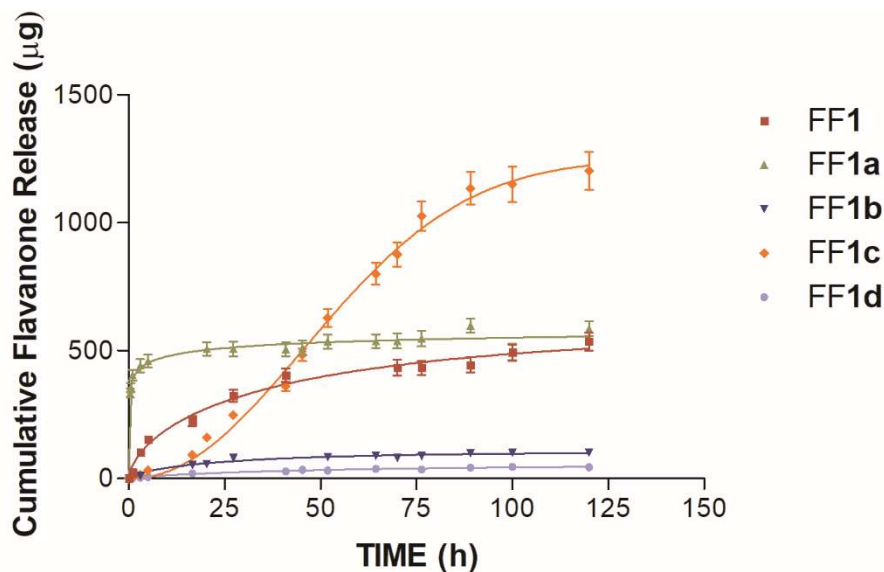


Figure 24. *In vitro* flavanone release from formulations FF1, FF1a, FF1b, FF1c and FF1d. The cumulative amount released was plotted against time. Data represent mean \pm SD ($n = 3$).

Data obtained from the *in vitro* release study were fitted to different functions. The correlation coefficient (r^2) of each mathematical model was calculated (see Table 9).

Table 9. Mean parameter obtained after fitting the release of flavanones **1**, **1a-1d** from FF data to different kinetic models.

MODEL	PARAMETER	FF1	FF1a	FF1b	FF1c	FF1d
FIRST ORDER	r^2	0.989	0.975	0.927	Nf	0.974
HYPERBOLA	r^2	0.992	0.988	0.927	0.990	0.977
WEIBULL	r^2	0.998	0.994	0.929	0.999	0.979
KORMEYER-PEPPAS	r^2	0.994	0.992	0.921	0.990	0.979

The highest r^2 value for the entire FF was that of the Weibull function. The β data (a dimensionless shape parameter from the Weibull function) allow the elucidation of drug release mechanisms. A combined mechanism (Fickian diffusion and swelling controlled release) is associated to the range $0.75 < \beta < 1$. In other cases, for values of β higher than 1, the drug transport follows a complex release mechanism [94]. From the Weibull function modeling data for all FF, the FF1c β value was 2.09 ± 0.21 , indicating a complex mechanism. In contrast, for the rest of FF with a β value between 0.19–0.88 it reflects a

combined mechanism. In the case of the flavanone amount released at time t (Q), FF1c was greater with $1249 \pm 64.59 \mu\text{g}$ followed by FF1, FF1a, FF1b and, FF1d $592.0 \pm 162.43 \mu\text{g}$, $606.7 \pm 159.21 \mu\text{g}$, $98.86 \pm 9.02 \mu\text{g}$ and $53.46 \pm 13.56 \mu\text{g}$, respectively (see Table 10).

Table 10. Equation parameters for the kinetic release of flavanones from FF.

	FF1	FF1a	FF1b	FF1c	FF1d
Q (μg)	592.0 ± 162.43	606.7 ± 159.21	98.04 ± 9.02 ^{1, a}	1249 ± 64.59 ^{1, a, b, d}	53.46 ± 13.56 ^{1, a}
td (h)	42.46 ± 36.37	0.94 ± 2.30	21.74 ± 6.30	62.39 ± 3.66 ^a	51.70 ± 22.63 ^a
β	0.64 ± 0.17	0.19 ± 0.12	0.88 ± 0.30	2.09 ± 0.21	0.78 ± 0.19

A parametric Turkey test showed significant statistical differences ($p < 0.05$). Therefore, there were statistical differences between the FF except in the case of FF1b with FF1d and, FF1 with FF1a, as can be appreciated visually in the graphic (Figure 25) in the same way. Correspondingly, the td (time required to 63.2 % of the maximum amount release) for the FF was 42.46 ± 36.37 h, 21.74 ± 6.30 h, 62.39 ± 3.66 and 51.70 ± 22.63 h for FF1, FF1b, FF1c and FF1d, respectively. If we turn to FF1a, the release revealed an even faster rush effect; td was only 0.94 ± 2.30 h (Table 10) and showed significant difference ($p < 0.05$) with FF1c and FF1d. The differences could be explained by the occurrence of substances in the FF that would act as promoters or inhibitors.

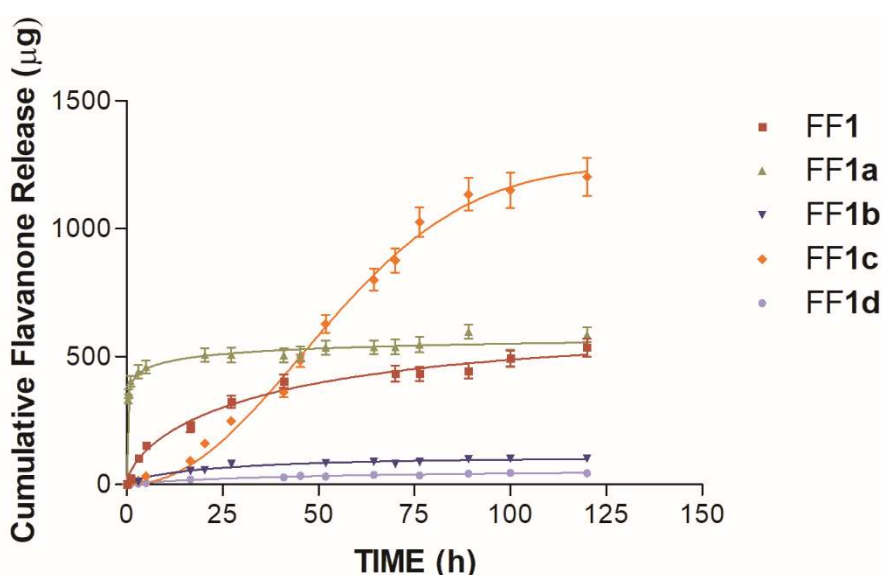


Figure 25. *In vitro* flavanones release from formulations FF1, FF1a, FF1b, FF1c and FF1d. The cumulative amount released was plotted against time. Data represent mean \pm SD ($n = 3$).

4.6. *Ex vivo* FF Studies

The permeation studies parameters of the studied flavanones are depicted in Table 11 as median values as the drug permeation follows a long-normal distribution more than a normal one (Gaussian) [94]. FF1a achieved the maximum flux with $105.83 \mu\text{g}/\text{h}/\text{cm}^2$, followed by FF1b, FF1c and FF1d with fluxes of 1.26, 0.85 and $0.10 \mu\text{g}/\text{h}/\text{cm}^2$, respectively. The T_l parameter indicates the time required for reaching the steady state and that this time is inversely proportional to the drug's diffusivity through the skin. Therefore, the results suggested that the FF1a had a higher diffusion with the lowest T_l of 1.9 h and FF1b had a lower diffusion with the highest T_l with 21.28 h. Similarly, FF1a exhibited the highest permeability K_p coefficient of $211.66 \times 10^{-4} \text{ cm}/\text{h}$. One of the factors, which controls the drug permeability between the formulation and the skin, is the partition coefficient (P_l). It is directly proportional to the distribution of the drug in the skin. Thus, once again, FF1a was shown to have the highest distribution of flavanone with a P_l of $14.90 \times 10^{-2} \text{ cm}$. In the case of the diffusion parameter P_2 , the results had the same tendency; $8.77 \text{ h}^{-1} \times 10^{-2} (1/\text{h})$ for FF1a was the maximum, followed by FF1d with $2.11 \times 10^{-2} (1/\text{h})$; FF1c with $0.99 \times 10^{-2} (1/\text{h})$ and finally, FF1b with $0.82 \times 10^{-2} (1/\text{h})$. The total flavanone that crosses the skin after 29 h of application corresponds to the Q_p parameter. The flavanone that could cross in the highest quantity to the receptor chamber was FF1a with $1082.85 \mu\text{g}$, followed by $82.56 \mu\text{g}$ for FF1, $7.17 \mu\text{g}$ for FF1b, $2.94 \mu\text{g}$ for FF1c and, $1.44 \mu\text{g}$ for FF1d turned out to be the one that crossed in the lowest quantity. In the same way, the highest retained flavanone amount (Q_r) was present in FF1a with $2277.24 \text{ g}/\text{g}_{\text{skin}}/\text{cm}^2$. In contrast to FF1d, in which the retained flavanone in the skin after permeation was smaller than in the other ones. The permeation parameters J , T_l , P_l , P_2 , K_p , Q_p and Q_r were compared by the application of the nonparametric statistical Mann–Whitney U test. This test compares the distribution of two unmatched groups. Significant

statistical differences ($p < 0.05$) in J , P_1 , K_p and Q_p parameters were found among all FF, except for FF1b with FF1c. The assayed FF formulations did not present significant statistical differences ($p > 0.05$) in T_l and P_2 parameters except for FF1b with FF1d and FF1c with FF1d. Additionally, the test showed significant statistical differences ($p < 0.05$) between FF assayed except in the case of FF1c and FF1d.

Table 11. Median (maximum-minimum) values of flux (J), lag time (T_l), P_1 and P_2 parameters, permeability coefficient (K_p), retained amount (Q_r) and permeated amount at 29 hours (Q_p) of flavanones **1**, **1a**, **1b**, **1c** and **1d** from FF in human skin.

	FF1*	FF1a	FF1b	FF1c	FF1d
$J/\text{sur}(\mu\text{g}/\text{h}/\text{cm}^2)$	0.81 (0.82 - 0.79)	105.828 (186.563 - 65.391)	1.258 ^a (1.382 - 1.135)	0.851 ^a (1.538 - 0.116)	0.101 ^{a, b, c} (0.142 - 0.025)
T_l (h)	7.95 (7.99 - 7.88)	1.9 (17.28 - 0.60)	21.28 (25.84 - 16.71)	16.91 (19.41 - 8.9)	7.89 ^{b, c} (12.34 - 7.06)
$P_2 \times 10^{-2}$ (1/h)	0.208 (0.209 - 0.203)	8.77 (27.95 - 0.96)	0.82 (1.00 - 0.64)	0.99 (1.87 - 0.86)	2.11 ^{b, c} (2.36 - 1.35)
$P_1 \times 10^{-2}$ (cm)	0.786 (0.787 - 0.757)	14.90 (386.9 - 7.6)	3.14 ^a (3.52 - 2.77)	1.73 ^a (3.58 - 0.12)	0.01 ^{a, b, c} (0.21 - 0.02)
$K_p \times 10^{-4}$ (cm/h)	1.60 (1.61 - 1.58)	211.66 (373.1 - 130.8)	2.52 ^a (2.76 - 2.27)	1.70 ^a (3.08 - 0.23)	0.202 ^{a, b, c} (0.28 - 0.05)
Q_r (g/gskin/cm ²)	0.0215 (0.243 - 0.013)	2277.24 (3735.5 - 1080.57)	1.10 ^a (1.19 - 1.01)	0.23 ^{a, b} (1.05 - 0.17)	0.19 ^{a, b} (0,26 - 0.09)
Q_p (μg)	82.56 (85.93 - 74.31)	1082.85 (1819.97 - 502.39)	7.17 ^a (11.52 - 2.83)	2.94 ^a (7.35 - 1.55)	1.44 ^{a, b, c} (1.57 - 0.05)

sur = surface.

^a Differences with FF1a

^b Differences with FF1b

^c Differences with FF1c

^d Differences with FF1d.

*Data obtained from Domínguez *et al* [55].*

4.7. In vivo FF and FS Studies

4.7.1. Model of mice ear inflammation induced with TPA

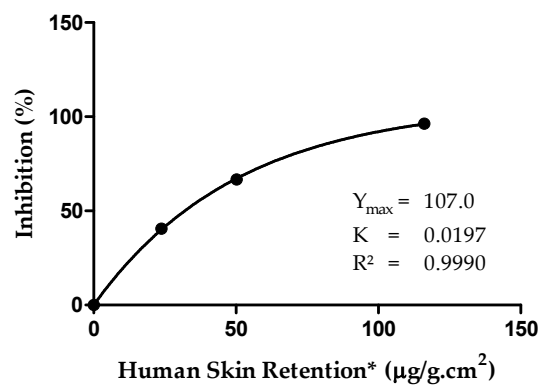
The results of the *in vivo* anti-inflammatory effects of the flavanones using the TPA induced edema model are depicted in Figure 26.A as mean values \pm standard deviation

(SD). The flavanone solutions showed good results in the anti-inflammatory efficacy studies. The flavanone natural **1** revealed a significant reduction of the dermal edema, with a % inhibition of 66.67 ± 1.55 . However, only the flavanone derivative **1d** showed an inhibition percentage (96.27 ± 1.93) higher than the indomethacin value (91.35 ± 0.47).

Solutions	% Inhibition	Human Skin Retention* ($\mu\text{g}/\text{g}\cdot\text{cm}^2$)
FS1	66.67 ± 1.55	50.22 ± 7.51
FS1a	10.27 ± 0.21	321.52 ± 45.23
FS1b	25.69 ± 0.52	381.75 ± 57.26
FS1c	40.61 ± 0.81	23.78 ± 5.46
FS1d	96.27 ± 1.93	116.14 ± 17.24
Indomethacin	91.35 ± 0.47	ND

* Results of the permeation studies expressed by mean and SD ($n = 3$) reported (Table 4) [78].
ND = Not Determined

(A)



(B)

Figure 26. (A) *In vivo* anti-inflammatory efficacy after TPA (12-O-tetradecanoylphorbol 13-acetate) induced mouse edema. Mean \pm SD ($n = 3$). (B) Correlated Function Inhibition vs Human Skin Retention.

The solutions of the flavanone natural **1** and the derivatives flavanones **1a-1d** were evaluated in *ex vivo* diffusional studies in Franz cells using human skin (Table 4) [78]. This was used to evaluate their intrinsic permeation and human skin retention (Figure 26.A). The skin retention results of this study were correlated with the inhibition percentage of mouse edema induced by TPA. The function that best fitted to FS1, FS1c and FS1d was the first order function with a correlation coefficient (R^2) equal to 1 (Figure 26.B).

4.7.2. *In vivo* rat Model and Anti-inflammatory Response after FS and FF treatment induced by AA

The edema reduction, associated with the FS1, FS1a- FS1d treatment in an *in vivo* ear rat model of inflammation induced by AA was evaluated by the difference in thickness compared to the initial ear measurements. The nFS and a solution of the drug reference

(diclofenac sodic) were also evaluated. The results are depicted in Figure 27.A. The FS reduced the ear thickness more than the RS. In the same way, the treatment with FS1 and nFS produced the same effect in the edema ear. Therefore, the flavanone **1** had not contributed to any additional anti-inflammatory effect compared with the effect produced by the excipients derivatives. Moreover, the FS1a with the FS1c presented almost the same edema reduction. On the other hand, it was worthy of mention that the FS1b displayed the highest efficacy since it reduced the thickness of the rat ears after 20 minutes of their application. It is important to point out that the ethanol per se can produce the effect of constriction and dehydration, which may contribute to the anti-inflammatory action.

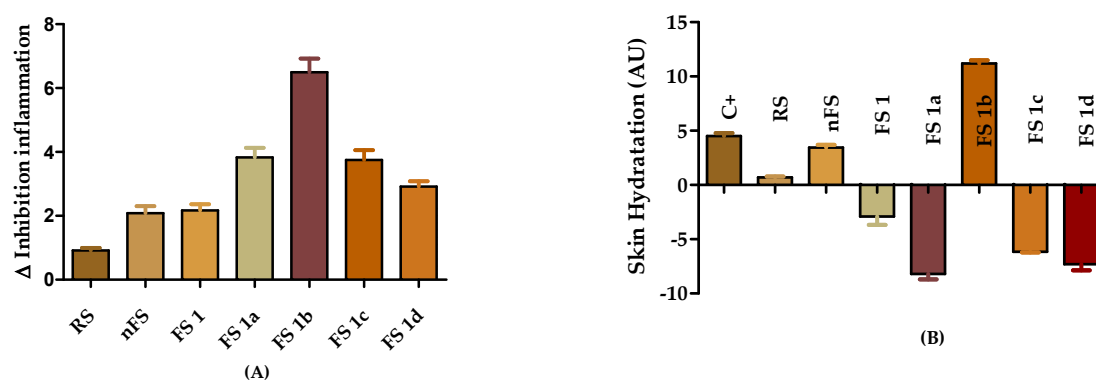


Figure 27. (A) *In vivo* rat model anti-inflammatory response after FS treatment in AA-induced edema model as shown in the increment or decrement of thickness with respect to initial conditions. (B) *In vivo* skin hydration after the application of FS treatments in AA-induced rat ear edema as the difference in hydration compared to initial conditions. Results are expressed as Mean \pm SD ($n = 5$). C+ = positive control, RS= reference drug solution, nFS = ethanol: water, FS = flavanone solution (**1**, **1a** – **1d**).

The skin hydration data may also reveal the importance of the treatment with FS. In this regard, the skin hydration of rat ears was measured, and the results are shown in Figure 27.B as the difference in stratum corneum hydration (SCH) after the solution treatment on swelled ears and the basal SCH conditions as arbitrary units (AU). It was found that the hydration of the skin changed with the application of all flavanone solutions. All of them reduced the skin hydration except FS1b, which increased the initial hydration value.

On the other hand, the results of the edema reduction of FF flavanone treatment in an *in vivo* ear rat model of inflammation induced by AA are set out in Figure 28. As can be seen, the commercial gel of diclofenac sodic (m) reduced the ear thickness compared with the positive control (C+), and so did FF1a. There were no statistical differences between them. On the contrary, the treatment with nFF did not present significant anti-inflammation activity, since it yielded a result comparable with that obtained with C+. On the other hand, it was interesting that the FF1d had a higher efficacy and was followed by FF1b, FF1c and FF1, since they reduced the thickness of the rat ears after 20 min of their application. All of them resulted in statistically significant differences to the positive control, commercial gel of diclofenac and nFF.

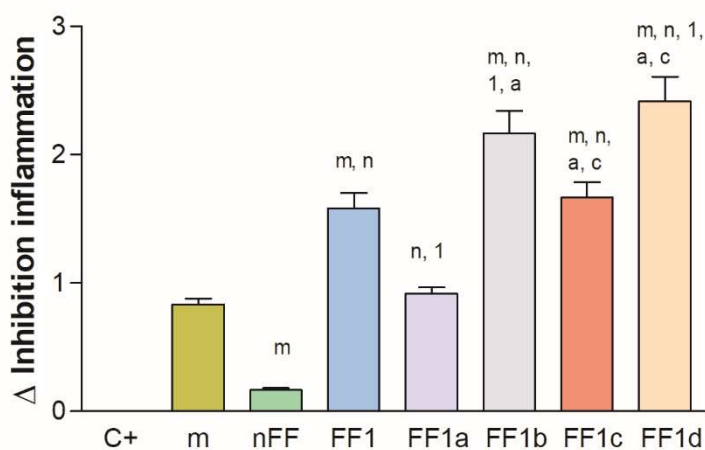


Figure 28. *In vivo* anti-inflammatory efficacy after FF treatment in AA-induced rat ear edema model as the increment of inhibition inflammation respect to positive control (C+). Results are expressed as Mean \pm SD (n = 5). Statistically significant differences $p < 0.05$ regarding ⁺C+, ^mCommercial Gel of diclofenac sodic, ⁿnFF, ¹FF1, ^aFF1a, ^bFF1b, ^cFF1c and ^dFF1d ANOVA Tukey's multiple comparison test.

The skin inflammation biomechanical properties may also reveal the importance of the treatment with FF. To exam this, the skin hydration of rat ears was measured and the results are shown in Figure 29 as the difference in SCH after the formulation treatment on swollen ears and the basal SCH conditions as arbitrary units. The SCH values did not present any change during the study in nontreated skin (negative control) and commercial gel of diclofenac sodic (m). In contrast, as shown in Figure 29, the hydration of the skin changed with the application of all FF. Even the nFF increased the SCH value. No

statistically significant differences were found when the FF1c and FF1d values were compared.

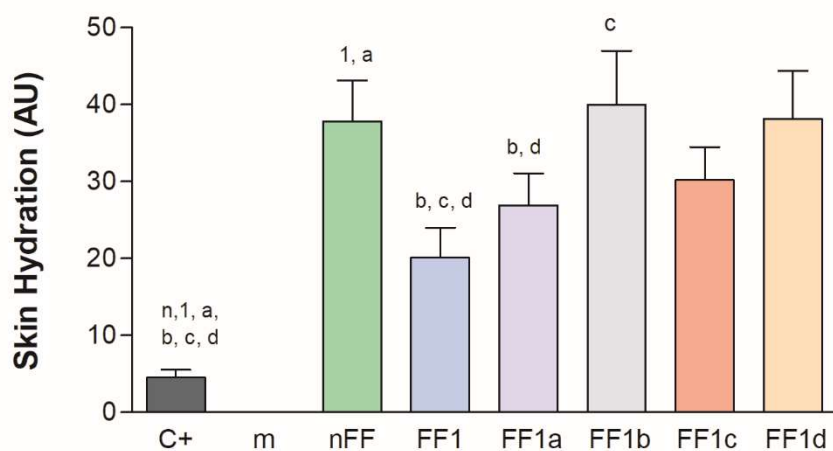


Figure 29. *In vivo* skin hydration after application of FF in AA-induced rat ear edema as the difference in hydration compared to initial conditions. Results are expressed as mean \pm SD, $n = 5$. Statistically significant differences $p < 0.05$ regarding ^{+C+}, ^mCommercial Gel, ⁿnFF, ¹FF1, ^aFF1a, ^bFF1b, ^cFF1c and ^dFF1d ANOVA Tukey's multiple comparison test.

4.8. Histological Analysis

Histological analysis of ear sections was also carried out for the assessment of the anti-inflammatory effect of the FS (Figure 30). Ears treated with AA (Figure 30.B) showed a mild inflammation characterized by edema, increased epidermal thickness, and the infiltration of polymorphonuclear (PMN) leukocytes. Histological analysis of the ear of FS-treated animals confirmed the reduction of edema and stratum corneum swelling (Figure 30.E-I).

Topical administration of the reference drug slightly decreased these inflammatory indicators. The effect of the solutions diluent (EtOH: H₂O) was also assayed in order to observe its effect on inflammation, and it showed some reduction of the edema (Figure 30.C). In addition, FS1b (Figure 30.G) was the best solution in reducing the inflammation induced by AA, showing better results than the reference drug (Figure 30.D). Another matter is that FS1 and FS1a showed less edema, although FS1 showed greater presence

of PMN. Furthermore, FS1c and FS1d were also able to reduce the edema but to a lower degree than FS1 and FS1a.

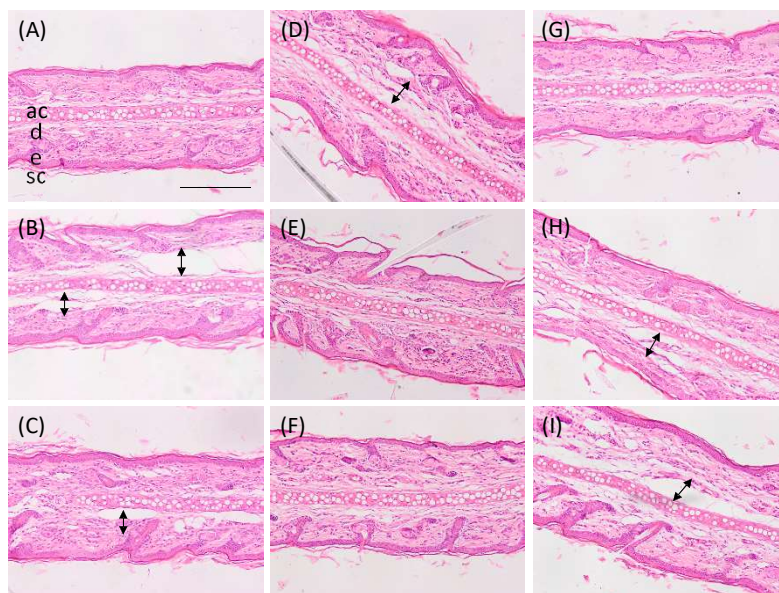


Figure 30. Representative micrographs of rat's ear (x100 magnification). (A): Control -, (B): Control +, (C): non-flavanone solution (nFS), (D): reference drug solution (RS), (E): FS1, (F): FS1a, (G): FS1b, (H): FS1c, (I): FS1d. e-epidermis, d-dermis, ac-auricular cartilage, sc-stratum corneum. Arrows indicate presence of edema. Scale bar = 200 μm .

Similarly, for the assessment of the anti-inflammatory effect of the formulations, histological analysis of ear biopsies was performed. Ears treated with arachidonic acid (AA, Figure 31.B) showed a mild inflammation characterized by edema, increased epidermal thickness, and infiltration of polymorphonuclear (PMN) leukocytes.

Topical administration of diclofenac decreased these inflammatory indicators. The placebo was also tested and did not show any anti-inflammatory effect. FF1d (Figure 31.I) was the best formulation in reducing the inflammation induced by AA. FF1, FF1a and FF1b (Figure 31.E, F, G) partially reduced the inflammation. All three formulations showed less PMN infiltrate. However, only FF1 and FF1b (Figure 31.E, G) were able to reduce the epidermal thickness. Only FF1c (Figure 31.H) showed an anti-inflammatory pattern similar to the positive control ear with the presence of PMN, even when the edema and the epidermal thickness were less pronounced than in AA-treated ears.

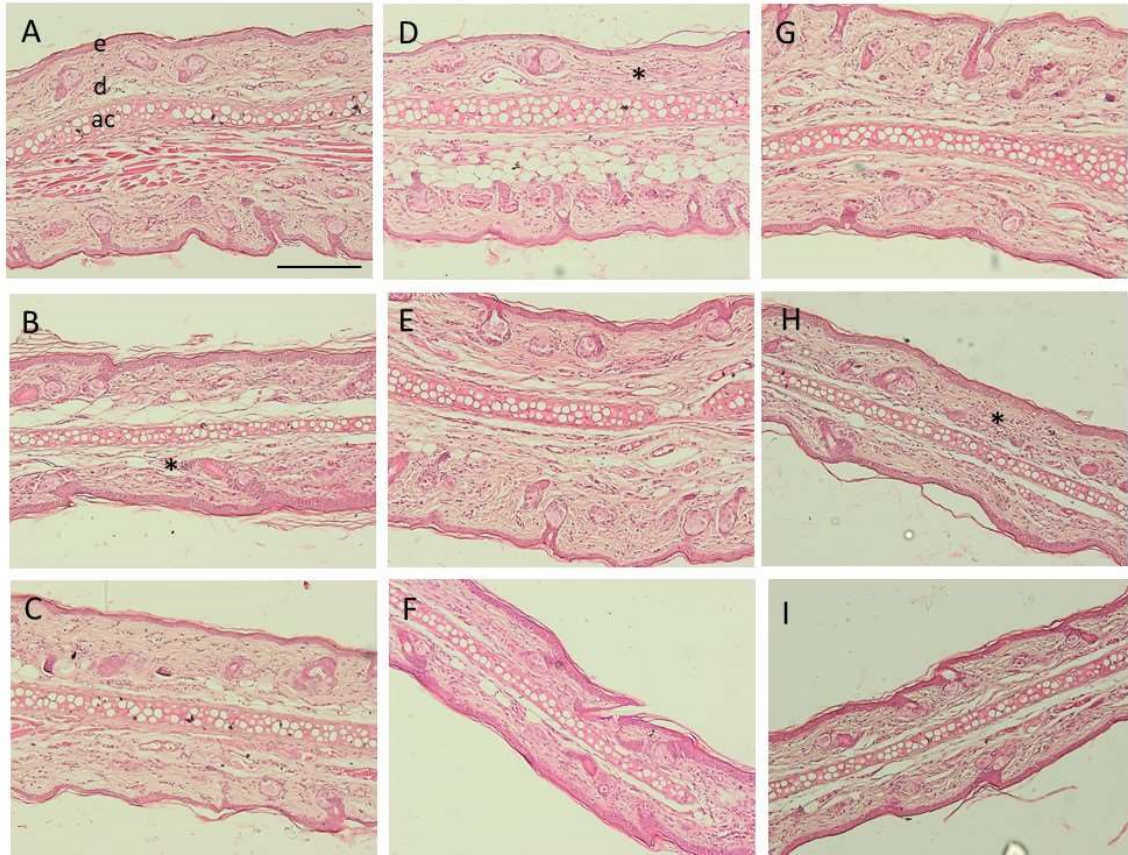


Figure 31. Histological sections of swollen ears stained with Hematoxylin and Eosin. A- Control (-), B-Control (+), C-Commercial Gel, D- nFF, E-FF1, F-FF1a, G-FF1b, H-FF1c, I- FF1d. e-epidermis, d-dermis, ac-auricular cartilage, * leukocytic infiltrate. 100X magnification. Scale bar = 200 μ m.

4.9. Gene Expression analysis by RT-qPCR

Results from the RT-qPCR analysis are presented in Figure 32. Rat ear samples from the positive control group showed significant higher mRNA expression of pro-inflammatory cytokines IL-6, IL-1 β and TNF- α than samples from non-treated rats (negative control), thus confirming the inflammatory effect of AA. A trend of reduced expression of the pro-inflammatory cytokines IL-6 and IL-1 β was also observed with the application of all the flavanone solutions as well as the reference solution (RS) (Figures 32.B-C). On the other hand, regarding TNF- α , only the FS1 and FS1a diminished the expression of this cytokine to levels that were not significantly different from those of the negative control group.

Moreover, no significant differences were observed between FS1 and FS1a results (Figure 32.A).

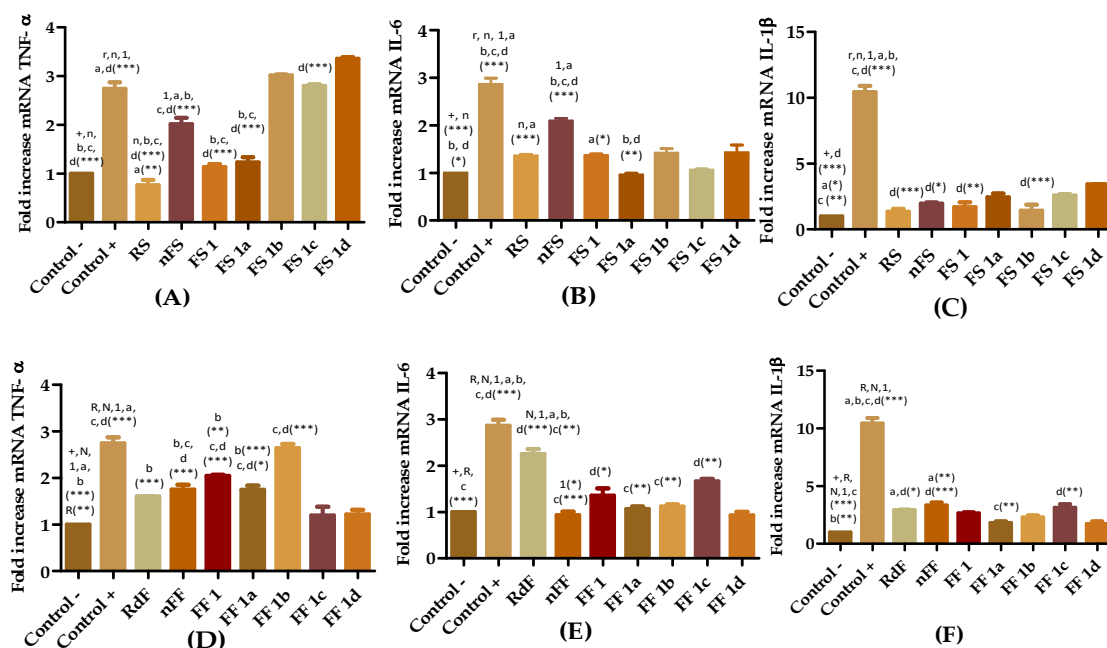


Figure 32. Relative expression of cytokines: (A, D): TNF- α ; (B, E): IL-6; (C, F): IL-1 β . Non-treated rat (Control -), rat treated only with AA (Control +), rat treated with ethanol: water (nFS), rat treated with diclofenac sodic solution (reference anti-inflammatory drug) after inducing inflammation (RS), rat treated with flavanone solutions FS1, FS1a- FS1d. Rat treated with flavanone formulation without flavanone (nFF), rat treated with diclofenac gel (reference anti-inflammatory drug) after inducing inflammation (RdF), rat treated with flavanone solutions FF1, FF1a- FF1d. Significant difference between Control + (+), nFS (n), RS (r), FS or FF1 (1), FS or FF 1a (a), FS or FF 1b (b), FS or FF 1c (c), FS or FF 1d (d) * $p < 0.05$, ** $p < 0.01$, *** $p < 0.001$ by non-parametric Tukey's t-test ($n = 5$).

As it can be seen, the treatment with all FF showed an anti-inflammatory potential as evidenced by a decreased production of IL-6 and IL-1 β (Figure 32.E, 32.F). For IL-6 expression, the inhibitory activity of all FF was higher than the reference anti-inflammatory drug formulation (RdF). Notice that the anti-inflammatory capacity of the non-flavanone formulation (nFF) was similar to FF1, FF1a-FF1d. Furthermore, TNF- α levels were decreased after treatment with all FF except with 1b. The best anti-inflammatory activity was observed for FF1c and FF1d.

DISCUSSION

5. DISCUSSION

Natural products continue to be a source of bioactive compounds and offer a possibility for the development of drugs to be used for the treatment of a huge diversity of diseases [15,95,96]. Using adequate methods, structural changes facilitate the altering of the physicochemical properties and bioactivities of natural compounds [23]. The present work carried out a range of structural changes such as esterification, methylation, cyclization or vinylogous cyclization match up well with the obtention of new compounds with improved biological efficacy. In addition, it provides a strategy to evaluate the influence of the substitution pattern on the structure–activity relationship [67].

The semi-synthesis of derivatives (**1a** and **1b**) by the introduction of new substituents into the structure of a lead flavanone **1** resulted in compounds with bioactive characteristics and different chemical properties. The shape has also been changed in **1c** and **1d**, which resulted in conformational restrictions that could affect the binding to the target site [3].

Modern drug discovery is based on high data screening of small molecules against macromolecular disease targets, as there is high demand about molecular screening libraries containing drug-like compounds [89]. The PASS computer program allows to estimate the probable profile of biological activity of a drug-like organic compound based on its structural formula [28].

The prediction of the biological activity spectra obtained using the PASS computer program showed that all the flavanones are predicted to display anti-inflammatory action and have a probability of being active (Pa) up to 0.6 similar to the common drug references (Table 2). The *in vivo* anti-inflammatory evaluation was carried out with the aim of confirming these predictions.

The $\text{Log}P$ (octanol/water partition coefficient) is used in drug design to measure the molecular lipophilicity. Lipophilicity affects drug absorption, bioavailability, hydrophilic drug-receptor interactions, metabolism, as well as their toxicity. The method for predicting $\text{log}P$ developed in Molinspiration[®] (miLog P) is one of the best methods

available for predicting this parameter. It has been reported that there is a very good correlation between Molinspiration[®] calculated $\text{Log}P$ and several drug transport properties [97]. The calculated $\text{miLog}P$ values for the investigated flavanones (**1**, **1a-1b**) were in the range of 3.82 to 4.57 (Table 2), which were acceptable values. Thus, these compounds were expected to present good bioavailability.

Molecular polar surface area (TPSA) is a very useful descriptor for predicting drug absorption and transport properties, for which the area of the polar surface is defined as the sum of the surfaces of the polar atoms like oxygen, nitrogen and hydrogen attached to a molecule. Therefore, TPSA is a molecular property related to the polarity, hydrogen-bonding potential and water solubility of organic molecules. Molecules with TPSA values around 160 or more are expected to exhibit problems to cross the membrane barriers [98]. In this regard, the TPSA flavanones were less than 78.92 values (Table 2). Therefore, this meant they could efficiently cross the skin. In biochemistry, a ligand is defined as a substance that is able to bind to and form a complex with a biomolecule so that it serves as a biological purpose [99]. Interestingly, flavanones **1c** and **1d** qualified as potential nuclear-receptor-ligands, and displayed the highest bioactivity scores of 0.71 and 0.67 respectively (Table 2).

As mentioned in the introduction section, due to the fact of the biological properties of flavanones, it is of utmost importance to have a good analytical method validation in order to promote future studies. HPLC is highly sensitive in the determination of small quantities of natural molecules in biopharmaceutical studies based on previous studies [73].

According to our data, the method developed was linear, accurate and precise. In addition, the method can be used in the quantification of prenylated flavanones samples from permeation and retention studies in human skin. Furthermore, the method was selective since the chromatograms allowed the observer to identify the signal for each prenylated flavanone without interference. This method was suitable for the analysis of flavanones **1**, **1a-1d** in biological systems and for other biopharmaceutical studies.

The main problem with natural products is their low stability, poor bioavailability and solubility parameter. Dermal drug delivery, the topical application of active products to the skin surface to treat local skin diseases, is a good strategy to formulate natural product compounds to solve the solubility problems, and thus enhancing their bioavailability [46,100]. Other advantages are that they are painless and easy to be applied, suggesting a good patient compliance [47]. Nevertheless, most natural active products are not suitable for this mode of administration. Recently, nanotechnology-based formulations such as nanoemulsions (NE), have been successfully employed for encapsulating and delivering lipophilic bioactive components targeted at delivery in a tissue [48]. Many previous studies demonstrated that permeation rates from nanostructured formulations were significantly higher than those of conventional formulations [101,102].

The evaluation of physical and biopharmaceutical properties of FF were possible because all the derivative flavanones were loaded in formulations in identical conditions. With regard to this, the flavanones **1**, **1a**, **1b**, **1c** and **1d** were successfully incorporated into FF. TEM images permitted the observation of the droplet structure, and confirmed the efficiency of the emulsion preparation method used [93]. In other studies, it has been observed that the molecular structure of emulsifiers had a great effect on the droplet size of the final emulsions [103]. The droplet size and stability of the emulsion is also affected by the type and concentration of the surfactant used [84].

Nevertheless, as shown in Table 5, the mean droplet size changed after the loading of flavanones. It could be hypothesized that the incorporated flavanones played an important role in the structure of the system and may affect it due to molecular interactions, similar to the effect of the emulsifiers and the surfactants used to prepare them. Those molecular interactions could compress or expand the drop of emulsion and determine its magnitude.

Viscosity plays an important role in the texture perception of the FF when applied to inflamed skin. In line with this, the assayed FF exhibited a Newtonian behavior since it showed characteristics suitable for topical flavanone delivery. In addition, the viscosity data can point to the option of dosing these formulations in a dispenser spray or roll on. In consequence, contamination of the formulation can be avoided, as well as it have the

advantage of easy application. The viscosity data would allow us to use it as a quality control measure when the formulation is taken to an industrial level [104]. Further to this, the formulation extensibility measurements demonstrate the ease or difficulty in spreading the FF on damaged skin. With the results of the extensibility study set out in Figure 22, it is possible to ascertain that all the FF studied can be applied on skin easily because with a low weight (200 g) the formulation has spread to the maximum possible.

In general, protection from physical and chemical degradation is one of the advantages in drug delivery of the majority of nanostructured systems [102]. From a practical viewpoint, it is important that formulations remain physically stable during storage. All the foregoing indicates the slow re-coalescence rate of FF drops because of continuous Brownian motion of the smaller droplets. However, the fact that nano-structured systems are transparent means that UV and visible light can penetrate into them, which may promote light-sensitive chemical degradation reactions to sensible components [105]. As shown by the data from FF1, FF1b, FF1c and FF1d, this is how it is possible that flavanones in these formulations interact in some way with the excipients that contain them, obtaining a kind of protection to degradation. On the other hand, the flavanone **1a** was unstable to chemical degradation when stored at 4 °C in the formulation. The ester moiety in FF1a could suffer hydrolysis by the action of atmospheric water, therefore, the flavanone **1a** content was reduced [3]. Consequently, it may be necessary to improve the chemical stability of labile components by adding antioxidants or chelating agents [105]. The physicochemical origin of this effect is currently unknown and requires further study.

The aim of the *in vitro* studies was to assess the effect of formulation factors, to establish an *in vitro-in vivo* correlation-relationship and, to confirm that the flavanones are capable of releasing the formulations. Therefore, if the skin allows this, and regardless of whether the excipients help or not, the flavanones could pass through the skin. There is more than one factor involved in the release process, including the flavanones' physicochemical properties, structural characteristics of the material system, release environment, and the possible interactions among others [92].

The increase of contact in the surface area with decreasing particle size offers a great potential of higher dissolution rates for molecules. Hence, particle size is crucial for appreciating a better release profile. Therefore, it is possible that the drop size was the reason why FF**1c** released a greater quantity than the other FF. Nevertheless, not only the size is important, but also other factors like the molecular polarizability. More polarizable molecules may interact more strongly with the excipients so the quantity released may be lower. In addition, the π interactions and hydrogen bonds can also influence drug release [106]. In sum, the probable combination of all these interactions may have been the cause of the results.

The *ex vivo* human skin permeation studies were carried out to define the permeation profile of flavanones formulations and the retained amounts in the tissue, which could be correlated to the efficacy of the treatment. The results for FF**1a** can be explained by the fact that ester moiety masks polar groups such as hydroxyl group (OH) contained in flavanone **1**, favoring passage through fatty cell membranes. In the case of methyl substituents, the molecule lipophilicity increased and was able to facilitate the absorption [3]. That may explain why FF**1b** had Q_r higher than FF**1**. Although FF**1a** presented the highest Q_r , it is also the formulation that was able to reach easily the systemic system, and therefore that could exert its function into a local and systemic level. In addition, FF**1a** is the formulation with most chemical degradation, and it is not possible to guaranty the treatment without changes in the formulation. Therefore, the formulation should be enriched with an antioxidant and a desiccant to avoid degradation [105].

The *in vivo* study was carry out to evaluate the anti-inflammatory efficacy of the assayed FF. The results (Figure 5) can be put down to the fact that the excipients of formulations did not have any anti-inflammatory activity per se. Thus, the efficacy of the FF were intrinsically due to the flavanones. It might be assumed that the anti-inflammatory effect could be related to the amount of flavanone retained. Even though the flavanone **1d** in the *in vivo* assay turned out to be the most active while it was the least retained ($Q_r = 0.19$ g/g_{skin}/cm²).

In several studies, the SARs of flavonoids revealed among other things that a planar ring system is essential in the flavonoid molecules to exhibit the activity and that hydroxyl

groups at 5- and 7- position of A-ring seem to be favorable to structural features to the inhibition of AA-induced mouse ear edema [15,52,53]. Hence, the molecules **1c** and **1d** present a planar system and a higher rigidity and were able to support interaction more easily with the target, it reduces inflammation more than the other molecules used in the *in vivo* assay. In the case of flavanone **1a**, it should be pointed out that it was synthesized from the acetylation of flavanone **1**, thus the hydroxyl groups at 5- and 7- position were somehow eliminated, and thus probably caused less *in vivo* activity compared to FF**1**. In addition, the fact is that the methylation of one of the functional hydroxyl groups moiety **1** yielded **1b**, and caused an increase in the anti-inflammatory activity compared with FF**1** due to an increase in lipophilicity, as suggested by its higher skin retention. Probably, the introduction of the methyl group may improve the binding of the ligand to its receptor by filling a pocket on the target site [3]. That is why the presence of those structural conditions in flavanone **1** and **1b** was the cause of FF**1** and FF**1b** reducing the epidermal thickness.

Finally, the SCH values after application of FF could indicate their hydration power due to the formation of an occlusive film on the skin thanks to the excipients. In the light of the foregoing, this permits the flavanones to penetrate easily through occluded hydrated skin and exert their action in the skin [38]. In addition, this hydration could reduce the physical discomfort associated with skin diseases like dryness and irritation [82].

The results obtained from *in vivo* studies using different irritant agents (TPA and AA) are shown in Figures 26.A and 27.A. They make clear that the natural flavanone extracted **1** and the derivatives flavanones (**1a-1d**) have topical anti-inflammatory activity, and of these flavanones **1d** stands out. All five FS were able to reduce the epidermal thickness present in the AA-treated ears. Furthermore, it is important to point out that ethanol per se can produce constriction and dehydration effects that can turn into an anti-inflammatory action [107]. The natural flavanone **1** and derivatives flavanones **1c** and **1d** showed a correlation of accumulation into the human skin with their local anti-inflammation effect evaluated in the TPA-induced model. The explanation to this correlation could be that these three flavanones have similar physicochemical properties, such as area and molecular mass, as well as that they bond energy.

Cytokines are regulatory proteins which play a key role in inflammatory responses [65,66]. The inhibition of some pro-inflammatory cytokines can alleviate many inflammatory diseases [108–110]. Continuing with our interest in the evaluation of the biological potential of flavanones, and in order to prove their anti-inflammatory potential, the gene expression of IL-1 β , IL-6, and TNF- α , involved in cellular inflammation were analyzed in small sections of the rat ear tissue after FS**1**, FS**1a**- FS**d** and FF**1**, FF**1a**- FF**d** treatment [64]. It is reported that flavonoids inhibit pro-inflammatory mediators such as cytokines/chemokines, eicosanoids, and adhesion molecules [111]. Overall, the FS**1**, FS**1a**- FS**d**, and FF**1**, FF**1a**- FF**d** inhibited the production of IL-1 β and IL-6 with respect to the positive control (Figure 32.B, 32.C, 32.E and 32.F). Some topical FF were able to decrease the cytokines (IL-1 β , IL-6, and TNF- α) to baseline control specially FF**d**, which again confirm that flavanone **d** was the most active. In addition, the FS**1b** showed better results when IL-1 β was evaluated. In general, all FF have greater capacity to reduce cytokine expression with respect to the reference drug. Contrastingly, even though the flavanones dissolved in ethanol: water (FS), diminished cytokines levels, they were not more effective than the reference drug solution (RS). In general, all FF tested showed greater capacity to reduce cytokine expression than the reference anti-inflammatory drug. We also explore the effect of the excipients (nFS and nFF) in the reduction of cytokine expression. It can be seen that TNF- α expression was significantly repressed by nFS and nFF but their activity was lower than the reference drug. For IL-1 β , the nFS caused the same inhibitory effect as the reference (RS). In the same way, nFF significantly reduced the IL-6 expression with respect to RdF.

Comparative results of each flavanone dissolved in solution (ethanol: water) or formulated in nanostructure (FF) did not reveal significant differences between them. Nevertheless, a significant difference in IL-1 β reduction by **d** was observed, being better in NE formulation than in solution. Likewise, FF**d** decreased IL-6 and TNF- α mRNA levels better than FS**d** with statistically significant differences between them. These findings suggest that the administration of flavanones loaded in nanostructured formulation could improve their anti-inflammatory activity.

The fact that both FS and FF showed inhibitory capacity of inflammation suggest that both formulations could well be used to treat skin inflammation but this specifically

depends on the skin area to be treated and this leads to the choosing of one option or another. For example, if there were intense pain in the inflamed skin, the FS should be administrated in spray form to avoid contact with the damaged area and to take advantage of the cooling and antiseptic effect of the alcohol contained in it. On the other hand, if the inflammation is on the face, the alcoholic spray would be harmful to both the eye and nasal mucosa and the use of FF would favor its application [112].

The better anti-inflammatory effect displayed by flavanones **1b** and **1d** suggested that the chemical modification of flavanone **1** played an important role in improving the anti-inflammatory activity. As in previous studies [113], these results again confirm that a planar ring system and hydroxyl groups at the 5- and 7- position of the A-ring seem to be vital in the flavonoid molecules so that they exhibit the anti-inflammatory action revealed in SARs studies [15,52,53]. These facts could be the reasons why the structure of flavanones **1b** that possess hydroxyl group at 5-position and flavanone **1d** with a more rigidity structure favored the anti-inflammatory effect in the models evaluated in this work.

CONCLUSIONS

6. CONCLUSIONS

- 6.1. The preparation of the flavanones derived **1a-1d** from the flavanone **1** was achieved and their identification was assessed by direct comparison with an authentic sample in the laboratory used as a standard.
- 6.2. The *in silico* tools (*Molinspiration* and *PASS Online*) has allowed the physicochemical properties of flavanones and the estimation, prior to *in vivo* studies, of their probable bioactivity profile. It was found that their anti-inflammatory action was highly probably part of this profile.
- 6.3. The results obtained in the validation of the analytical method for the quantification of the different flavanones by HPLC proved to be linear, exact and precise for concentrations ranging tested from 1.56 to 200 µg/mL. The detection and quantification limits averaged 0.4 µg/mL and 1.2 µg/mL, respectively. The validated method seems to be selective since during the test of the flavanones' permeation in solution in human skin, no interferences of the skin components were observed and this thus verified the applicability of the analytical method of the flavanones' quantification in this type of tissue.
- 6.4. The nanostructured formulations (FF) that individually and independently contain natural flavanone **1** and its derivatives **1a-1d** were successfully prepared. This obtained isotropic, transparent and slightly viscous substances (Newtonian behavior with values in the range from 80.01 ± 0.04 to 86.83 ± 0.03 mPa·s). The physicochemical and morphological characterization of the formulations by transmission electron microscopy (TEM) revealed that they have adequate characteristics for dermal administration with a droplet size ranging from 12.56 nm for FF**1c** to 370.64 nm for FF**1d**.
- 6.5. According to the study of short-term physical stability (stored at 4 ± 1 °C for a period of 180 days), the FF maintained their physical properties without changes in visual appearance, without phase separation, or sedimentation. In turn, no significant changes in pH were recorded. Turning to the evaluation of the

chemical stability during storage, the formulations **FF1**, **FF1b** and **FF1d** maintained an amount of original flavanone above 90 %.

- 6.6. The FFs maintained a sustained release behavior with a tendency to increase the release inversely proportional to their droplet size (observed by TEM) following the Weibull mathematical model. This type of *in vitro* evaluation made it possible to guarantee that the formulation releases flavanones and allows a sufficient quantity of compound to be left and that it is capable of being permeated into human skin.
- 6.7. The results obtained from the *ex vivo* permeation of human skin from FF of flavanones revealed that the amount permeated after 29 hours was different depending on the flavanone that was being tested. The values were in the range of 1082.85 μg for **FF1a** to 1.44 μg for **FF1d**. In the same way, the maximum amount of flavanone retained in the skin was presented by **FF1a** with 2277.24 $\text{g}/\text{g}_{\text{piel}}/\text{cm}^2$ and the minimum observed was 0.19 $\text{g}/\text{g}_{\text{piel}}/\text{cm}^2$ for **FF1d**. The different functional groups that characterize each of the different chemical structures of flavanones may well have favored to a greater or lesser degree their passage through the natural membrane. The amount of flavanone retained in the skin for all derived flavanones (**1a-1d**) was greater than that presented by natural flavanone **1**.
- 6.8. The results of the *in vivo* study to evaluate the anti-inflammatory efficacy of FFs showed that the excipients do not exert a biological activity by themselves and that the anti-inflammatory activity observed was due to the intrinsic strength of the flavanones studied *per se*. The FFs and the flavanones' solutions (**FS**) were found to be more effective in treating the surface of inflamed skin than the reference drug tested (diclofenac sodium gel and solution). The histological analysis of the ears treated with both the flavanone solutions and the formulations confirmed the reduction of edema and the reduction of the thickness of the stratum corneum, without affecting the treated tissue, highlighting the action of **FF1d** and **FS1b**. According to the results of this investigation, it can be considered that Flavone F1 presents better anti-inflammatory activity and therefore can potentially be an anti-inflammatory agent for topical use.

6.9. The modification of the chemical structure of natural flavanone **1** to obtain flavanones **1a**, **1b**, **1c** and **1d** allowed us to understand the importance of the molecular structure that results in the anti-inflammatory action on the skin. It can be concluded that the molecules that present a planar system, as in the case of **1c** and **1d**, showed better results than natural flavanone **1**, probably because its molecular rigidity could cause a greater interaction with the therapeutic targets in the inflammatory process. Similarly, the increase in lipophilicity of molecule **1b** with respect to molecule **1** caused an increase in the anti-inflammatory activity.

6.10. In general, all **FFs** were able to reduce the expression of the cytokines evaluated with respect to the reference drug. However; the flavanones in solution decreased the levels of cytokines. They were not more effective than the reference drug solution (Diclofenac sodium). With this observation, it can be concluded that the formulation of flavanones in nanostructured systems represents a notable advantage which improves their bioavailability and thus one observes an efficient pharmacological effect when its results are compared with that of the flavanones contained in solution.

REFERENCES

1. Thring, T. S.; Hili, P.; Naughton, D. P. Antioxidant and potential anti-inflammatory activity of extracts and formulations of white tea, rose, and witch hazel on primary human dermal fibroblast cells. *J. Inflamm.* **2011**, *8*, 1–7. <https://doi.org/10.1186/1476-9255-8-27>.
2. Lin, T.; Zhong, L.; Santiago, J. L. Anti-Inflammatory and Skin Barrier Repair Effects of Topical Application of Some Plant Oils. *Int. J. Mol. Sci.* **2018**, *19* (1), 70. <https://doi.org/10.3390/ijms19010070>.
3. Gareth, T. *Medicinal Chemistry An Introduction*, 2nd ed; John Wiley & Sons: England, 2007. <https://doi.org/10.1021/ie50495a015>.
4. Villarino, N. F.; Landoni, M. F. Administración Transdérmica De Fármacos: Una Alternativa Terapéutica. *Analecta Vet.* **2006**, *26* (1), 28–37.
5. Rauh, L. K.; Horinouchi, C. D. S.; Loddi, A. M. V.; Pietrovski, E. F.; Neris, R.; Souza-Fonseca-Guimarães, F.; Buchi, D. F.; Biavatti, M. W.; Otuki, M. F.; Cabrini, D. A. Effectiveness of Vernonia scorpioides ethanolic extract against skin inflammatory processes. *J. Ethnopharmacol.* **2011**, *138* (2), 390–397. <https://doi.org/10.1016/j.jep.2011.09.012>.
6. de Souza, M. L.; Oliveira, D. D.; Pereira, N. de P.; Soares, D. M. Nanoemulsions and dermatological diseases: contributions and therapeutic advances. *Int. J. Dermatol.* **2018**, *57* (8), 894–900. <https://doi.org/10.1111/ijd.14028>.
7. Chi, Y. S.; Lim, H.; Park, H.; Kim, H. P. Effects of wogonin, a plant flavone from Scutellaria radix, on skin inflammation: In vivo regulation of inflammation-associated gene expression. *Biochem. Pharmacol.* **2003**, *66* (7), 1271–1278. [https://doi.org/10.1016/S0006-2952\(03\)00463-5](https://doi.org/10.1016/S0006-2952(03)00463-5).
8. Castardo, J. C.; Prudente, A. S.; Guimaraes, C. L.; Monache, F. D.; Filho, V. C.; Otuki, M. F.; Cabrini, D. A. Anti-inflammatory effects of hydroalcoholic extract and two biflavonoids from Garcinia gardneriana leaves in mouse paw oedema. **2008**, *118*, 405–411. <https://doi.org/10.1016/j.jep.2008.05.002>.
9. Boller, S.; Soldi, C.; Marques, M. C. A.; Santos, E. P.; Cabrini, D. A.; Pizzolatti, M. G.; Zampronio, A. R.; Otuki, M. F. Anti-inflammatory effect of crude extract and isolated compounds from Baccharis illinita DC in acute skin inflammation. *J. Ethnopharmacol.* **2010**, *130* (2), 262–266.

- <https://doi.org/10.1016/j.jep.2010.05.001>.
10. Passos, G. F.; Medeiros, R.; Marcon, R.; Nascimento, A. F. Z.; Calixto, J. B.; Pianowski, L. F. The role of PKC/ERK1/2 signaling in the anti-inflammatory effect of tetracyclic triterpene euphol on TPA-induced skin inflammation in mice. *Eur. J. Pharmacol.* **2013**, *698* (1–3), 413–420. <https://doi.org/10.1016/j.ejphar.2012.10.019>.
 11. Rincón, M.; Calpena, A. C.; Fabrega, M. J.; Garduño-Ramírez, M. L.; Espina, M.; Rodríguez-Lagunas, M. J.; García, M. L.; Abrego, G. Development of pranoprofen loaded nanostructured lipid carriers to improve its release and therapeutic efficacy in skin inflammatory disorders. *Nanomaterials* **2018**, *8* (12). <https://doi.org/10.3390/nano8121022>.
 12. Siddiqui, F.; Naqvi, S.; Abidi, L.; Faizi, S.; Lubna; Avesi, L.; Mirza, T.; Farooq, A. D. *Opuntia dillenii* cladode: Opuntiol and opuntioside attenuated cytokines and eicosanoids mediated inflammation. *J. Ethnopharmacol.* **2016**, *182*, 221–234. <https://doi.org/10.1016/j.jep.2016.02.016>.
 13. Salinas, R.; Arellano-García, J.; Perea-Arango, I.; Álvarez, L.; Garduño-Ramírez, M. L.; Marquina, S.; Zamilpa, A.; Castillo-España, P. Production of the anti-inflammatory compound 6-o-palmitoyl-3-O-β-D- glucopyranosylcampesterol by callus cultures of *lopezia racemosa* cav. (onagraceae). *Molecules* **2014**, *19* (6), 8679–8690. <https://doi.org/10.3390/molecules19068679>.
 14. Kim, H. P.; Son, K. H.; Chang, H. W.; Kang, S. S. Anti-inflammatory Plant Polyphenolics and Cellular Action Mechanisms. *J. Pharmacol. Sci.* **2004**, *16* (6), 809–817. <https://doi.org/10.2174/1573407215666190419205317>.
 15. Gautam, R.; Jachak, S. M. Recent Developments in Anti Inflammatory Natural Products. *Harv. Bus. Rev.* **2008**, *86* (6), 84–92. <https://doi.org/10.1002/med>.
 16. Chen, J.; Li, W.; Yao, H.; Xu, J. Insights into drug discovery from natural products through structural modification. *Fitoterapia* **2015**, *103*, 231–241. <https://doi.org/10.1016/j.fitote.2015.04.012>.
 17. Durán-Iturbide, N. A.; Díaz-Eufracio, B. I.; Medina-Franco, J. L. In Silico ADME/Tox Profiling of Natural Products: A Focus on BIOFACQUIM. *ACS Omega* **2020**, *5* (26), 16076–16084. <https://doi.org/10.1021/acsomega.0c01581>.

18. Garcia-Campoy, A.; Garcia, E.; Muñiz-Ramirez, A. Phytochemical and pharmacological study of the eysenhardtia genus. *Plants* **2020**, *9* (9), 1–33. <https://doi.org/10.3390/plants9091124>.
19. Narváez-Mastache, J. M.; Garduño-Ramírez, M. L.; Alvarez, L.; Delgado, G. Antihyperglycemic activity and chemical constituents of Eysenhardtia platycarpa. *J. Nat. Prod.* **2006**, *69* (12), 1687–1691. <https://doi.org/10.1021/np060166z>.
20. Shi, L.; Feng, X. E.; Rong, J.; Hua, L.; Hua, G.; Shan, Q. Synthesis and biological activity of flavanone derivatives. *Bioorg. Med. Chem. Lett.* **2010**, *20* (18), 5466–5468. <https://doi.org/10.1016/j.bmcl.2010.07.090>.
21. Domínguez-Villegas, V.; Domínguez-Villegas, V.; García, M. L.; Calpena, A.; Clares-Naveros, B.; Garduño-Ramírez, M. L. Anti-inflammatory, Antioxidant and Cytotoxicity Activities of Methanolic Extract and Prenylated Flavanones Isolated from Leaves of Eysenhardtia platycarpa. *Nat. Prod. Commun.* **2013**, *8* (2), 177–180. <https://doi.org/10.1177/1934578x1300800211>.
22. Gómez Estrada, H. A.; González Ruiz, K. N.; Medina, J. D. Actividad antiinflamatoria de productos naturales. *Bol. Latinoam. y del Caribe Plantas Med. y Aromat.* **2011**, *10* (3), 182–217.
23. Li, S.; Xiong, Q.; Lai, X.; Li, X.; Wan, M.; Zhang, J.; Yan, Y.; Cao, M.; Lu, L.; Guan, J.; et al. Molecular Modification of Polysaccharides and Resulting Bioactivities. *Compr. Rev. Food Sci. Food Saf.* **2016**, *15*, 237–250.
24. Delgado Cirilo, A.; Minguillón Llombart, C.; Joglar Tamargo, J. *Introducción a la química terapéutica.*, 2^a.; 2000.
25. Andrade-Carrera, B.; Clares, B.; Noé, V.; Mallandrich, M.; Calpena, A.; García, M.; Garduño-Ramírez, M. Cytotoxic Evaluation of (2S)-5,7-Dihydroxy-6-prenylflavanone Derivatives Loaded PLGA Nanoparticles against MiaPaCa-2 Cells. *Molecules* **2017**, *22* (9), 1553. <https://doi.org/10.3390/molecules22091553>.
26. Terstappen, G. C.; Reggiani, A. In silico research in drug discovery. *Trends Pharmacol. Sci.* **2001**, *22* (1), 23–26. [https://doi.org/10.1016/S0165-6147\(00\)01584-4](https://doi.org/10.1016/S0165-6147(00)01584-4).
27. Scior, T.; Martínez Morales, E.; Salinas Stefanón, E. Los modelos in silico , una herramienta para el conocimiento farmacológico. *Elementos* **2007**, *68* (1), 45–48.

28. Filimonov, D. A.; Lagunin, A. A.; Glorizova, T. A.; Rudik, A. V.; Druzhilovskii, D. S.; Pogodin, P. V.; Poroikov, V. V. Prediction of the biological activity spectra of organic compounds using the pass online web resource. *Chem. Heterocycl. Compd.* **2014**, *50* (3), 444–457. <https://doi.org/10.1007/s10593-014-1496-1>.
29. Tugores, Y. M.; Marcel, A. M.; Ponce, Y. M.; Aran, V. J.; García-Trevijano, J. A. E.; Thu, H. L. T.; García Sánchez, R. N.; Barrio, A. G. Descubrimiento de nuevos antimaláricos a partir de fármacos conocidos mediante cribado in silico e in vitro. *An. la Real Acad. Nac. Farm.* **2012**, *78* (4), 401–416.
30. Bajorath, J. Integration of virtual and high-throughput screening. *Nat. Rev. Drug Discov.* **2002**, *1* (11), 882–894. <https://doi.org/10.1038/nrd941>.
31. Fleisher, M.; Belyakov, S.; Jansone, D.; Poroikov, V.; Leite, L.; Lukevics, E. Investigation of the structure and prediction of the biological activity of 1,3-bis(3-cyano-6,6-dimethyl-2-oxo-5,6-dihydro-2H-pyran-4-yl)-2-(4-methoxyphenyl)propane. *Chem. Heterocycl. Compd.* **2009**, *45* (5), 531–535. <https://doi.org/10.1007/s10593-009-0303-x>.
32. Mishra, S. S.; Kumar, N.; Sirvi, G.; Sharma, C. S.; Singh, H. P.; Pandiya, H. Computational Prediction of Pharmacokinetic, Bioactivity and Toxicity Parameters of Some Selected Anti arrhythmic Agents. *Pharm. Chem. J.* **2017**, *4* (5), 143–146.
33. Ertl, P.; Rohde, B.; Selzer, P. Fast calculation of molecular polar surface area as a sum of fragment-based contributions and its application to the prediction of drug transport properties. *J. Med. Chem.* **2000**, *43* (20), 3714–3717. <https://doi.org/10.1021/jm000942e>.
34. Green, J. M. Peer Reviewed: A Practical Guide to Analytical Method Validation. *Anal. Chem.* **1996**, *68* (9), 305A-309A. <https://doi.org/10.1021/ac961912f>.
35. Gómez-Segura, L.; Parra, A.; Calpena, A. C.; Gimeno, Á.; Boix-Montañes, A. Carprofen permeation test through porcine ex vivo mucous membranes and ophthalmic tissues for tolerability assessments: Validation and histological study. *Vet. Sci.* **2020**, *7* (4), 1–17. <https://doi.org/10.3390/vetsci7040152>.
36. Chibli, L. A.; Rodrigues, K. C. M.; Gasparetto, C. M.; Pinto, N. C. C.; Fabri, R. L.; Scio, E.; Alves, M. S.; Del-Vechio-Vieira, G.; Sousa, O. V. Anti-inflammatory

- effects of *Bryophyllum pinnatum* (Lam.) Oken ethanol extract in acute and chronic cutaneous inflammation. *J. Ethnopharmacol.* **2014**, *154* (2), 330–338. <https://doi.org/10.1016/j.jep.2014.03.035>.
37. B Sánchez, A.; Calpena, A. C.; Soriano, J. L.; Gálvez, P.; Clares, B. Anti-inflammatory nanomedicines: what does the future hold? *Nanomedicine* **2020**, *15* (14), 1357–1360. <https://doi.org/https://doi.org/10.2217/nmm-2020-0064>.
 38. Tanner, T.; Marks, R. Delivering Drugs by the Transdermal Route: Review and Comment. *Ski. Res. Technol.* **2008**, *14* (3), 249–260. <https://doi.org/10.1111/j.1600-0846.2008.00316.x>.
 39. Shakeel, F.; Shafiq, S.; Haq, N.; Alanazi, F. K.; Alsarra, I. A. Nanoemulsions as potential vehicles for transdermal and dermal delivery of hydrophobic compounds: An overview. *Expert Opin. Drug Deliv.* **2012**, *9* (8), 953–974. <https://doi.org/10.1517/17425247.2012.696605>.
 40. Saneja, A.; Panda, A. K.; Lcihtfouse, E. *Sustainable Agriculture Reviews*; Springer, Red; Cham, Switzerland, 2012; Vol 44. <https://doi.org/10.1007/978-94-007-5449-2>.
 41. Ahmad, S.; Ali, M. S.; Alam, M. S.; Alam, M. I.; Alam, N. Nanoemulsion as a novel carrier for drug delivery system: an overview. *Adv. Environmental Biol.* **2016**, *10* (10), 120–130.
 42. Kale, S. N.; Deore, S. L. Emulsion Micro Emulsion and Nano Emulsion : A Review. *Syst. Rev. Pharmacy. Rev. Pharm.* **2017**, *8* (1), 39–47.
 43. Gharibzahedi, S. M. T.; Mohammadnabi, S. Characterizing the novel surfactant-stabilized nanoemulsions of stinging nettle essential oil: Thermal behaviour, storage stability, antimicrobial activity and bioaccessibility. *J. Mol. Liq.* **2016**, *224*, 1332–1340. <https://doi.org/10.1016/j.molliq.2016.10.120>.
 44. Ali, A.; Mekhloufi, G.; Huang, N.; Agnely, F. β -lactoglobulin stabilized nanemulsions - Formulation and process factors affecting droplet size and nanoemulsion stability. *Int. J. Pharm.* **2016**, *500* (1–2), 291–304. <https://doi.org/10.1016/j.ijpharm.2016.01.035>.
 45. Shah, P.; Bhalodia, D.; Shelat, P. Nanoemulsion: A pharmaceutical review. *Syst. Rev. Pharm.* **2010**, *1* (1), 24–32. <https://doi.org/10.4103/0975-8453.59509>.

46. Piazzini, V.; Monteforte, E.; Luceri, C.; Bigagli, E.; Rita, A.; Bergonzi, M. C.; Piazzini, V.; Monteforte, E.; Luceri, C.; Bigagli, E.; et al. Nanoemulsion for Improving Solubility and Permeability of Vitex agnus-castus extract : Formulation and in vitro Evaluation using PAMPA and Caco-2 approaches. *Drug Deliv.* **2017**, *24* (1), 380–390. <https://doi.org/10.1080/10717544.2016.1256002>.
47. Martins Pinheiro, I.; Pereira Carvalho, I.; Sousa de Carvalho, C. E.; Moreira Brito, L.; Soares da Silva, A. B.; Mendes Conde Júnior, A.; Amorim de Carvalho, F. A.; Menezes Carvalho, A. L. Evaluation of the in vivo Leishmanicidal Activity of Amphotericin B Emulgel: An Alternative for the Treatment of Skin Leishmaniasis. *Exp. Parasitol.* **2016**, *164*, 49–55. <https://doi.org/10.1016/j.exppara.2016.02.010>.
48. Gopi, S.; Amalraj, A.; Haponiuk, J.; Thomas, S. Introduction of Nanotechnology in Herbal Drugs and Nutraceutical: A Review. *J. Nanomedicine. Biotherapeutic Discov.* **2016**, *6* (2), 1–8. <https://doi.org/10.4172/2155-983x.1000143>.
49. Prasad, M.; Lambe, U. P.; Brar, B.; Shah, I.; J, M.; Ranjan, K.; Rao, R.; Kumar, S.; Mahant, S.; Khurana, S. K.; et al. Nanotherapeutics: An insight into healthcare and multi-dimensional applications in medical sector of the modern world. *Biomed. Pharmacother.* **2018**, *97* (October 2017), 1521–1537. <https://doi.org/10.1016/j.biopha.2017.11.026>.
50. Lovelyn, C.; Attama, A. A. Current State of Nanoemulsions in Drug Delivery. *J. Biomater. Nanobiotechnol.* **2011**, *02* (05), 626–639. <https://doi.org/10.4236/jbnb.2011.225075>.
51. Navarrete-Vázquez, G.; Moreno-Díaz, H.; Aguirre-Crespo, F.; León-Rivera, I.; Villalobos-Molina, R.; Muñoz-Muñiz, O.; Estrada-Soto, S. Design, microwave-assisted synthesis, and spasmolytic activity of 2-(alkyloxyaryl)-1H-benzimidazole derivatives as constrained stilbene bioisosteres. *Bioorganic Med. Chem. Lett.* **2006**, *16* (16), 4169–4173. <https://doi.org/10.1016/j.bmcl.2006.05.082>.
52. Gomes, A.; Fernandes, E.; Lima, J.; Mira, L.; Corvo, M. Molecular Mechanisms of Anti-Inflammatory Activity Mediated by Flavonoids. *Curr. Med. Chem.* **2008**, *15* (16), 1586–1605. <https://doi.org/10.2174/092986708784911579>.
53. Jiang, C.; Liang, L.; Guo, Y. Natural Products Possessing Protein Tyrosine Phosphatase 1B (PTP1B) Inhibitory Activity Found in the Last Decades. *Acta Pharmacol. Sin.* **2012**, *33*, 1217–1245. <https://doi.org/10.1038/aps.2012.90>.

54. Espinoza, L. C.; Vera-García, R.; Silva-Abreu, M.; Domènech, Ò.; Badia, J.; Rodríguez-Lagunas, M. J.; Clares, B.; Calpena, A. C. Topical pioglitazone nanoformulation for the treatment of atopic dermatitis: Design, characterization and efficacy in hairless mouse model. *Pharmaceutics* **2020**, *12* (3). <https://doi.org/10.3390/pharmaceutics12030255>.
55. Domínguez-Villegas, V.; Clares-Naveros, B.; García-López, M. L.; Calpena-campmany, A. C.; Bustos-Salgado, P.; Garduño, M. L. Development and Characterization of two Nano-Structured Systems for Topical Application of Flavanones Isolated from *Eysenhardtia platycarpa*. *Colloids Surfaces B Biointerfaces* **2014**, *116*, 183–192. <https://doi.org/10.1016/j.colsurfb.2013.12.009>.
56. Kreilgaard, M. Influence of microemulsions on cutaneous drug delivery. *Adv. Drug Deliv. Rev.* **2002**, *54* (SUPPL.). [https://doi.org/10.1016/S0169-409X\(02\)00116-3](https://doi.org/10.1016/S0169-409X(02)00116-3).
57. Forgiarini, A.; Marquez, L.; Salager, J.-L. Nanoemulsions. *Nanosci. Colloid. Interfacial Asp.* **2006**, *1*, 395. <https://doi.org/10.1201/EBK1420065008>.
58. Costa, P.; Sousa Lobo, J. M. Modeling and comparison of dissolution profiles. *J. Pharm. Sci.* **2001**, *13*, 123–133. <https://doi.org/10.14227/DT160209P41>.
59. Xian, Y. F.; Hu, Z.; Ip, S. P.; Chen, J. N.; Su, Z. R.; Lai, X. P.; Lin, Z. X. Comparison of the anti-inflammatory effects of *Sinapis alba* and *Brassica juncea* in mouse models of inflammation. *Phytomedicine* **2018**, *50* (November 2017), 196–204. <https://doi.org/10.1016/j.phymed.2018.05.010>.
60. Feldmann, M.; Brennan, F. M.; Maini, R. N. Role of cytokines in rheumatoid arthritis. *Annu. Rev. Immunol.* **1996**, *14*, 397–440. <https://doi.org/10.1146/annurev.immunol.14.1.397>.
61. Alturkistani, H. A.; Tashkandi, F. M.; Mohammedsaleh, Z. M. Histological Stains: A Literature Review and Case Study. *Glob. J. Health Sci.* **2016**, *8* (3), 72–79. <https://doi.org/10.5539/gjhs.v8n3p72>.
62. Paramitha, D.; Ulum, M. F.; Purnama, A.; Wicaksono, D. H. B.; Noviana, D.; Hermawan, H. *Monitoring degradation products and metal ions in vivo*; Elsevier Ltd, 2017. <https://doi.org/10.1016/B978-0-08-100603-0.00002-X>.
63. Rincón, M.; Calpena, A. C.; Clares, B.; Espina, M.; Garduño-Ramírez, M. L.;

- Rodríguez-Lagunas, M. J.; García, M. L.; Abrego, G. Skin-controlled release lipid nanosystems of pranoprofen for the treatment of local inflammation and pain. *Nanomedicine* **2018**, *13* (19), 2397–2413. <https://doi.org/10.2217/nmm-2018-0195>.
64. Sarango-Granda, P.; Silva-Abreu, M.; Calpena, A. C.; Halbaut, L.; Fábrega, M. J.; Rodríguez-Lagunas, M. J.; Díaz-Garrido, N.; Badia, J.; Espinoza, L. C. Apremilast microemulsion as topical therapy for local inflammation: Design, characterization and efficacy evaluation. *Pharmaceuticals* **2020**, *13* (12), 1–25. <https://doi.org/10.3390/ph13120484>.
65. Peinnequin, A.; Mouret, C.; Birot, O.; Alonso, A.; Mathieu, J.; Clarençon, D.; Agay, D.; Chancerelle, Y.; Multon, E. Rat pro-inflammatory cytokine and cytokine related mRNA quantification by real-time polymerase chain reaction using SYBR green. *BMC Immunol.* **2004**, *5*, 1–10. <https://doi.org/10.1186/1471-2172-5-3>.
66. Spies, M.; Nestic, O.; Barrow, R. E.; Perez-Polo, J. R.; Herndon, D. N. Liposomal IGF-1 gene transfer modulates pro- and anti-inflammatory cytokine mRNA expression in the burn wound. *Gene Ther.* **2001**, *8* (18), 1409–1415. <https://doi.org/10.1038/sj.gt.3301543>.
67. Alalaiwe, A.; Lin, C.; Hsiao, C.; Chen, E.; Lin, C. Development of Flavanone and its Derivatives as Topical Agents Against Psoriasis : The Prediction of Therapeutic efficiency through Skin Permeation Evaluation and Cell-based Assay. *Int. J. Pharm.* **2020**, *581* (March), 119256. <https://doi.org/10.1016/j.ijpharm.2020.119256>.
68. Andrade-Carrera, B.; Clares, B.; Noé, V.; Mallandrich, M.; Calpena, A.; García, M.; Garduño-Ramírez, M. Cytotoxic Evaluation of (2S)-5,7-Dihydroxy-6-prenylflavanone Derivatives Loaded PLGA Nanoparticles against MiaPaCa-2 Cells. *Molecules* **2017**, *22* (9), 1553. <https://doi.org/10.3390/molecules22091553>.
69. Tariq, M.; Sirajuddin, M.; Ali, S.; Khalid, N.; Tahir, M. N.; Khan, H.; Ansari, T. M. Pharmacological investigations and Petra/Osiris/Molinspiration (POM) analyses of newly synthesized potentially bioactive organotin(IV) carboxylates. *J. Photochem. Photobiol. B Biol.* **2016**, *158*, 174–183. <https://doi.org/10.1016/j.jphotobiol.2016.02.028>.
70. Imran, M.; Aziz, M.; Kumar, N.; Kousar, Z.; Shabnam, S.; Nohri, F. SYNTHESIS

- , SPECTROSCOPIC CHARACTERIZATION AND PETRA OSIRIS MOLINSPIRATION (POM) ANALYSES OF DICARBOXYLIC ACID AMIDES. *Int. J. Pharm. Sci. Res.* **2016**, *7* (5), 1915–1927. [https://doi.org/10.13040/IJPSR.0975-8232.7\(5\).1915-27](https://doi.org/10.13040/IJPSR.0975-8232.7(5).1915-27).
71. EMA, C. for M. P. for H. U. Guideline on Bioanalytical Method Validation https://www.ema.europa.eu/en/documents/scientific-guideline/guideline-bioanalytical-method-validation_en.pdf (accessed Okt 9, 2019).
 72. Shabir, G. A. Validation of high-performance liquid chromatography methods for pharmaceutical analysis. *J. Chromatogr. A* **2003**, *987* (1–2), 57–66. [https://doi.org/10.1016/s0021-9673\(02\)01536-4](https://doi.org/10.1016/s0021-9673(02)01536-4).
 73. Alvarado, H. L.; Abrego, G.; Garduño-Ramírez, M. L.; Clares, B.; García, M. L.; Calpena, A. C. Development and validation of a high-performance liquid chromatography method for the quantification of ursolic/oleanic acids mixture isolated from *Plumeria obtusa*. *J. Chromatogr. B Anal. Technol. Biomed. Life Sci.* **2015**, *983–984*, 111–116. <https://doi.org/10.1016/j.jchromb.2015.01.009>.
 74. Surve, D. H.; Jindal, A. B. Development and validation of reverse-phase high-performance liquid chromatographic (RP-HPLC) method for quantification of Efavirenz in Efavirenz-Enfuvirtide co-loaded polymer-lipid hybrid nanoparticles. *J. Pharm. Biomed. Anal.* **2019**, *175*, 112765. <https://doi.org/10.1016/j.jpba.2019.07.013>.
 75. Cañadas-Enrich, C.; Abrego, G.; Alvarado, H. L.; Calpena-Campmany, A. C. Pranoprofen Quantification in ex vivo corneal and scleral permeation samples : Analytical validation. *J. Pharm. Biomed. Anal.* **2018**, *160*, 109–118. <https://doi.org/10.1016/j.jpba.2018.07.015>.
 76. Rozet, E.; Marini, R. D.; Ziemons, E.; Boulanger, B.; Hubert, P. Advances in validation, risk and uncertainty assessment of bioanalytical methods. *J. Pharm. Biomed. Anal.* **2011**, *55* (4), 848–858. <https://doi.org/10.1016/j.jpba.2010.12.018>.
 77. Causon, R. Validation of chromatographic methods in biomedical analysis viewpoint and discussion. *J. Chromatogr. B Biomed. Sci. Appl.* **1997**, *689* (1), 175–180. [https://doi.org/10.1016/S0378-4347\(96\)00297-6](https://doi.org/10.1016/S0378-4347(96)00297-6).
 78. Bustos-Salgado, P.; Andrade-Carrera, B.; Garduño-Ramírez, M. L.; Alvarado, H.;

- Calpena-Campmany, A. Quantification of One Prenylated Flavanone from *Eysenhardtia platycarpa* and Four Derivatives in Ex Vivo Human Skin Permeation Samples Applying a Validated HPLC Method. *Biomolecules* **2020**, *10*, 889. <https://doi.org/10.3390/biom10060889>.
79. Benmeradi, N.; Payre, B.; Goodman, S. L. Easier and Safer Biological Staining: High Contrast Uranyl-less Staining of TEM Grids using mPrep/g Capsules. *Microsc. Microanal.* **2015**, *21* (S3), 721–722. <https://doi.org/10.1017/s1431927615004407>.
80. Suñer, J.; Calpena, A. C.; Clares, B.; Cañadas, C.; Halbaut, L. Development of Clotrimazole Multiple W/O/W Emulsions as Vehicles for Drug Delivery: Effects of Additives on Emulsion Stability. *AAPS PharmSciTech* **2017**, *18* (2), 539–550. <https://doi.org/10.1208/s12249-016-0529-8>.
81. Provenza Bernal, N.; Calpena, A. C.; Mallandrich, M.; Ruiz, A.; Clares, B. Development, Physical-Chemical Stability, and Release Studies of Four Alcohol-Free Spironolactone Suspensions for Use in Pediatrics. *Dissolution Technol.* **2014**, *21* (1), 19–30. <https://doi.org/10.14227/DT210114P19>.
82. Carvajal-Vidal, P.; González-Pizarro, R.; Araya, C.; Espina, M.; Halbaut, L.; Gómez de Aranda, I.; García, M. L.; Calpena, A. C. Nanostructured Lipid Carriers Loaded with Halobetasol Propionate for Topical Treatment of Inflammation: Development, Characterization, Biopharmaceutical Behavior and Therapeutic Efficacy of Gel Dosage Forms. *Int. J. Pharm.* **2020**, *585*, 119480. <https://doi.org/10.1016/j.ijpharm.2020.119480>.
83. Suñer-Carbó, J.; Boix-Montañés, A.; Halbaut-Bellowa, L.; Velázquez-Carralero, N.; Zamarbide-Ledesma, J.; Bozal-de-Febrer, N.; Calpena-Campmany, A. C. Skin permeation of econazole nitrate formulated in an enhanced hydrophilic multiple emulsion. *Mycoses* **2017**, *60* (3), 166–177. <https://doi.org/10.1111/myc.12575>.
84. Kumar, N.; Mandal, A. Surfactant Stabilized Oil-in-Water Nanoemulsion: Stability, Interfacial Tension, and Rheology Study for Enhanced Oil Recovery Application. *Energy and Fuels* **2018**, *32* (6), 6452–6466. <https://doi.org/10.1021/acs.energyfuels.8b00043>.
85. Rachmawati, H.; Budiputra, D. K.; Mauludin, R. Curcumin Nanoemulsion for Transdermal Application: Formulation and Evaluation. *Drug Dev. Ind. Pharm.*

- 2015**, *41* (4), 560–566. <https://doi.org/10.3109/03639045.2014.884127>.
86. Mallandrich, M.; Fernández-Campos, F.; Clares, B.; Halbaut, L.; Alonso, C.; Coderch, L.; Garduño-Ramírez, M. L.; Andrade, B.; del Pozo, A.; Lane, M. E.; et al. Developing Transdermal Applications of Ketorolac Tromethamine Entrapped in Stimuli Sensitive Block Copolymer Hydrogels. *Pharm. Res.* **2017**, *34* (8), 1728–1740. <https://doi.org/10.1007/s11095-017-2181-8>.
87. Espinoza, L. C.; Silva-Abreu, M.; Calpena, A. C.; Rodríguez-Lagunas, M. J.; Fábrega, M. J.; Garduño-Ramírez, M. L.; Clares, B. Nanoemulsion Strategy of Pioglitazone for the Treatment of Skin Inflammatory Diseases. *Nanomedicine Nanotechnology, Biol. Med.* **2019**, *19*, 115–125. <https://doi.org/10.1016/j.nano.2019.03.017>.
88. Close, B.; Banister, K.; Baumans, V.; Bernoth, E. M.; Bromage, N.; Bunyan, J.; Erhardt, W.; Flecknell, P.; Gregory, N.; Hackbarth, H.; et al. Recommendations for Euthanasia of Experimental Animals: Part 2. *Lab. Anim.* **1997**, *31* (1), 1–32. <https://doi.org/10.1258/002367797780600297>.
89. Nadeem, S.; Sirajuddin, M.; Ahmad, S.; Tirmizi, S. A.; Ali, M. I.; Hameed, A. Synthesis, spectral characterization and in vitro antibacterial evaluation and Petra/Osiris/Molinspiration analyses of new Palladium(II) iodide complexes with thioamides. *Alexandria J. Med.* **2016**, *52* (3), 279–288. <https://doi.org/10.1016/j.ajme.2015.10.003>.
90. Farias, I. V.; Faqueti, L. G.; Noldin, V. F.; Franchi Junior, G.; Nowil, A. E.; Schuquel, I. T. A.; Delle Monache, F.; García, P. A.; López-Pérez, J. L.; San Feliciano, A.; et al. Cytotoxic phloroglucinol meroterpenoid from *Eugenia umbelliflora* fruits. *Phytochem. Lett.* **2018**, *27* (July), 187–192. <https://doi.org/10.1016/j.phytol.2018.07.004>.
91. Mostafa, D. M.; Ammar, N. M.; Basha, M.; Hussein, A.; Awdan, S. El; Awad, G.; Mahmoud, D.; Ammar, N. M.; Basha, M.; Ali, R.; et al. Transdermal microemulsions of *Boswellia carterii* Bird: formulation, characterization and in vivo evaluation of anti-inflammatory activity. *Drug Deliv.* **2015**, *22* (6), 748–756. <https://doi.org/10.3109/10717544.2014.898347>.
92. Souza, S. D. A Review of In Vitro Drug Release Test Methods for Nano-Sized Dosage Forms. *Adv. Pharm.* **2014**, *2014*, 12.

93. Fernández Campos, F.; Calpena Campmany, A. C.; Rodríguez Delgado, G.; López Serrano, O.; Clares Naveros, B. Development and Characterization of A Novel Nystatin-Loaded Nanoemulsion for the Buccal Treatment of Candidosis: Ultrastructural Effects and Release Studies. *J. Pharm. Sci.* **2012**, *101* (10), 3739–3752. <https://doi.org/DOI 10.1002/jps.23249>.
94. Alvarado, H. L.; Abrego, G.; Souto, E. B.; Garduño-Ramirez, M. L.; Clares, B.; García, M. L.; Calpena, A. C. Nanoemulsions for Dermal Controlled Release of Oleanolic and Ursolic Acids: In vitro, Ex vivo and In Vivo Characterization. *Colloids Surfaces B Biointerfaces* **2015**, *130*, 40–47. <https://doi.org/10.1016/j.colsurfb.2015.03.062>.
95. Yuan, H.; Ma, Q.; Ye, L.; Piao, G. The Traditional Medicine and Modern Medicine from Natural Products. *Molecules* **2016**, *21*, 559. <https://doi.org/10.3390/molecules21050559>.
96. Nagula, R. L.; Wairkar, S. Recent Advances in Topical Delivery of Flavonoids: A Review. *J. Control. Release* **2019**, *296* (December 2018), 190–201. <https://doi.org/10.1016/j.jconrel.2019.01.029>.
97. Jarrahpour, A.; Fathi, J.; Mimouni, M.; Hadda, T. Ben; Sheikh, J.; Chohan, Z.; Parvez, A. Petra, Osiris and Molinspiration (POM) together as a successful support in drug design: Antibacterial activity and biopharmaceutical characterization of some azo Schiff bases. *Med. Chem. Res.* **2012**, *21* (8), 1984–1990. <https://doi.org/10.1007/s00044-011-9723-0>.
98. Baskar, V.; Jayalakshmi, C.; Pavithra, N.; Veronica Grite, S. Validating therapeutically active phytochemical compounds for anti-ageing by in silico pharmacokinetic approach. *J. Biol. Inf. Sci.* **2014**, *3* (1), 1–7.
99. Sladek, F. What are Nuclear Receptor Ligands? *Mol Cell Endocrinol.* **2011**, *334* (1–2), 3–13. <https://doi.org/10.1016/j.mce.2010.06.018>.What.
100. Abdel-Mottaleb, M. M.; Try, C.; Pellenquer, Y.; Lamprecht, A. Nanomedicine Strategies for Targeting Skin Inflammation. *Nanomedicine* **2014**, *9* (11), 1–20. <https://doi.org/https://doi.org/10.2217/nnm.14.74>.
101. Chaiyana, W.; Anuchapreeda, S.; Leelapornpisid, P.; Phongpradist, R.; Viernstein, H.; Mueller, M. Development of Microemulsion Delivery System of Essential Oil

- from Zingiber cassumunar Roxb. Rhizome for Improvement of Stability and Anti-Inflammatory Activity. *AAPS PharmSciTech* **2017**, *18* (4), 1332–1342. <https://doi.org/10.1208/s12249-016-0603-2>.
102. Saraf, S. Applications of Novel Drug Delivery System for Herbal Formulations. *Fitoterapia* **2010**, *81* (7), 680–689. <https://doi.org/10.1016/j.fitote.2010.05.001>.
 103. Noor El-Din, M. R.; El-Hamouly, S. H.; Mohamed, H. M.; Mishrif, M. R.; Ragab, A. M. Water-in-Diesel Fuel Nanoemulsions: Preparation, Stability and Physical Properties. *Egypt. J. Pet.* **2013**, *22* (4), 517–530. <https://doi.org/10.1016/j.ejpe.2013.11.006>.
 104. Gasperlin, M.; Tusar, L.; Tusar, M.; Smid-Korbar, J.; Zupan, J.; Kristl, J. Viscosity Prediction of Lipophilic Semisolid Emulsion Systems by Neural Network Modelling. *Int. J. Pharm.* **2000**, *196*, 37–50.
 105. McClements, D. J. Edible Nanoemulsions : Fabrication , Properties , and Functional Performance. *Soft Matter* **2011**, *7*, 2297–2316. <https://doi.org/10.1039/c0sm00549e>.
 106. Heng, D.; Cutler, D. J.; Chan, H. K.; Yun, J.; Raper, J. A. What is a Suitable Dissolution Method for Drug Nanoparticles? *Pharm. Res.* **2008**, *25* (7), 1696–1701. <https://doi.org/10.1007/s11095-008-9560-0>.
 107. Eby, J. M.; Majetschak, M. Effects of ethanol and ethanol metabolites on intrinsic function of mesenteric resistance arteries. *PLoS One* **2019**, *14* (3), 1–13. <https://doi.org/10.1371/journal.pone.0214336>.
 108. Xiao, S.; Yu, H.; Xie, Y.; Guo, Y.; Fan, J.; Yao, W. The anti-inflammatory potential of Cinnamomum camphora (L.) J.Presl essential oil in vitro and in vivo. *J. Ethnopharmacol.* **2021**, *267* (April), 113516. <https://doi.org/10.1016/j.jep.2020.113516>.
 109. Giongo, J. L.; de Almeida Vaucher, R.; Sagrillo, M. R.; Vianna Santos, R. C.; Duarte, M. M. M. F.; Rech, V. C.; Soares Lopes, L. Q.; Beatriz da Cruz, I.; Tatsch, E.; Moresco, R. N.; et al. Anti-inflammatory effect of geranium nanoemulsion macrophages induced with soluble protein of Candida albicans. *Microb. Pathog.* **2017**, *110*, 694–702. <https://doi.org/10.1016/j.micpath.2017.01.056>.
 110. Wang, H.; Peters, T.; Kess, D.; Sindrilaru, A.; Oreshkova, T.; Van Rooijen, N.;

- Stratis, A.; Renkl, A. C.; Sunderkötter, C.; Wlaschek, M.; et al. Activated macrophages are essential in a murine model for T cell-mediated chronic psoriasiform skin inflammation. *J. Clin. Invest.* **2006**, *116* (8), 2105–2114. <https://doi.org/10.1172/JCI27180>.
111. Owona, B. A.; Abia, W. A.; Moundipa, P. F. Natural compounds flavonoids as modulators of inflammasomes in chronic diseases. *Int. Immunopharmacol.* **2020**, *84* (March), 106498. <https://doi.org/10.1016/j.intimp.2020.106498>.
112. Wohlrab, J. Topical preparations and their use in dermatology. *JDDG - J. Ger. Soc. Dermatology* **2016**, *14* (11), 1061–1071. <https://doi.org/10.1111/ddg.13151>.
113. Bustos-Salgado, P.; Andrade-Carrera, B.; Domínguez-Villegas, V.; Rodríguez-Lagunas, M. J.; Boix-Montañes, A.; Calpena-Campmany, A.; Garduño-Ramírez, M. L. Biopharmaceutic study and in vivo efficacy of natural and derivatives flavanones formulations. *Nanomedicine* **2021**, *16* (3), 368. <https://doi.org/https://doi.org/10.2217/nmm-2020-0368>.

ANNEXED

“Quantification of One Prenylated Flavanone from *Eysenhardtia platycarpa* and Four Derivatives in *Ex Vivo* Human Skin Permeation Samples Applying a Validated HPLC Method”

Paola Bustos-Salgado¹, Berenice Andrade-Carrera², Ma. Luisa. Garduño-Ramírez³, Helen Alvarado¹ and Ana Calpena-Campmany^{1,4, *}

¹ Department of Pharmacy and Pharmaceutical Technology and Physical Chemistry, Faculty of Pharmacy and Food Science, University of Barcelona, Joan XXIII Av. 29-31, Barcelona 08028, Spain.

² Facultad de Ciencias Química e Ingeniería, Universidad Autónoma del Estado de Morelos; Av. Universidad 1001, Cuernavaca, Morelos, México.

³ Centro de Investigaciones Químicas, Instituto de Investigación en Ciencias Básicas y Aplicadas, Universidad Autónoma del Estado de Morelos; Av. Universidad 1001 Cuernavaca, Morelos, México.

⁴ Institute of Nanoscience and Nanotechnology (IN²UB), University of Barcelona, Spain.

Revista: *Biomoleculas* (MDPI) ISSN: 2218-273X

Año de publicación: 2020

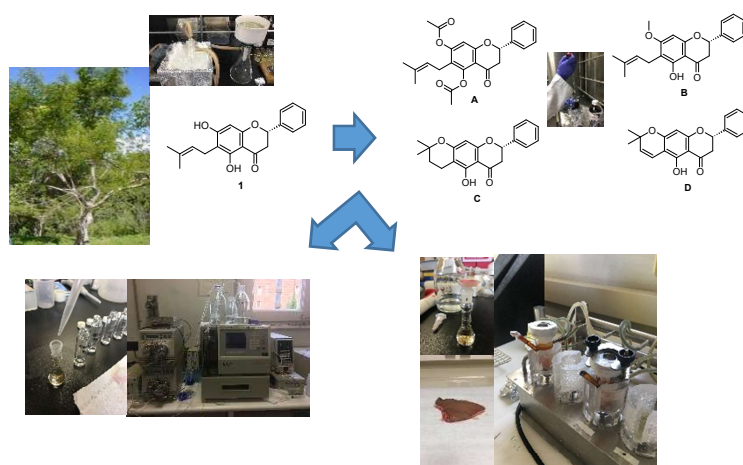
Factor de impacto: JCR: 4.082 (Datos del año 2019)

Percentil: JCR Categoría Q2 (Biochemistry & Molecular Biology),

DOI: 10.3390/biom10060889

Resumen

En este artículo se enfocaron los esfuerzos en obtener un método de validación por la técnica de HPLC (cromatografía de alta eficacia) para la cuantificación de las flavanonas **1**, **A-D** aplicadas en estudios biofarmacéuticos. El método mostró ser lineal con coeficientes de correlación $R^2 > 0.999$ en un rango de concentraciones de 1.56 a 200 $\mu\text{g/mL}$ con bajos límites de detección y cuantificación en promedio de 0.4 y 1.2 $\mu\text{g/mL}$ respectivamente para todas las flavanonas. El método también resultó ser exacto y preciso con valores de error relativo y desviación estándar relativa menores al 15 %. La desviación estándar relativa de la repetibilidad del sistema instrumental fue menor al 0.6 % para todas las flavanonas. La aplicabilidad del método de cuantificación de las flavanonas en muestras provenientes de permeación de piel humana fue establecido utilizando el sistema de celdas de Franz. No se encontraron interferencias debidas a los componentes de la piel humana utilizando el método analítico propuesto.



Article

Quantification of One Prenylated Flavanone from *Eysenhardtia platycarpa* and Four Derivatives in Ex Vivo Human Skin Permeation Samples Applying a Validated HPLC Method

Paola Bustos-Salgado ¹, Berenice Andrade-Carrera ², María Luisa Garduño-Ramírez ³,
Helen Alvarado ¹ and Ana Calpena-Campmany ^{1,4,*}

¹ Department of Pharmacy and Pharmaceutical Technology and Physical Chemistry, Faculty of Pharmacy and Food Science, University of Barcelona, Joan XXIII Av. 29–31, 08028 Barcelona, Spain; pbustosa19@alumnes.ub.edu (P.B.-S.); hl_alvarado@ub.edu (H.A.)

² Facultad de Ciencias Química e Ingeniería, Universidad Autónoma del Estado de Morelos, Av. Universidad 1001, Cuernavaca 62209, Morelos, Mexico; bereniceac@uaem.mx

³ Centro de Investigaciones Químicas, Instituto de Investigación en Ciencias Básicas y Aplicadas, Universidad Autónoma del Estado de Morelos, Av. Universidad 1001 Cuernavaca, Cuernavaca 62209, Morelos, Mexico; lgarduno@ciq.uaem.mx

⁴ Institute of Nanoscience and Nanotechnology (IN²UB), University of Barcelona, 08007 Barcelona, Spain

* Correspondence: anacalpena@ub.edu; Tel.: +34-934-02-4578

Received: 8 April 2020; Accepted: 2 June 2020; Published: 10 June 2020

Abstract: Prenylated flavanones are polyphenols that have diverse biological properties. The present paper focuses on a HPLC method validation for the quantification of prenylated flavanones (2*S*)-5,7-dihydroxy-6-(3-methyl-2-buten-1-yl)-2-phenyl-2,3-dihydro-4*H*-1-Benzopyran-4-one **1** and derivatives (2*S*)-5,7-bis(acetyloxy)-6-(3-methyl-2-buten-1-yl)-2-phenyl-2,3-dihydro-4*H*-1-Benzopyran-4-one **A**; (2*S*)-5-hydroxy-7-methoxy-6-(3-methyl-2-buten-1-yl)-2-phenyl-2,3-dihydro-4*H*-1-Benzopyran-4-one **B**; (8*S*)-5-hydroxy-2,2-dimethyl-8-phenyl-3,4,7,8-tetrahydro-2*H*,6*H*-Benzo[1,2-*b*:5,4-*b'*]dipyran-6-one **C**; and (8*S*)-5-hydroxy-2,2-dimethyl-8-phenyl-7,8-dihydro-2*H*,6*H*-Benzo[1,2-*b*:5,4-*b'*]dipyran-6-one **D** applied in biopharmaceutic studies. The linear relationships are proven with significant correlation coefficients ($R^2 > 0.999$) in the range of 1.56 to 200 $\mu\text{g/mL}$ with low limits of detection and quantification, on average of 0.4 $\mu\text{g/mL}$ and 1.2 $\mu\text{g/mL}$, respectively. The validation method used in this work is highly accurate and precise, with values lower than 15%. The relative standard deviation values of repeatability of the instrumental system are demonstrated with less than 0.6% for all studied flavanones. Therefore, the applicability method of the quantification of the prenylated flavanones was established using the permeation of human skin in the Franz cell system. During the method previously described, there was no interference observed from human skin components in ex vivo permeation studies.

Keywords: prenylated flavanones; HPLC; ex vivo permeation; bioanalytical method validation

1. Introduction

Prenylated flavanones are part of a diverse class of natural flavonoids conformed of oxygen-containing heterocycles and prenyl substituents. They have proven to have antibacterial and anti-fungal properties conferring protection to plants against diseases [1–4]. Nowadays, several studies have confirmed their biological effects against oxidation, obesity, and inflammation, which may be useful in the prevention of several diseases, including cancer [5–7].

The genus *Eysenhardtia* comprises 14 species, and some of them, including *E. platycarpa*, which contains prenylated flavanones, are widely used in traditional Mexican medicine for the treatment of

kidney and bladder infections [8]. *E. platycarpa* is a tree found throughout southern Mexico and is popularly known as “taray”, “palo dulce” and “palo azul”. Previous studies on *Eysenhardtia* species have highlighted hypoglycemic and antidiabetic properties [9]. The antioxidant activity of the alcoholic extract of *E. platycarpa* was also confirmed [10,11]. Domínguez-Villegas et al. isolated five flavanones from a methanolic extract obtained from the aerial parts of *E. platycarpa*, one of them were (2*S*)-5,7-dihydroxy-6-(3-methyl-2-buten-1-yl)-2-phenyl-2,3-dihydro-4*H*-1-Benzopyran-4-one **1** (Figure 1). The formerly mentioned compounds proved to have anti-inflammatory activity. Furthermore, flavanones revealed a high percentage reduction of free radical DPPH (2,2-Diphenyl-1-picrylhydrazyl), and thus exhibited strong cytotoxic activity on brine shrimp [12].

In addition, the prenylated flavanone **1**, as well as its derivatives obtained from structural modifications: (2*S*)-5,7-bis(acetyloxy)-6-(3-methyl-2-buten-1-yl)-2-phenyl-2,3-dihydro-4*H*-1-Benzopyran-4-one **A**; (2*S*)-5-hydroxy-7-methoxy-6-(3-methyl-2-buten-1-yl)-2-phenyl-2,3-dihydro-4*H*-1-Benzopyran-4-one **B**; (8*S*)-5-hydroxy-2,2-dimethyl-8-phenyl-3,4,7,8-tetrahydro-2*H*,6*H*-Benzo[1,2-*b*:5,4-*b'*]dipyran-6-one **C**; and (8*S*)-5-hydroxy-2,2-dimethyl-8-phenyl-7,8-dihydro-2*H*,6*H*-Benzo[1,2-*b*:5,4-*b'*]dipyran-6-one **D** (Figure 1); were loaded into polymeric nanoparticles exhibiting cytotoxic potential against pancreatic cell line MiaPaCa-2 [13].

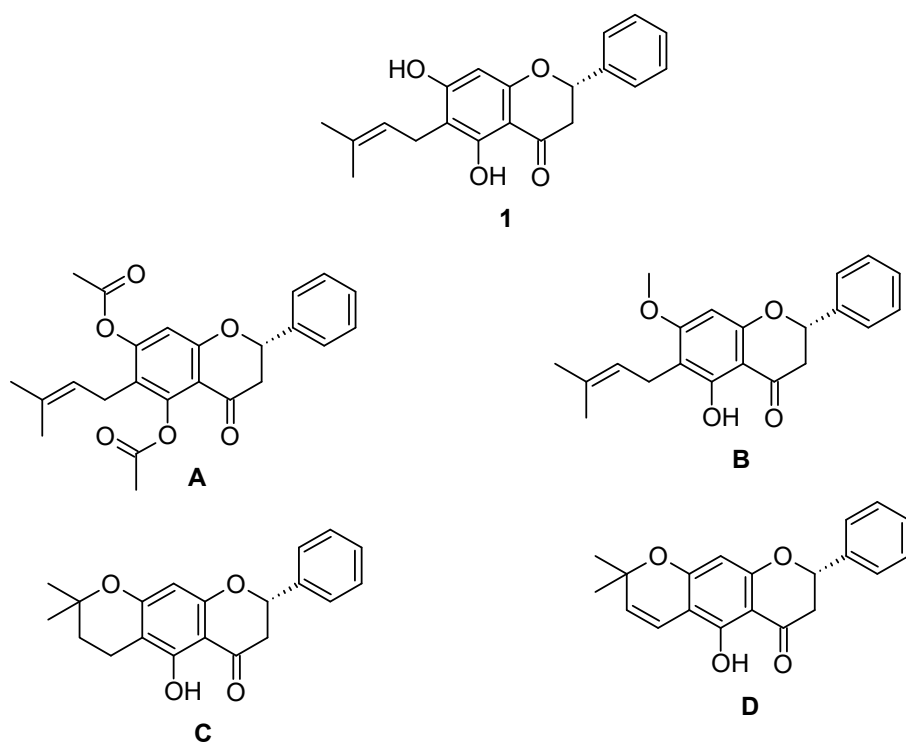


Figure 1. Chemical structures of studied compounds. (2*S*)-5,7-dihydroxy-6-(3-methyl-2-buten-1-yl)-2-phenyl-2,3-dihydro-4*H*-1-Benzopyran-4-one (**1**); (2*S*)-5,7-bis(acetyloxy)-6-(3-methyl-2-buten-1-yl)-2-phenyl-2,3-dihydro-4*H*-1-Benzopyran-4-one (**A**); (2*S*)-5-hydroxy-7-methoxy-6-(3-methyl-2-buten-1-yl)-2-phenyl-2,3-dihydro-4*H*-1-Benzopyran-4-one (**B**); (8*S*)-5-hydroxy-2,2-dimethyl-8-phenyl-3,4,7,8-tetrahydro-2*H*,6*H*-Benzo[1,2-*b*:5,4-*b'*]dipyran-6-one (**C**); and (8*S*)-5-hydroxy-2,2-dimethyl-8-phenyl-7,8-dihydro-2*H*,6*H*-Benzo[1,2-*b*:5,4-*b'*]dipyran-6-one (**D**).

The increasing interest in the medicinal properties of flavanones, with specific anti-inflammatory activity on skin diseases [14], has led to a demand for accurate, reproducible, and sensitive analytical methods to quantify new compounds that have not been validated yet. High-performance liquid chromatography (HPLC) is the most widely used separation method for quantifying phenolic compounds [15,16]. The conditions include mainly the use of C18 reverse phase

columns and a diode array and a fluorescence detector. Aqueous solutions and acetonitrile or methanol are usually the mobile phases. Notwithstanding, there are HPLC validated methods to quantify compounds similar to flavanones assayed [17]. The present job focused on the validation method of unpublished molecules prenylated flavanone **1** extracted from *E. platycarpa* and its derivatives **A–D**; considering the human skin as the principal biologic matrix. Moreover, this method was used to determine the concentration of prenylated flavanones in permeation and retention samples of ex vivo diffusional studies, using human skin and following bioanalytical guidelines to evaluate their intrinsic permeation, before they were analyzed in vivo as potential anti-inflammatory drugs candidates.

2. Materials and Methods

2.1. Chemicals and Reagents

The purified water used in all experiments was obtained from the MilliQ® Plus System lab supply. All other chemical reagents used in this study were purchased from Fisher Scientific (Leicestershire, UK). The solvents were appropriately filtered through a 0.45 µm Millipore membrane filter (Merck, Darmstadt, Germany) and degassed in an ultrasonic bath for 20 min.

2.2. Extraction and Isolation of Plant Material

E. platycarpa leaves were collected in Tetipac, Guerrero, Mexico, and identified by Prof. Ramiro Cruz (Registration Number: Ramiro Cruz 1325 from the Sciences Faculty Herbarium Facilities of the Autonomous University of the State of Morelos). The leaves were dried at room temperature, then pulverized and extracted by three consecutive macerations with methanol at room temperature (100g of dried vegetal material per 1000 mL methanol). The extraction solvent was removed under reduced pressure. Next, the prenylated flavanone **1** was isolated by column chromatography at reduced pressure. Finally, it was purified and characterized by direct thin-layer chromatography (TLC) comparison with original samples available in the laboratory. The product was a yellow powder precipitate with a melting point of 200.2 °C. The compound obtained was characterized by comparison with previously published melting point data and with ¹H-NMR results [9].

2.3. Semi-synthesis from Natural Prenylated Flavanone

Each prenylated flavanone was prepared following the method as previously reported [13] getting (2*S*)-5,7-bis(acetyloxy)-6-(3-methyl-2-buten-1-yl)-2-phenyl-2,3-dihydro-4*H*-1-Benzopyran-4-one **A**; (2*S*)-5-hydroxy-7-methoxy-6-(3-methyl-2-buten-1-yl)-2-phenyl-2,3-dihydro-4*H*-1-Benzopyran-4-one **B**; (8*S*)-5-hydroxy-2,2-dimethyl-8-phenyl-3,4,7,8-tetrahydro-2*H*,6*H*-Benzo[1,2-*b*:5,4-*b'*]dipyran-6-one **C**; and (8*S*)-5-hydroxy-2,2-dimethyl-8-phenyl-7,8-dihydro-2*H*,6*H*-Benzo[1,2-*b*:5,4-*b'*]dipyran-6-one **D**.

2.4. Chromatographic Operating Conditions

The HPLC system consisted of a Waters 515 HPLC pump, a 717 Plus autosampler, and a dual λ absorbance UV-vis 2487 detector (Waters, Milford, MA, USA). The analytical column was Atlantis® C18 5 µm 250 mm × 4.6 mm, Waters. The analyte separation was performed with 10 µL sample injection volume. The separations were done in isocratic mode at room temperature. The mobile phase with a flow rate of 1 mL/min comprised of W-water and AcN-acetonitrile (%W: %AcN) with a different composition for each prenylated flavanone studied: **1** (30:70), **A** (20:80), **B** (40:60), **C** (20:80) and **D** (10:90). The detection wavelengths determined by spectrum scan were 300 nm for **1**, **B**, **C**, **D**, and 320 nm for **A**. The Peak area was used to quantify each analyte.

2.5. Ex Vivo Human Skin Permeation

A blank sample (ethanol: water; 70:30; v/v) was used as a negative control and the samples of prenylated flavanones (**1**, **A**, **B**, **C**, and **D**) with a concentration of 200 µg/mL were permeated through

human skin membrane in the receptor compartment of the Franz diffusion cells (FDC 400, Crown Glass, Somerville, NY, USA), with a diffusion area of 2.54 cm². Human skin from abdominal plastic surgery of healthy patients was used as a permeation membrane. The skin was cut into 400 µm thickness and placed between the donor, and the receptor compartment of the Franz diffusion cells, avoiding the formation of bubbles [18]. The flavanone samples **1**, **A**, **B**, **C**, and **D** (300 µL) were applied to the donor compartment and the receptor compartment was filled with ethanol: water (70:30) solution. The receptor compartment was kept at 32 ± 1 °C. Twenty-four h after the application of the tests, 300 µL aliquots were collected from the receptor side. Sink conditions were always followed. The flavanones amount permeated (Q) through human skin were determined by HPLC analysis described in Section 2.4.

2.6. Prenylated Flavanone Extraction

At the end of the ex vivo human skin permeation study, the flavanones amounts remaining in the skin were quantified by calculating the flavanone amount extracted from the skin to the flavanone amount added. For this purpose, the skin was removed from the Franz cells, cleaned with gauze soaked in a 0.05% solution of dodecyl sulfate and washed with distilled water. The permeated areas of the skin were then excised and weighed. The flavanone contained in the skin was extracted with ethanol: water (70:30) mixture under sonication (20 min) in an ultrasonic bath. The resulting solutions were measured with HPLC, quantifying the flavanone amount retained in the skin in micrograms of prenylated flavanone per grams of skin and per area unit µg/g_{skin}.cm²).

2.7. Recovery from Human Skin Tissues and Prenylated Flavanone Retained

The accuracy of the extraction was evaluated by adding 1 mL of each prenylated flavanone solution (200 µg/mL) to their corresponding vials containing approximately 100 mg of human skin. These vials remained for 24 h at 32 °C to simulate the permeation conditions experiments. This experiment was conducted in triplicate. After the time of the study, the skin was submitted to drug extraction, as described in Section 2.6. The initial solutions and the eluates from each assay were collected and analyzed with HPLC. The differences obtained between the initial flavanone amount in the solution and the final flavanone amount in the collected solutions after 24 h were considered to be the value of the respective flavanone amount bound to tissue. Recovery percentage was calculated comparing the corresponding drug extraction results with the flavanone amount bound to the tissue [19]. A comparison of the amount of prenylated flavanone extracted and the recovery percentage was made in order to find out the real amount of flavanone retained in the skin.

2.8. Analytical Method Validation

The method was validated according to the International Conference on Harmonization guidelines (ICH) [20,21] for linearity, the limit of detection (LOD), the limit of quantification (LOQ), accuracy, and precision. Calibration curves were analyzed in two ranges; from 200 to 12.5 µg/mL in a high concentration level, and from 12.5 to 1.56 µg/mL in a low concentration level.

2.8.1. Standard Solutions for Calibration Curves

Standard stock solutions of each compound (**1**, **A**, **B**, **C**, and **D**) were prepared daily by dissolving the appropriate amount of each analyte in ethanol: water (7:3; v/v) to obtain a final concentration of (200 µg/mL). The working solutions were elaborated by the dilution of appropriate aliquots of the stock solutions with the diluting solvent to reach the concentration ranges 1.56, 3.12, 6.25, 12.5, 25, 50, 100 µg/mL.

2.8.2. Linearity

The linearity was evaluated by a one-way analysis of variance (ANOVA) test to compare peak areas versus nominal concentrations of each standard [22]. Differences were considered statistically significant when $p < 0.05$. The least-square linear regression analysis and mathematical

determinations were performed by Prism, V 5.0 software (Graph Pad Software Inc., San Diego, CA, USA).

2.8.3. Limit of Detection and Limit of Quantification

The limit of detection (LOD) and the limit of quantitation (LOQ) for each analyte (**1**, **A**, **B**, **C**, and **D**) were calculated based on the standard deviation of the response and the slope of the calibration curve, generated from six replicate analysis applying the formula 1 [23]:

$$LOD \text{ or } LOQ = k \frac{SD_{Sa}}{S_b} \quad (1)$$

where k is the factor related to the level of confidence ($k = 3.3$ and 10 for LOD and LOQ respectively), SD_{Sa} is the standard deviation of the intercept, and S_b is the slope.

2.8.4. Repeatability, Accuracy, and Precision

The instrumental repeatability was assayed by analyzing the concentration sample of $200 \mu\text{g/mL}$ for each flavanone (**1**, **A**, **B**, **C**, and **D**) repeatedly seven times, consecutively. The accuracy and precision were investigated by measuring samples in three concentrations 1.56 , 12.5 , and $200 \mu\text{g/mL}$ [24]. The inter-day test was conducted by analyzing each analyte (**1**, **A**, **B**, **C**, and **D**) with each of the three concentration levels mentioned before, once a day for six consecutive days. The accuracy was expressed as a relative error (RE%). The precision was defined as the relative standard deviation (RSD%) of the measurement. The method is considered accurate and precise if RE% and RSD%, respectively, are within $\pm 15\%$.

2.8.5. Specificity

Specificity is defined as the ability of the method to distinguish the analyte from all other substances present in the sample. This can be proven by comparing the analyte chromatographic retention time in extracted matrix samples and with its retention time in at least one reference solution [19,25]. To test the specificity of the analytical method, the ex vivo human permeation procedure described in Section 2.5 was followed. The blank sample peaks should not appear at the same retention times of the prenylated flavanones.

3. Results and Discussions

Due to the fact of the biological properties of prenylated flavanones, it is of utmost importance to count on analytical method validation in order to promote future studies. HPLC is highly sensitive in the determination of small quantities of natural molecules in biopharmaceutical studies based on previous studies [22].

3.1. Analytical Method Validation

3.1.1. Linearity

The linearity of the analytical method is the capability over a range of data to obtain proportional results. The applied HPLC method for the flavanone's quantification (**1**, **A**, **B**, **C**, and **D**) showed satisfactory linearity in the tested concentrations. In order to have a better mathematical analysis, the linearity was evaluated in two concentration ranges: from 200 to $12.5 \mu\text{g/mL}$ and from 12.5 to $1.56 \mu\text{g/mL}$. Two linear calibration curves were fitted for each flavanone. The R^2 value for each analyte was found above 0.999 for all studied flavanones, indicating the linear relationship between the analyte concentration and the peak area. No statistical differences were found ($p > 0.05$) after the ANOVA test of the calibration curves of each flavanone **1**, **A**, **B**, **C**, and **D** with p values for each two levels of 0.12 and 0.08 , 0.93 and 0.08 , 0.38 and 0.47 , 0.63 and 0.56 , and 0.53 and 0.46 , respectively (see Table 1).

Table 1. Linearity (expressed in R^2 and p with two ranges, one by row), Precision, Accuracy (calculated at maximum, medium, and minimum concentration values), and Repeatability of the HPLC Method for the determination of flavanones.

Compound	Linearity		LOD	LOQ	Accuracy	Precision	R.I.S
	R^2	p					
	200–12.5 ($\mu\text{g/mL}$)	12.5–1.56 ($\mu\text{g/mL}$)	Mean ($\mu\text{g/mL}$) \pm SD ($\mu\text{g/mL}$)	200 ($\mu\text{g/mL}$) 12.5 ($\mu\text{g/mL}$) 1.56 ($\mu\text{g/mL}$)	RE (%)	RSD (%)	RSD (%)
1	0.9998	0.12	0.51 ± 0.13	1.53 ± 0.38	–0.23	0.20	0.36
	0.9991	0.08					
A	0.9997	0.93	0.28 ± 0.10	0.84 ± 0.29	–0.09	0.09	0.54
	0.9997	0.08					
B	0.9998	0.38	0.49 ± 0.12	1.48 ± 0.36	0.46	0.27	0.43
	0.9990	0.47					
C	0.9999	0.63	0.48 ± 0.43	1.45 ± 1.30	–0.19	0.29	0.37
	0.9996	0.56					
D	0.9999	0.53	0.30 ± 0.08	0.91 ± 0.24	–0.01	0.21	0.32
	0.9997	0.46					
					4.15	1.12	
					3.74	0.42	

LOD = limit of detection; LOQ = limit of quantitation; RE = relative error; RSD = relative standard deviation; and R.I.S = Repeatability of Instrumental System.

3.1.2. Limit of Detection and Limit of Quantification

LODs and LOQs for all the investigated flavanones were calculated using the response standard deviation and the calibration curve slope of 12.5 to 1.56 $\mu\text{g/mL}$ for each flavanone, described in Section 2.8.3. The values of LODs and LOQs for each flavanone are listed in Table 1. These results indicate that the method is sensitive enough for flavanones determination in the range of 1.56 to 200 $\mu\text{g/mL}$.

3.1.3. Repeatability, Accuracy, and Precision

Precision and accuracy values were obtained from sample analyses of the 1.56, 12.5, and 200 $\mu\text{g/mL}$ flavanones concentrations (**1**, **A**, **B**, **C**, and **D**). The inter-day precision and accuracy were calculated after analyzing the samples on six different days. The results are reported in Table 1. Both parameters were lower than the 15 % limit value in EMA (European Medicines Agency) guidelines. These results suggest that the proposed method has satisfactory accuracy and precision. Repeatability studies of the instrumental system showed RSD % not greater than 0.6% for all flavanones.

3.1.4. Specificity

The analytical methodology was implemented for the flavanone's quantitation (**1**, **A**, **B**, **C**, and **D**) in skin permeation studies. In order to show the specificity, 300 μL of the flavanones at 200 $\mu\text{g/mL}$ concentration was permeated into human skin using Franz cells. The amount of each flavanone normalized by the surface (Q) in the receptor compartment during percutaneous permeation experiments ($n = 3$) is indicated in Table 2. Percentages of permeation were calculated, accounting for the experimental flavanone content of each assay. At the end of each experiment, skin samples were removed from the diffusion cell, flavanones amount retained (Q_{ret}) were quantified as previously described and expressed in micrograms of prenylated flavanone per grams of skin and per area unit ($\mu\text{g/g}_{\text{skin}} \cdot \text{cm}^2$) in Table 2. As shown in Table 2, the prenylated flavanone **1** is the one which most permeates, followed by **D** and **C**. In the case of **A** and **B**, Q was detectable but not quantifiable because their values were below LOQ determinate before (see Table 1). On the contrary, **A** and **B** are found

retained in the skin in a greater amount, so we can infer that it is possible that these molecules have greater interactions with the different skin components due to their physicochemical characteristics. Therefore, they have prevented permeation as **1**, **C**, and **D** did too.

Table 2. Results of the permeation studies expressed by mean and SD ($n = 3$).

Compound	24 h Permeated Amount	Degree Of Permeation	Recovery	Skin Retention
	Q ($\mu\text{g}/\text{cm}^2$)	(%)	(%)	Q _{ret} ($\mu\text{g}/\text{g}\cdot\text{cm}^2$)
1	1.29 ± 0.12	2.15	46.20 ± 6.46	50.22 ± 7.51
A	NQ	NQ	0.38 ± 0.05	321.52 ± 45.23
B	NQ	NQ	3.43 ± 0.5	381.75 ± 57.26
C	0.75 ± 0.07	1.26	NQ	23.78 ± 5.46 *
D	0.91 ± 0.08	1.52	38.1 ± 5.23	116.14 ± 17.24

¹ NQ = non quantifiable; value below LOQ, * skin extracted not corrected by percentage recovery.

The chromatograms showed the absence of interference of any other peak corresponding to each flavanone (Figure 2: 1_a, 1_b; A_a, A_b; B_a, B_b; C_a, C_b; D_a, D_b). Furthermore, no interference from the human skin components assays were observed during the analysis in the ex vivo permeation studies (Figure 2: 1_c, 1_d; A_c, A_d; B_c, B_d; C_c, C_d; D_c, D_d).

3.1.5. Recovery

Flavanone extraction was done, as described in Section 2.6. Recovery was calculated comparing the corresponding extraction result with the amount of flavanone bound to the skin. The results were reported as the mean value of the percentage between the amount of flavanone in each sample and the weight of the skin sample (see in Table 2). The aforementioned results show the real quantity for each prenylated flavanone that can be recovered using the extraction method previously described. Thus, the exact quantity of flavanone retained can be known, and this quantity is responsible for the exercising of the biological effect.

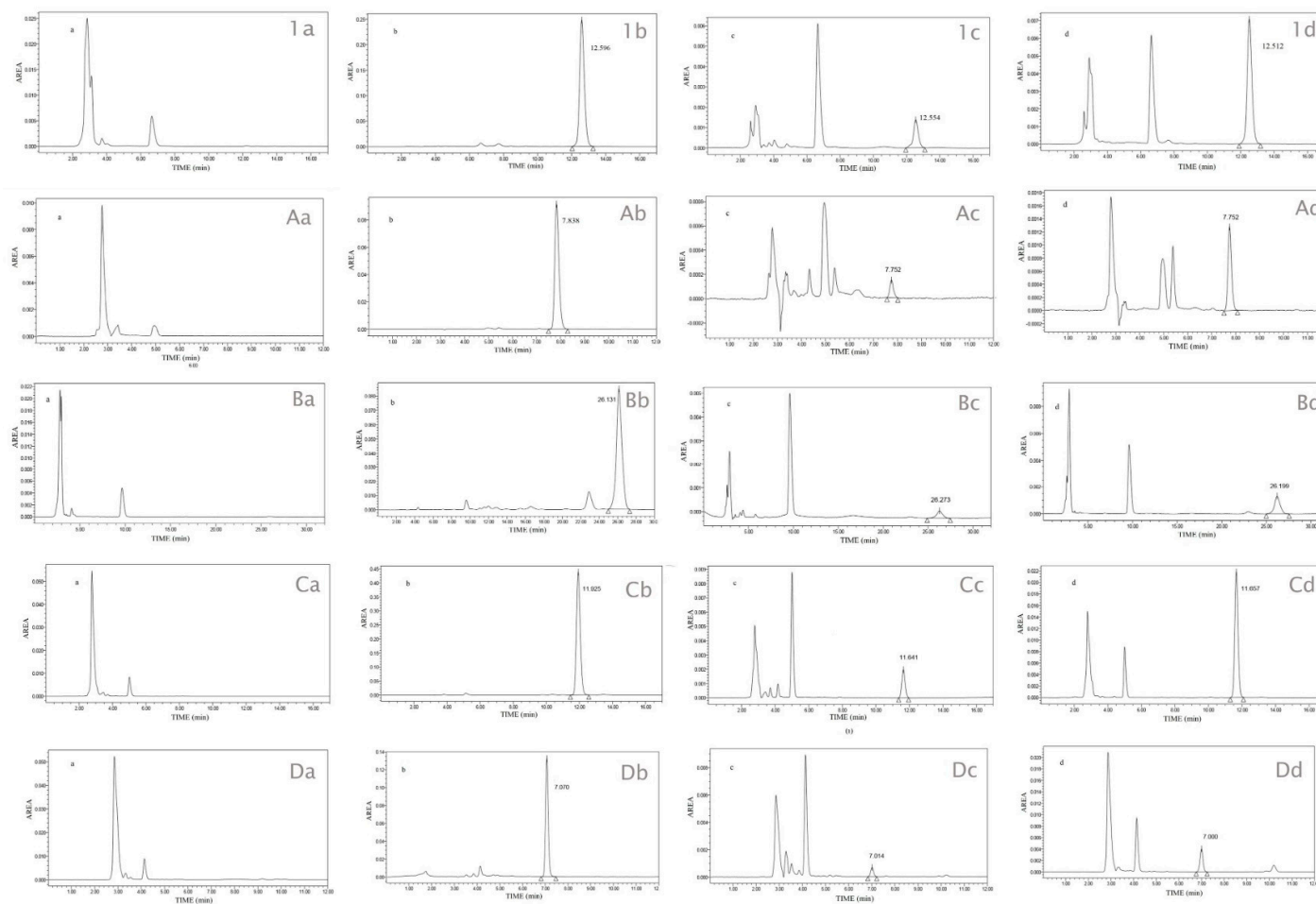


Figure 2. HPLC chromatograms of prenylated flavanones **1**, **A–D** classified with sub-index a, b, c, and d. a correspond to: Blank sample (ethanol: water, 70:30) permeated at chromatographic conditions of each prenylated flavanone; b correspond to prenylated flavanone standard; c correspond to prenylated flavanone from receptor compartment Franz diffusion cells; and, d correspond to prenylated flavanone extracted from human skin after permeation study.

4. Conclusions

The results in the present research describe a liquid chromatographic method validation for the analysis of prenylated flavanones **1, A–D** using UV-VIS detection. According to the data obtained, the method developed is linear, accurate, and precise. In addition, the method can be used in the quantification of prenylated flavanones samples from permeation and retention studies in human skin. Finally, the method is selective since the chromatograms allowed the observer to identify the signal for each prenylated flavanone without interference. We can conclude that this method is suitable for further analysis of prenylated flavanones **1, A–D** in biological systems, and for other biopharmaceutical studies.

Author Contributions: Conceptualization, P.B.-S.; validation, P.B.-S., B.A.-C. and H.A.; formal analysis, P.B.-S.; investigation, P.B.-S.; resources, A.C.-C. and M.L.G.-R.; writing—original draft preparation, P.B.-S., H.A., M.L.G.-R. and A.C.-C.; writing—review and editing, P.B.-S., B.A.-C., H.A., M.L.G.-R. and A.C.-C.; supervision, M.L.G.-R. and A.C.-C.; project administration, A.C.-C.; funding acquisition, P.B.-S. All authors have read and agreed to the published version of the manuscript.

Acknowledgments: The authors would like to thank CONACyT- México (grant number 709906) and acknowledge Silvia Nicolàs, Galia Lombardo, and Uriel Robles for their help in the review of the English language use.

Conflicts of Interest: The authors declare no conflict of interest. The funders had no role in the design of the study; in the collection, analyses, or interpretation of data; in the writing of the manuscript, or in the decision to publish the results.

References

1. Sohn, H.Y.; Son, K.H.; Kwon, C.S.; Kwon, G.S.; Kang, S.S. Antimicrobial and Cytotoxic Activity of 18 Prenylated Flavonoids Isolated from Medicinal Plants: *Morus alba* L., *Morus mongolica* Schneider, *Broussonetia papyrifera* (L.) Vent, *Sophora flavescens* Ait and *Echinosophora koreensis* Nakai. *Phytomedicine* **2004**, *11*, 666–672.
2. Li, J.; Chen, R.; Wang, R.; Liu, X.; Xie, K.; Chen, D.; Dai, J. Biocatalytic Access to Diverse Prenyl Flavonoids by Combining a Regiospecific C-Prenyltransferase and a Stereospecific Chalcone Isomerase. *Acta Pharm. Sinica* **2018**, *8*, 678–686.
3. Chen, X.; Mukwaya, E.; Wong, M.S.; Zhang, Y. A Systematic Review on Biological Activities of Prenylated Flavonoids. *Pharm. Biol.* **2014**, *52*, 655–660, doi:10.3109/13880209.2013.853809.
4. Sasaki, H.; Kashiwada, Y.; Shibata, H.; Takaishi, Y. Prenylated Flavonoids from *Desmodium caudatum* and Evaluation of Their Anti-MRSA Activity. *Phytochemistry* **2012**, *82*, 136–142.
5. Brewer, M.S. Natural Antioxidants: Sources, Compounds, Mechanisms of Action, and Potential Applications. *Compr. Rev. Food Sci. Food Saf.* **2011**, *10*, 221–247.
6. Venturelli, S.; Burkard, M.; Biendl, M.; Lauer, U.M.; Frank, J.; Busch, C. Prenylated Chalcones and Flavonoids for the Prevention and Treatment of Cancer. *Nutrition* **2016**, *32*, 1171–1178.
7. Yang, X.; Jiang, Y.; Yang, J.; He, J.; Sun, J.; Chen, F.; Zhang, M.; Yang, B. Prenylated Flavonoids, Promising Nutraceuticals with Impressive Biological Activities. *Trends Food Sci. Technol.* **2015**, *44*, 93–104.
8. Gopi, S.; Amalraj, A. Introduction of Nanotechnology in Herbal Drugs and Nutraceutical: A Review. *J. Nanomedicine. Biotherapeutic Discov.* **2016**, *6*, 1–8.
9. Narváez-Mastache, J.M.; Garduño-Ramírez, M.L.; Alvarez, L.; Delgado, G. Antihyperglycemic Activity and Chemical Constituents of *Eysenhardtia platycarpa*. *J. Nat. Prod.* **2006**, *69*, 1687–1691.
10. Narváez Mastache, J.M.; Soto, C.; Delgado, G. Antioxidant Evaluation of *Eysenhardtia* Species (Fabaceae): Relay Synthesis of 3- O -Acetyl-11 α , 12 α -Epoxy-Oleanan-28, 13 β -Olide Isolated from *E. platycarpa* and Its Protective Effect in Experimental Diabetes. *Biol. Pharm. Bull.* **2007**, *30*, 1503–1510.
11. Pérez Gutierrez, R.M.; García Baez, E. Evaluation of Antidiabetic, Antioxidant and Antiglycating Activities of the *Eysenhardtia polystachya*. *Pharmacogn. Mag.* **2014**, *10*, 404–418.
12. Domínguez-Villegas, V.; Domínguez-Villegas, V.; García, M.L.; Calpena, A.; Clares-Naveros, B.; Garduño-Ramírez, M.L. Anti-Inflammatory, Antioxidant and Cytotoxicity Activities of Methanolic Extract and Prenylated Flavanones Isolated from Leaves of *Eysenhardtia platycarpa*. *Nat. Prod. Commun.* **2013**, *8*, 177–180.

13. Andrade-Carrera, B.; Clares, B.; Noé, V.; Mallandrich, M.; Calpena, A.; García, M.; Garduño-Ramírez, M. Cytotoxic Evaluation of (2S)-5,7-Dihydroxy-6-Prenylflavanone Derivatives Loaded PLGA Nanoparticles against MiaPaCa-2 Cells. *Molecules* **2017**, *22*, 1553.
14. Alalaiwe, A.; Lin, C.; Hsiao, C.; Chen, E.; Lin, C. Development of Flavanone and Its Derivatives as Topical Agents against Psoriasis: The Prediction of Therapeutic Efficiency through Skin Permeation Evaluation and Cell-Based Assay. *Int. J. Pharm.* **2020**, *581*, 119256.
15. Pyrzynska, K.; Sentkowska, A. Recent Developments in the HPLC Separation of Phenolic Food Compounds. *Crit. Rev. Anal. Chem.* **2015**, *45*, 41–51.
16. Villiers, A.; De Venter, P.; Pasch, H. Recent Advances and Trends in the Liquid-Chromatography–Mass Spectrometry Analysis of Flavonoids. *J. Chromatogr. A* **2016**, *1430*, 16–78.
17. Sus, N.; Schlienz, J.; Calvo-Castro, L.A.; Burkard, M.; Venturelli, S.; Busch, C.; Frank, J. Validation of a Rapid and Sensitive Reversed-Phase Liquid Chromatographic Method for the Quantification of Prenylated Chalcones and Flavanones in Plasma and Urine. *NFS J.* **2018**, *10*, 1–9.
18. Abrego, G.; Alvarado, H.; Souto, E.B.; Guevara, B.; Halbaut, L.; Luisa, M.; Luisa, M.; Calpena, A.C. Biopharmaceutical Profile of Hydrogels Containing Pranoprofen-Loaded PLGA Nanoparticles for Skin Administration: In Vitro, Ex Vivo and in Vivo Characterization. *Int. J. Pharm.* **2016**, *501*, 350–361.
19. Causon, R. Validation of Chromatographic Methods in Biomedical Analysis Viewpoint and Discussion. *J. Chromatogr. B Biomed. Sci. Appl.* **1997**, *689*, 175–180.
20. EMA, C. for M. P. for H. U. Guideline on Bioanalytical Method Validation. Available online: https://www.ema.europa.eu/en/documents/scientific-guideline/guideline-bioanalytical-method-validation_en.pdf (accessed on 9 October 2019).
21. Shabir, G.A. Validation of High-Performance Liquid Chromatography Methods for Pharmaceutical Analysis. *J. Chromatogr. A* **2003**, *987*, 57–66.
22. Alvarado, H.L.; Abrego, G.; Garduño-Ramírez, M.L.; Clares, B.; García, M.L.; Calpena, A.C. Development and Validation of a High-Performance Liquid Chromatography Method for the Quantification of Ursolic/Oleanic Acids Mixture Isolated from *Plumeria obtusa*. *J. Chromatogr. B Anal. Technol. Biomed. Life Sci.* **2015**, *983*, 111–116.
23. Surve, D.H.; Jindal, A.B. Development and Validation of Reverse-Phase High-Performance Liquid Chromatographic (RP-HPLC) Method for Quantification of Efavirenz in Efavirenz-Enfuvirtide Co-Loaded Polymer-Lipid Hybrid Nanoparticles. *J. Pharm. Biomed. Anal.* **2019**, *175*, 112765.
24. Abrego, G.; Alvarado, H.L.; Calpena-Campmany, A.C. Analysis of Pranoprofen Quantification in Ex Vivo Corneal and Scleral Permeation Samples: Analytical Validation. *J. Pharm. Biomed. Anal.* **2018**, *160*, 109–118.
25. Rozet, E.; Marini, R.D.; Ziemons, E.; Boulanger, B.; Hubert, P. Advances in Validation, Risk and Uncertainty Assessment of Bioanalytical Methods. *J. Pharm. Biomed. Anal.* **2011**, *55*, 848–858.



ARTÍCULO 2

“Biopharmaceutic Study and *In vivo* Efficacy of Natural and Derivatives Flavanones Formulations”



P. Bustos-Salgado^a, B. Andrade-Carrera^b, V. Domínguez-Villegas^b, María J. Rodríguez-Lagunas^c, A. Boix-Montañes^a, A. Calpena-Campmany^{*a,c}, M.L. Garduño-Ramírez^d

^aDepartment of Pharmacy and Pharmaceutical Technology and Physical Chemistry, Faculty of Pharmacy and Food Science, University of Barcelona, Av. Joan XXIII 29-31, Barcelona 08028, Spain.

^bFacultad de Ciencias Químicas e Ingeniería, Universidad Autónoma del Estado de Morelos; Av. Universidad 1001, Cuernavaca, Morelos, México.

^cDepartment of Biochemistry and Physiology, Faculty of Pharmacy and Food Sciences, University of Barcelona, 08028 Barcelona, Spain

^dCentro de Investigaciones Químicas, Instituto de Investigación en Ciencias Básicas y Aplicadas, Universidad Autónoma del Estado de Morelos; Av. Universidad 1001, Cuernavaca, Morelos, México.

*Institute of Nanoscience and Nanotechnology (IN²UB), University of Barcelona, Spain.

Revista: *Nanomedicine (Future Medicine)* ISSN (online): 1748-6963

Año de publicación: 2020

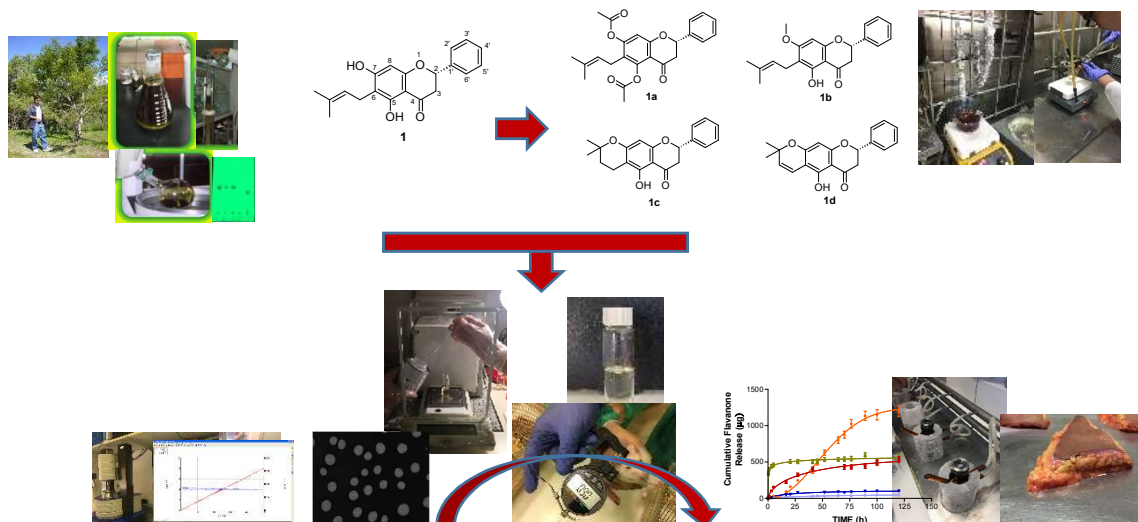
Factor de impacto: JCR: 4.3 (Datos del año 2019)

Percentil: JCR Categoría Q1 (Biotechnology & Apply Microbiology)

DOI: 10.2217/nnm-2020-0368








Resumen

El objetivo de este artículo fue el desarrollo y caracterización de formulaciones nanoestructuradas (FF) que contenían a la flavanona natural **1** extraída de *Eysenhardtia platycarpa* y a las flavanonas derivadas **1a-1d** obtenidas mediante modificación molecular de la flavanona **1** como candidatos para el tratamiento local de la inflamación en la piel. Primeramente, las FF fueron fisicoquímicamente caracterizadas seguido de su comportamiento de liberación, permeación en piel humana y eficacia antiinflamatoria *in vivo* en modelo de rata. Las FF mostraron una liberación sostenida de las flavanonas y una lenta penetración en piel humana. Las FF redujeron la inflamación con valores comparados a las formulaciones estándar para el tratamiento de esta patología. Se concluyó que las FF podrían ser sistemas efectivos para la liberación controlada de flavanonas en la piel y que la modificación química de la flavanona líder **1** mejoró la eficacia.





Biopharmaceutic study and *in vivo* efficacy of natural and derivatives flavanones formulations

Paola Bustos-Salgado¹ , Berenice Andrade-Carrera² , Valeri Domínguez-Villegas² ,
 María José Rodríguez-Lagunas³ , Antonio Boix-Montañes¹ , Ana
 Calpena-Campmany^{*.1.4}  & María Luisa Garduño-Ramírez⁵ 

¹Department of Pharmacy & Pharmaceutical Technology & Physical Chemistry, Faculty of Pharmacy & Food Science, University of Barcelona, Av. Joan XXIII 29-31, Barcelona 08028, Spain

²Facultad de Ciencias Químicas e Ingeniería, Universidad Autónoma del Estado de Morelos; Av. Universidad 1001, Cuernavaca, Morelos, México

³Department of Biochemistry & Physiology, Faculty of Pharmacy & Food Sciences, University of Barcelona, Barcelona 08028, Spain

⁴Institute of Nanoscience & Nanotechnology (IN²UB), University of Barcelona, Barcelona 08028, Spain

⁵Centro de Investigaciones Químicas, Instituto de Investigación en Ciencias Básicas y Aplicadas, Universidad Autónoma del Estado de Morelos; Av. Universidad 1001, Cuernavaca, Morelos, México

*Author for correspondence: Tel.: +34 93 402 4578; anacalpena@ub.edu

Aim: The development and characterization of nanostructured flavanone formulations (FF) of **1** extracted from *Eysenhardtia platycarpa* and **1a**, **1b**, **1c** and **1d** derivatives by structural modification of **1** as anti-inflammatory candidates for topical treatment of local inflammation. **Materials & methods:** The FF were physicochemical characterized and the behavior release, *skin* permeation and, *in vivo* anti-inflammatory efficacy in the rat model were studied. **Results:** The FF revealed sustained drug release and showed slow drug penetration in human skin. The FF reduced inflammation in comparison with the standard formulation. **Conclusion:** The FF could be effective systems for the delivery and controlled release of flavanones on the skin, and the chemical modification of lead molecule **1** improved the efficacy.

First draft submitted: 19 September 2020; Accepted for publication: 7 December 2020; Published online: 22 January 2020

Keywords: *ex vivo* permeation • *in vitro* release • *in vivo* anti-inflammation • nanostructured formulations • natural and derivatives flavanones

Natural products continue to be a source of bioactive compounds and offer a possibility for the development of drugs for the treatment of a diversity of diseases [1–3]. *Eysenhardtia platycarpa*, which is widely distributed throughout Southern Mexico, is a small tree, commonly called “taray”, “palo dulce” and “palo azul”, which contains flavanones. Flavanones have been reported to present several biological activities, such as antimicrobial, anti-oxidant and even anti-inflammatory effects [4–7]. *E. platycarpa* has been used traditionally as a diuretic, antidiabetic, antiseptic and for the treatment of kidney and bladder infections [8]. The methanolic extract of *E. platycarpa* and a solution containing only flavanone **1** (2*S*)-5,7-dihydroxy-6-(3-methyl-2-buten-1-yl)-2-phenyl-2,3-dihydro-4*H*-1-Benzopyran-4-one (Figure 1) isolated from this extract, showed an anti-inflammatory percentage of 77.5 ± 1.0 and 66.7 ± 1.1 , respectively when the TPA-induced acute inflammation model in mice’s ears was used [9].

The main problem with natural products is their low stability, poor bioavailability and solubility parameter. Dermal drug delivery, the topical application of active products to the skin surface to treat local skin diseases, is a good strategy to formulate natural product compounds to solve the solubility problems, and thus enhancing their bioavailability [10,11]. Other advantages are that they are painless and easy to be applied, suggesting a good patient compliance [12]. Nevertheless, most natural active products are not suitable for this mode of administration. Recently, nanotechnology-based formulations, such as nanoemulsions (NE), have been successfully employed for encapsulating and delivering lipophilic bioactive components targeted at delivery in a tissue [13]. NE are

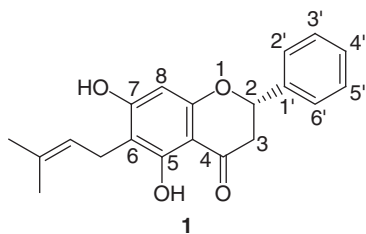


Figure 1. Chemical structure of flavanone **1** extracted from *Eysenhardtia platycarpa*.

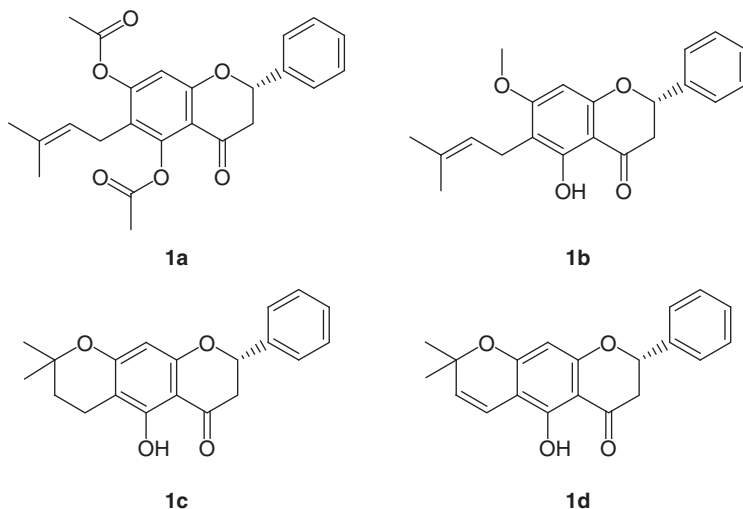


Figure 2. Chemical structure of derivative flavanones **1a**, **1b**, **1c** and **1d**.

colloidal nanocarriers of low viscosity formed by droplets, the size on a nanometer scale and characterized by being thermodynamically unstable but kinetically stable systems with a transparent and translucent appearance [14–17]. Many previous studies demonstrated that permeation rates from nanostructured formulations were significantly higher than those of conventional formulations [18–20].

If we continue with this reasoning, in previous reports the flavanone **1** was formulated as being effective in drug delivery systems: NE and polymeric nanoparticles NP for topical use as novel anti-inflammatory topical formulations. The topical anti-inflammatory activities of **1** (free drug and encapsulated) were determined by assessing the result of the formulations on mice's ear edema induced by TPA. The figures concluded that there was an inhibition percentage of inflammation of 82.91 ± 0.95 for NE**1** and 80.97 ± 1.48 for NP**1**. This seems to indicate that NE**1** and NP**1** are valid as potential topical anti-inflammatory formulations and have the most advantageous properties for the treatment of inflammatory disorders [21].

Molecular modification is the structural modification of compounds by chemical, physical and biological means so that numerous structural types of derivatives are obtained. Using adequate methods, structural changes facilitate the altering of the physicochemical properties and bioactivities of natural compounds [22]. A range of structural modifications, such as esterification, methylation, cyclization or vinylogous cyclization match up well with the obtaining of new compounds offering improved biological efficacy as well as providing a strategy to evaluate the influence of the substitution pattern on the structure–activity relationship [23].

Based on previous studies and considering the flavanone **1** anti-inflammatory potential, the main purpose of this work was the development of innovative drug delivery systems with an improved biopharmaceutical profile for dermal administration of flavanones. The systems included the flavanone **1** and derivatives obtained from structural modifications: (2*S*)-5,7-bis(acetyloxy)-6-(3-methyl-2-buten-1-yl)-2-phenyl-2,3-dihydro-4*H*-1-Benzopyran-4-one (**1a**); (2*S*)-5-hydroxy-7-methoxy-6-(3-methyl-2-buten-1-yl)-2-phenyl-2,3-dihydro-4*H*-1-Benzopyran-4-one (**1b**); (8*S*)-5-hydroxy-2,2-dimethyl-8-phenyl-3,4,7,8-tetrahydro-2*H*,6*H*-Benzo(1,2-*b*:5,4-*b'*)dipyrano-6-one (**1c**) and (8*S*)-5-hydroxy-2,2-dimethyl-8-phenyl-7,8-dihydro-2*H*,6*H*-Benzo(1,2-*b*:5,4-*b'*)dipyrano-6-one (**1d**) (Figure 2). We expected to enhance the penetration of the flavanones through the skin, improving their in-skin retention, thus increasing their bioavailability. We explored the relationship between chemical structure and

skin delivery. The *in vivo* therapeutic efficiency of flavanones was checked by gross observation and histopathology in the rat ear edema model induced by arachidonic acid (AA).

Materials & methods

Chemicals

Polyglyceryl-6-dioleate (Plurol[®] oleique), triglycerides medium-chain EP/NF/JPE (Labrafac[®] lipophile), and caprylocaproyl macrogol-polyoxyl-8-glyceride (Labrasol[®]) were gifted by Gattefossé (Gennevilliers, France). Propylene glycol, ethanol, HPLC-grade Acetonitrile, DMSO and, all other chemicals and reagents used in the study were acquired from Sigma-Aldrich (Madrid, Spain). Dialysis cellulose membrane molecular weight cutoff (MWCO) 12 kDa was purchased from Iberlabo (Madrid, Spain). The purified water used in the experiments was obtained from a MilliQ[®] Plus System (Millipore Corporation, MA, USA).

Flavanone natural **1** was extracted as set out in the method described before [24]. Briefly; *E. platycarpa* leaves (Registration Number: Ramiro Cruz 1325 from the Sciences Faculty Herbarium Facilities of the Autonomous University of the State of Morelos) were dried, pulverized and macerated with methanol (100 g of dried vegetal material per 1000 ml methanol three-times). Finally, the flavanone **1** was isolated by column chromatography and purified by thin layer chromatography. The melting point product was a yellow powder precipitate at 200.2°C. The compound obtained was characterized by comparison with the previous published melting point data and with the ¹H-NMR results. Correspondingly, the flavanones derivatives were synthesized, and as previously reported in the protocol [24] this obtained (2*S*)-5,7-bis(acetyloxy)-6-(3-methyl-2-buten-1-yl)-2-phenyl-2,3-dihydro-4*H*-1-Benzopyran-4-one **1a**; (2*S*)-5-hydroxy-7-methoxy-6-(3-methyl-2-buten-1-yl)-2-phenyl-2,3-dihydro-4*H*-1-Benzopyran-4-one **1b**; (8*S*)-5-hydroxy-2,2-dimethyl-8-phenyl-3,4,7,8-tetrahydro-2*H*,6*H*-Benzo(1,2-*b*:5,4-*b'*)dipyran-6-one **1c** and (8*S*)-5-hydroxy-2,2-dimethyl-8-phenyl-7,8-dihydro-2*H*,6*H*-Benzo(1,2-*b*:5,4-*b'*)dipyran-6-one **1d**.

Experimental animals

Adult male Sprague Dawley[®] rats (200–240 g) were brought from the Bellvitge animal facility services and approved by the Ethics Committee of Animal Experimentation of the University of Barcelona. Prior to the experiments, they were fed with standard food and water *ad libitum*. The experiments reported in this study were carried out following the guidelines stated in the protocol “Principles of Laboratory Animal Care” (publication 214/97 of 30 July).

Preparation of flavanone formulations

The flavanone formulations (FF) were elaborated by an ultrasonic homogenization method as described previously [21]. In short, independently flavanones **1**, **1a**, **1b**, **1c** and **1d** (0.5% w/w) were dissolved into the excipients mixture (see Supplementary Table 1) by sonication of the components in an Elma Transonic Digital S T490 DH ultrasonic bath (Elma, Singen, Germany) for 15 min. They were then stirred in a water bath at 32°C for 15 min. In the next step, the mixture was sonicated for 15 min more and finally the resulting solutions were cooled at -20°C for 24 h to yield FF**1**, FF**1a**, FF**1b**, FF**1c** and FF**1d**. Non flavanone formulation (**nFF**) was prepared with the same procedure described before but without adding any flavanone.

Determination of physical parameters

Morphological studies

The transmission electron microscopy (TEM) was used for the morphological and structural examination of FF. First, one drop of each FF was adsorbed into carbon-coated copper grids (EMS, London, UK) for 1 min and filter papers were used to remove the excess. Then, they were stained with Uranylless (EMS) for 1 min. The excess of liquid was manually blotted from the edge of the grids. The sample was observed in a Tecnai[™] Spirit microscope (EM; FEI, Maastricht, The Netherlands) equipped with a tungsten filament, at the Cryomicroscopy Unit from the CCiTUB. Finally, images were acquired at 120 kV and at room temperature with a 1376 × 1024 pixel CCD Mega view camera [25].

Determination of physical parameters

Morphological studies

The TEM was used for the morphological and structural examination of FF. First, one drop of each FF was adsorbed into carbon-coated copper grids (EMS) for 1 min and filter papers were used to remove the excess. Then, they

were stained with Uranylless (EMS) for 1 min. The excess of liquid was manually blotted from the edge of the grids. The sample was observed in a Tecnai Spirit microscope (EM) (FEI) equipped with a tungsten filament, at the Cryomicroscopy Unit from the CCIiTUB. Finally, images were acquired at 120 kV and room temperature with a 1376×1024 pixel CCD Mega view camera [25].

Rheology studies

The FF (**n**, **1**, **1a**, **1b**, **1c** and **1d**) viscosity was measured at $25 \pm 2^\circ\text{C}$ in triplicate with a Haake Rheo Stress 1 rheometer (Thermo Fisher Scientific, Karlsruhe, Germany) with a cone rotor C60/2-Ti (60 mm diameter, 2° angle, 0.105 mm gap between cone-plate). The rheometer executed the tests and run the analyses connected to a thermostatic circulator Thermo Haake Phoenix II + Haake C25P and to a computer (Haake Rheowin[®] Job Manager and Data Manager v3.3 software; Thermo Electron Corporation, Karlsruhe, Germany). As described by Suñer *et al.*: Ramp-up from 0 to 100/s in 3 min, a constant shear rate of 100/s during 1 min and Ramp-down from 100 to 0/s in 3 min [26,27].

Extensibility studies

A volume of 50 μl of FF (**n**, **1**, **1a**, **1b**, **1c** and **1d**) was placed on a steel plate circle (10 cm diameter) then a glass plate was placed over it. Increasing standard weight pieces (1, 2, 5, 10, 20, 50, 100 and 200 g) were replaced and allowed to rest on the upper glass plate for 1 min. The increase in the diameter due to the formulation spreading was noted. Each formulation was tested in triplicate at room temperature. The increase in surface area (mm^2) of the FF was plotted as a function of the increasing weights applied [28]. The two-site binding hyperbola model described as equation 1 was the best fitted to formulations.

$$y = \frac{B_{\max 1} \cdot x}{K_{d1} + x} + \frac{B_{\max 2} \cdot x}{K_{d2} + x}; \quad (\text{Eq. 1})$$

where $B_{\max 1}$ and $B_{\max 2}$ are the maximal surfaces, and K_{d1} and K_{d2} are the weights required to reach the half-maximal surfaces.

Stability studies

To assess physical stability, aliquots of 1 ml of the FF (**n**, **1**, **1a**, **1b**, **1c** and **1d**) were deposited in glass vials. The samples were stored for 180 days and kept at $4 \pm 1^\circ\text{C}$. The FF macroscopic characteristics were studied to detect any instability by visual observation over the storage period. Their physical appearance was captured by high-resolution digital camera (Panasonic DMC-FZ20). The clarity, the precipitation appearance, phase separation and any other macroscopic changes were compared with the initial formulations [29,30]. The pH of FF was measured at room temperature using a calibrated digital pH meter GLP 22 (Crison Instruments S.A., Barcelona, Spain), once FF had been elaborated and after 180 days of storage. Measurements were done in triplicate and mean and standard deviation (SD) values were reported.

The chemical stability was evaluated by measuring the quantity of flavanone present in the FF (**1**, **1a**, **1b**, **1c** and **1d**) to verify if potential changes occurred during the storage at $4 \pm 1^\circ\text{C}$ for 30, 60 and 180 days. For this purpose, an exact volume of 100 μl of each formulation was dissolved in 5 ml of DMSO by stirring for 10 min in an ultrasonic bath [31]. The amount of flavanone extracted was determined by HPLC described in reference 33. If the flavanones profiles had variations of more than 10%, they were indicated as unstable formulations.

In vitro studies

The release study of flavanones (**1**, **1a**, **1b**, **1c** and **1d**) was performed using dialysis membrane (12 kDa, Dialysis Tubing Visking, Medicell International Ltd, London, UK) hydrated for 24 h before being fixed in the Franz diffusion cell with an effective diffusional area of 2.54 cm^2 . The experiment was performed under “sink conditions”. The receptor phase was filled with 12 ml of ethanol: water (7:3) maintained at $32 \pm 1^\circ\text{C}$ under continuous stirring. Afterward, 0.3 ml of FF samples were placed into the donor compartment. Moreover, aliquots of 0.3 ml were taken from the receptor compartment at fixed times for 120 h and replaced with the same volume of receptor medium. The concentration of each sample was quantified by HPLC with an UV detector [33]. Data were expressed as mean \pm SD ($n = 3$). Different kinetic models (first order, hyperbola, Korsmeyer–Peppas and Weibull, Equations 2–5) were evaluated to find out the flavanones release profile from FF. Coefficients of determination (r^2) were used

as discrimination criteria.

$$Q_t = K_d(t - t_0) \text{ Zero Order} \quad (\text{Eq. 2})$$

$$Q_t = Q_\infty(1 - e^{-K_d(t-t_0)}) \text{ First Order} \quad (\text{Eq. 3})$$

$$Q = At^n \text{ Korsmeyer - Peppas} \quad (\text{Eq. 4})$$

$$Q_t = Q_\infty \left[1 - e^{-\left(\frac{t}{t_d}\right)^\beta} \right] \text{ Weibull} \quad (\text{Eq. 5})$$

Where Q_t is the drug amount released at time t (μg), K_d is the release rate constant ($\mu\text{g}/\text{h}$),

Q_∞ is the maximum amount susceptible to release (μg), t_0 is the latency period (h), A is a kinetic constant ($\mu\text{g}/\text{h}^n$), n is the diffusion release exponent; t_d is the time in which the 63.2% of the drug is released, and β is the sigmoidicity.

Analysis of variance and t -test were calculated to evaluate the significant differences between release profiles of all the formulations. Data were considered statistically significant at $p < 0.05$.

Ex vivo studies

The permeation studies were carried out with vertical Franz diffusion cells of 0.64 cm^2 and dermatome human skin from the abdominal region (0.4 mm) for a unique donor as membrane. All provided from the plastic surgery unit (Hospital de Barcelona, SCIAS, Barcelona, Spain), with written informed consent. Three parallel determinations were addressed. The receptor phase was filled with 5 ml of ethanol: water (70:30), under the temperature of $32 \pm 1^\circ\text{C}$ kept by a circulating-water jacket and stirred at 700 r.p.m. with teflon[®]-coated magnetic stirring bars. The donor side was filled with 0.1 ml of each FF (**1a**, **1b**, **1c** and **1d**) covered with parafilm[®] in order to avoid evaporation. Samples were withdrawn at different points in time over 29 h and quantified by means of a validated HPLC method with 1 ml/min flow rate and Machery Nagel[®] C18 5mm, $25 \times 4.6 \text{ cm}$ column (section 2.5). At the end, the experimental data were analyzed using the Prism[®], V.5 software (GraphPad Software Inc., CA, USA). The cumulative amount of flavanones permeated through the human skin membrane were plotted as a function of time. The estimated permeation parameters such as the flux across the skin J ($\mu\text{g}/\text{cm}^2/\text{h}$) were calculated from the slope of the linear portion of cumulative amounts of each flavanone permeated through human skin per unit surface area Q ($\mu\text{g}/\text{cm}^2$), set out on a time plot. The intercept with X-axis (time) of this plot is equal to lag time T_l (h). The transdermal permeability coefficient K_p (cm/h) resulted by dividing the flux (J) by the initial concentration of the flavanones studied (C_0) in the donor compartment [32]. The partition coefficient P_1 (1/h) (Equation 7) and the diffusion coefficient P_2 (Equation 6) were also estimated as followed:

$$P_2 = \frac{1}{6T_l} \quad (\text{Eq. 6})$$

$$P_1 = \frac{J}{(A * C_0 * P_2)} \quad (\text{Eq. 7})$$

where T_l is the lag time; J is the flux across the skin, A is the membrane area, C_0 is the concentration of the flavanones at time zero in the donor compartment.

Once the experiment had finalized, the amount of flavanone retained (skin retention, Q_r , $\mu\text{g}/\text{g}$ skin/ cm^2) in the human skin membrane was determined. For that purpose, the flavanones skin extraction was carried out as followed: the skin was removed from the Franz cells at the end of the permeation studies, and then it was cleaned with 0.05% solution of dodecylsulphate and was washed with distilled water. The permeation areas of the skin were cut and weighed. The flavanone contained was extracted with ethanol: water (70:30) mixture under sonication (20 min) in an ultrasonic bath. Finally, the solutions were quantified by HPLC as described in section 2.5, yielding the amount of each flavanone that could be extracted Q_{ext} ($\mu\text{g}/\text{g}$) by this method from the skin study.

The recovery percentage (R%) was obtained as described in previous studies [33] in accordance with a mass-balance calculation. Briefly, 1 ml of each flavanone solution (200 $\mu\text{g}/\text{ml}$) was added to vials with 100 mg of human skin ($n = 3$). These vials remained for 24 h in a water bath at 32°C . Once 24 h had passed, the skin was extracted with ethanol: water (70:30) mixture under sonication (20 min) in an ultrasonic bath. Finally, the initial solutions

and the eluates were analyzed by HPLC (see section 2.5). The R% of each flavanone (**1**, **1a**, **1b**, **1c** and **1d**) was calculated comparing the corresponding drug extraction results, with the flavanone amount bound to the tissue (difference between initial flavanone amount and flavanone amount in the eluates at 24 h).

The amount of flavanone retained in tissue (Q_r) was calculated at the end by the comparison of the amount of flavanone extracted (Q_{ext}) and the recovery percentage as described above and in accordance with the equation 8:

$$Q_r = \frac{Q_{ext}}{R\%} \times 100 \quad (\text{Eq. 8})$$

where Q_{ext} is the amount of flavanone extracted and R% is the percentage of recovery of flavanones [34].

The statistical analysis and data comparisons were achieved using the nonparametric statistical Mann–Whitney U test with significant statistical differences when $p < 0.05$.

In vivo Studies: anti-inflammatory efficacy

The topical anti-inflammatory efficacy of the flavanones FF (**1**, **1a**, **1b**, **1c** and **1d**) was appraised using arachidonic acid (AA) in rat ear edema model. The experiment was carried out using a slight modification of the procedure described by Espinoza, *et al.* [35]. An irritant solution was prepared by dissolving AA (5 mg/ml) in phosphate-buffered saline. The inflammatory process was induced by one topical application of 60 μl of AA solution on both sides of the ears; and left for 20 min of exposure. Adult male Sprague Dawley rats were used with a weight ranging from 200 to 240 g. The animals were divided into nine groups (five animals in each). Group (1) was the negative control group; it was not treated at all. Group (2) was the positive control; it was treated only with AA solution. Group (3) was the drug reference group; both sides of the ears received 0.5 mg of commercial gel diclofenac sodium 10 mg/g (ATC Code: M02AA15). Group (4) the vehicle group nFF, received 50 μl of the formulation without flavanones only excipients. Finally, the Groups (5), (6), (7), (8) and (9) were groups treated with 50 μl of FF (**1**, **1a**, **1b**, **1c** and **1d**) correspondingly. All groups, except the negative and positive control, were treated with the respective formulation 20 min after AA exposition and the treatment was kept for 20 min. The measurements of stratum corneum hydration (SCH) were done before and after the AA application and treatments using a corneometer CM825 (Courage & Khazaka electronics GmbH, Köln-Germany). Values (arbitrary units) reported as the mean of five replications \pm SD. In the same way, ear thicknesses were recorded before and after the AA and the different treatments with a digital micrometer (Wisamic Digital Thickness Gauge 0–12.7 mm). The anti-inflammatory activity was expressed by means of the following equation 9 [21]:

$$\Delta \text{ Inhibition inflammation} = \frac{\text{difference in thickness, positive control} - \text{difference in thickness after treatment}}{\text{difference in thickness, positive control}} \quad (\text{Eq. 9})$$

Finally, at the end of the experiment, the rats were sacrificed using carbon dioxide, following the recommendations for euthanasia of experimental animals from the European Commission [36]. Then, the ears were cutoff and stored to assess ear edema and treatments activity performing a histological assay (section 2.10).

Histological analysis

After the *in vivo* study, the rats' ears were immediately removed from the treated animals. The positive and negative control groups were used to study the anti-inflammatory effect. First, the tissues were rinsed with PBS pH 7.4, and set overnight in 4% buffered formaldehyde and finally embedded in paraffin wax. Transversal sections (5 μm) were stained with hematoxylin and eosin and viewed for the evaluation of the ear inflammation under a light microscope (Olympus BX41 and camera Olympus XC50) on blind coded samples. Ears from the nontreated animals were used as the control condition.

Results

Characterization

Morphological studies

Flavanones formulations FF1, FF1a, FF1b, FF1c and FF1d and nFF were qualitatively and quantitatively assayed in terms of appearance, droplet and particle size. The FF obtained were isotropic, transparent and slightly viscous. TEM imaging is the most powerful and accurate technique to determine a sample's morphology, purity and particle size distribution [31]. As shown in Figure 3, the droplets were distributed uniformly in FF1a, FF1b and FF1c.

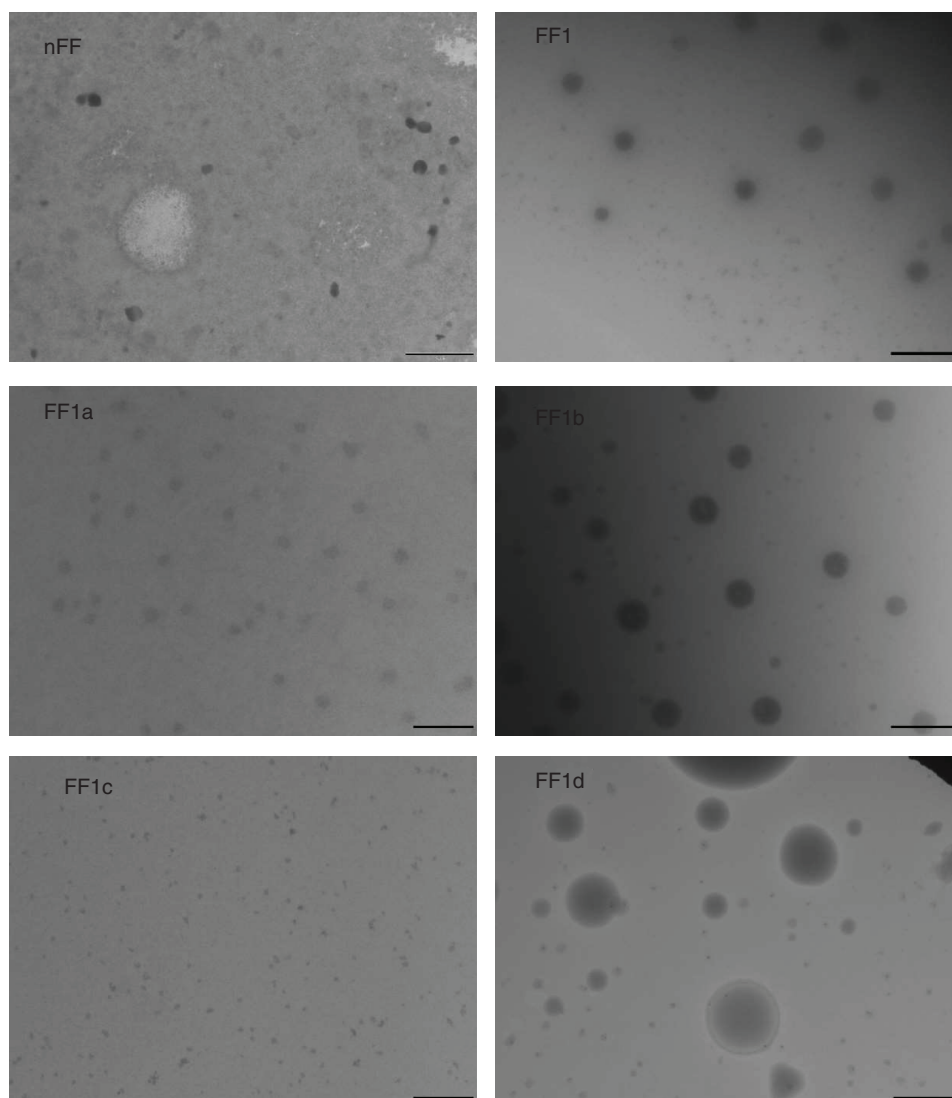


Figure 3. Transmission electron microscopy images of the flavanones formulations. Bar length 200 nm for FF1a and FF1c; 1 μm for nFF, FF1, FF1b and FF1d.

In addition, the droplets were spherical and no aggregation process was observed. The mean size from all the formulations is listed in [Supplementary Table 2](#). The formulation without flavanone **nFF** exhibited the size of 155.31 ± 27.64 nm and **FF1c** showed the least droplet, sized 12.56 ± 1.77 nm.

Rheology studies

The viscosity measurements are used to determine if the material is characterized by linear-viscous (Newtonian) behavior (shear-stress exponent $n = 1$) in the investigated shear rate range or if it shows power-law behavior ($n \neq 1$) [27]. The potential dependence of the FF viscosity on the shear rate is shown in [Supplementary Figure 1](#). The viscosity graph (η) for all FF is a line, thus the behavior was Newtonian. Therefore, the viscosity values at 100 s^{-1} were 80.01 ± 0.04 , 80.64 ± 0.04 , 81.29 ± 0.05 , 82.77 ± 0.03 , 85.2 ± 0.03 and 86.83 ± 0.03 mPa·s for **nFF**, **FF1**, **FF1a**, **FF1b**, **FF1c** and **FF1d**, respectively, at t_0 .

Extensibility studies

All the formulations were in accordance with the two-site binding hyperbola model (see [Supplementary Figure 2 & Table 3](#)). Extensibility values increases with loading weight. These results are in accordance with that obtained in the rheological characterization of FF. The **nFF** and **FF1** were the most extensible with $B_{\text{max}1}$ of 16.39 ± 4.05 and

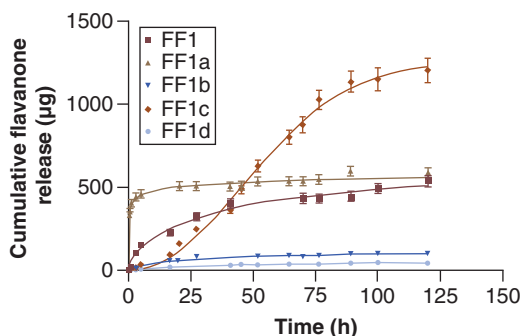


Figure 4. *In vitro* flavanone release from formulations FF1, FF1a-1d. The cumulative amount released was plotted against time. Data represent the mean \pm SD ($n = 3$).

$17.84 \pm 14.37 \text{ mm}^2$, respectively. Otherwise, the least extensible were FF1a, FF1b, FF1c and FF1d with $B_{\max 1}$ of 13.11 ± 3.08 , 9.61 ± 2.65 , 10.79 ± 1.19 and $3.19 \pm 2.15 \text{ mm}^2$, respectively. The parametric analysis of the t -test showed no significant influence of the FF composition FF except in nFF with FF1d.

Physical & chemical stability

Preparations were considered stable if the physical appearance did not change. As seen in, [Supplementary Figure 3](#), there was no sign of creaming action, phase separation or sedimentation even after 180 days of storage. Additionally, as mentioned in [Supplementary Table 4](#), there were no significant changes in pH values of FF at 180 storage days except in FF1a and FF1d where the pH were a little bit lower. Therefore, the data indicated that the examined FF were physically stable.

Moreover, the pH of FF after 180 days slightly decreased, being these values within the physiological range accepted for dermal and transdermal preparations (4.5–7) [37].

On the other hand, the results on chemical degradation of flavanones during storage showed that in all the FF except FF1a the flavanone content remained above 90% of the original amount of flavanone (see [Supplementary Table 5](#)) after 60 storage days. While after 180 storage days, only FF1, FF1b and FF1d showed the same stability tendency with percentages that could be considered stable.

In vitro studies

[Figure 4](#) shows the different release profiles of FF. The release process can be described in two phases. In the cases of FF1, FF1a, FF1b and FF1d, the initial phase displays a rush release, followed by a slower sustained release phase of the flavanone loaded FF. The cumulative release curve of FF1c presents a sigmoidal profile, which is in agreement with the fact that the experiments were developed with a finite dose and thus the donor compartment reaches a stage of flavanone depletion.

The mathematical modeling to describe drug release profiles offers several advantages. It allows the simplifying of the process elucidating the drug release mechanisms and it can be used to guide formulation development efforts [21,38]. Besides, the release model is useful for assessing the excipients effect on the drug release and for simulating different situations not assayed. The modeling is also used in quality control studies because the drug release parameters can detect changes in the formulation over time [39]. Data obtained from the *in vitro* release study were fitted to different functions. The correlation coefficient (r^2) of each mathematical model was calculated (see [Supplementary Table 6](#)). The highest r^2 value for the entire FF was that of the Weibull function

The β data (a dimensionless shape parameter from the Weibull function) allow the elucidation of drug release mechanisms. A combined mechanism (Fickian diffusion and swelling controlled release) is associated to the range $0.75 < \beta < 1$. In other cases, for values of β higher than 1, the drug transport follows a complex release mechanism [40]. From the Weibull function modeling data for all FF, the FF1c β value was 2.09 ± 0.21 , indicating a complex mechanism. In contrast, for the rest of FF with a β value between 0.19–0.88 it reflects a combined mechanism.

In the case of the flavanone amount released at time t (Q), FF1c was greater with $1249 \pm 64.59 \mu\text{g}$ followed by FF1, FF1a, FF1b and, FF1d $592.0 \pm 162.43 \mu\text{g}$, $606.7 \pm 159.21 \mu\text{g}$, $98.86 \pm 9.02 \mu\text{g}$ and $53.46 \pm 13.56 \mu\text{g}$, respectively (see [Supplementary Table 7](#)). A parametric Turkey test showed significant statistical differences ($p < 0.05$). Therefore, there were statistical differences between the FF except in the case of FF1b with FF1d and, FF1 with FF1a, as can be appreciated visually in the graphic ([Figure 4](#)) in the same way. Correspondingly, the t_d (time required to 63.2% of the maximum amount release) for the FF was $42.46 \pm 36.37 \text{ h}$, $21.74 \pm 6.30 \text{ h}$, 62.39 ± 3.66

Table 1. Median (maximum–minimum) values of flux (J), lag time (T_l), P_1 and P_2 parameters, permeability coefficient (K_p), retained amount (Q_r) and permeated amount at 29 h (Q_p) of flavanones 1, 1a, 1b, 1c and 1d from FF in human skin.

	FF1 [†]	FF1a	FF1b	FF1c	FF1d
J /sur($\mu\text{g}/\text{h}/\text{cm}^2$)	0.81 (0.82–0.79)	105.828 (186.563–65.391)	1.258 [‡] (1.382–1.135)	0.851 [‡] (1.538–0.116)	0.101 ^{‡,§,¶} (0.142–0.025)
T_l (h)	7.95 (7.99–7.88)	1.9 (17.28–0.60)	21.28 (25.84–16.71)	16.91 (19.41–8.9)	7.89 ^{§,¶} (12.34–7.06)
$P_2 \times 10^{-2}$ (1/h)	0.208 (0.209–0.203)	8.77 (27.95–0.96)	0.82 (1.00–0.64)	0.99 (1.87–0.86)	2.11 ^{§,¶} (2.36–1.35)
$P_1 \times 10^{-2}$ (cm)	0.786 (0.787–0.757)	14.90 (386.9–7.6)	3.14 [‡] (3.52–2.77)	1.73 [‡] (3.58–0.12)	0.01 ^{‡,§,¶} (0.21–0.02)
$K_p \times 10^{-4}$ (cm/h)	1.60 (1.61–1.58)	211.66 (373.1–130.8)	2.52 [‡] (2.76–2.27)	1.70 [‡] (3.08–0.23)	0.202 ^{‡,§,¶} (0.28–0.05)
Q_r (g/gskin/cm ²)	0.0215 (0.243–0.013)	2277.24 (3735.5–1080.57)	1.10 [‡] (1.19–1.01)	0.23 ^{‡,§} (1.05–0.17)	0.19 ^{‡,§} (0.26–0.09)
Q_p (μg)	82.56 (85.93–74.31)	1082.85 (1819.97–502.39)	7.17 [‡] (11.52–2.83)	2.94 [‡] (7.35–1.55)	1.44 ^{‡,§,¶} (1.57–0.05)

[†]Data obtained from Dominguez *et al* [21].*
[‡]Differences with FF1a.
[§]Differences with FF1b.
[¶]Differences with FF1c.

and 51.70 ± 22.63 h for FF1, FF1b, FF1c and FF1d, respectively. If we turn to FF1a, the release revealed an even faster rush effect; t_d was only 0.94 ± 2.30 h (Supplementary Table 7) and showed significant difference ($p < 0.05$) with FF1c and FF1d. The differences could be explained by the occurrence of substances in the FF that would act as promoters or inhibitors.

Ex vivo studies

The permeation studies parameters of the studied flavanones are depicted in Table 1 as median values as the drug permeation follows a long-normal distribution more than a normal one (Gaussian) [41]. FF1a achieved the maximum flux with $105.83 \mu\text{g}/\text{h}/\text{cm}^2$, followed by FF1b, FF1c and FF1d with fluxes of 1.26, 0.85 and $0.10 \mu\text{g}/\text{h}/\text{cm}^2$, respectively. The T_l parameter indicates the time required for reaching the steady state and that this time is inversely proportional to the drug's diffusivity through the skin. Therefore, the results suggested that the FF1a had a higher diffusion with the lowest T_l of 1.9 h and FF1b had a lower diffusion with the highest T_l with 21.28 h. Similarly, FF1a exhibited the highest permeability K_p coefficient of 211.66×10^{-4} cm/h. One of the factors, which controls the drug permeability between the formulation and the skin, is the partition coefficient (P_l). It is directly proportional to the distribution of the drug in the skin. Thus, once again, FF1a was shown to have the highest distribution of flavanone with a P_l of 14.90×10^{-2} cm. In the case of the diffusion parameter P_2 , the results had the same tendency; $8.77 \text{ h}^{-1} \times 10^{-2}$ (1/h) for FF1a was the maximum, followed by FF1d with 2.11×10^{-2} (1/h); FF1c with 0.99×10^{-2} (1/h) and finally, FF1b with 0.82×10^{-2} (1/h). The total flavanone that crosses the skin after 29 h of application corresponds to the Q_p parameter. The flavanone that could cross in the highest quantity to the receptor chamber was FF1a with 1082.85 μg , followed by 82.56 μg for FF1, 7.17 μg for FF1b, 2.94 μg for FF1c and, 1.44 μg for FF1d turned out to be the one that crossed in the lowest quantity. In the same way, the highest retained flavanone amount (Q_r) was present in FF1a with 2277.24 g/gskin/cm². In contrast to FF1d, in which the retained flavanone in the skin after permeation was smaller than in the other ones.

The permeation parameters J , T_l , P_1 , P_2 , K_p , Q_p and Q_r were compared by the application of the nonparametric statistical Mann–Whitney U test. This test compares the distribution of two unmatched groups. Significant statistical differences ($p < 0.05$) in J , P_l , K_p and Q_p parameters were found among all FF, except for FF1b with FF1c. The assayed FF formulations did not present significant statistical differences ($p > 0.05$) in T_l and P_2 parameters except for FF1b with FF1d and FF1c with FF1d. Additionally, the test showed significant statistical differences ($p < 0.05$) between FF assayed except in the case of FF1c and FF1d.

In vivo studies

The results are set out in Figure 5. As can be seen, the commercial gel of diclofenac sodic (m) reduced the ear thickness compared with the positive control (C+), and so did FF1a. There were no statistical differences between them. On the contrary, the treatment with nFF did not present significant anti-inflammation activity, since it yielded a result comparable with that obtained with C+. On the other hand, it was interesting that the FF1d had a higher efficacy and was followed by FF1b, FF1c and FF1, since they reduced the thickness of the rat ears after 20 min of their application. All of them resulted in statistically significant differences to the positive control, commercial gel of diclofenac and nFF.

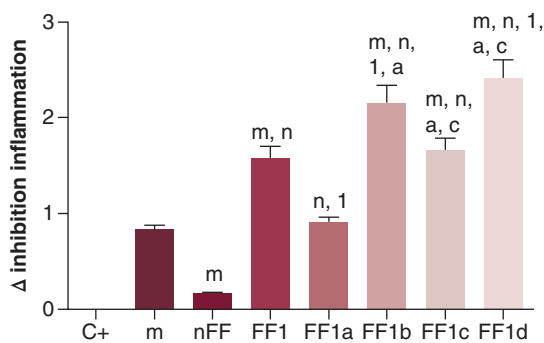


Figure 5. *In vivo* anti-inflammatory efficacy after FF treatment in AA-induced rat ear edema model as the increment of inhibition inflammation respect to positive control (C+). Results are expressed as mean \pm SD (n = 5). Statistically significant differences $p < 0.05$ regarding ⁺C+, ^mcommercial gel of diclofenac sodic, ⁿnFF, ¹FF1, ^aFF1a, ^bFF1b, ^cFF1c and ^dFF1d ANOVA Tukey's multiple comparison test.

ANOVA: Analysis of variance.

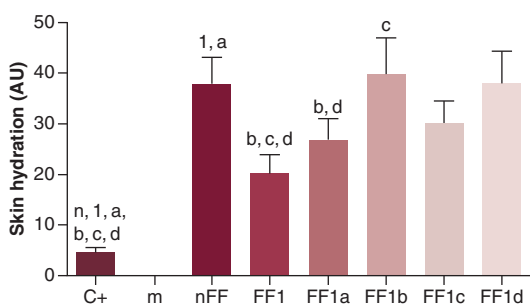


Figure 6. *In vivo* skin hydration after application of FF in AA-induced rat ear edema as the difference in hydration compared with initial conditions. Results are expressed as mean \pm SD, n = 5. Statistically significant differences $p < 0.05$ regarding ⁺C+, ^mcommercial gel, ⁿnFF, ¹FF1, ^aFF1a, ^bFF1b, ^cFF1c and ^dFF1d ANOVA Tukey's multiple comparison test. ANOVA: Analysis of variance.

The skin inflammation biomechanical properties may also reveal the importance of the treatment with FF. To exam this, the skin hydration of rat ears was measured and the results are shown in Figure 6 as the difference in SCH after the formulation treatment on swollen ears and the basal SCH conditions as arbitrary units.

The SCH values did not present any change during the study in nontreated skin (negative control) and commercial gel of diclofenac sodic (m). In contrast, as shown in Figure 6, the hydration of the skin changed with the application of all FF. Even the nFF increased the SCH value. No statistically significant differences were found when the FF1c and FF1d values were compared.

Histological analysis

For the assessment of the anti-inflammatory effect of the formulations, histological analysis of ear biopsies was performed. Ears treated with AA (Figure 7B) showed a mild inflammation characterized by edema, increased epidermal thickness and infiltration of polymorphonuclear (PMN) leukocytes.

Topical administration of diclofenac decreased these inflammatory indicators. The placebo was also tested and did not show any anti-inflammatory effect. FF1d (Figure 7I) was the best formulation in reducing the inflammation induced by AA. FF1, FF1a and FF1b (Figure 7E–G) partially reduced the inflammation. All three formulations showed less PMN infiltrate. However, only FF1 and FF1b (Figure 7E & G) were able to reduce the epidermal thickness. Only FF1c (Figure 7H) showed an anti-inflammatory pattern similar to the positive control ear with the presence of PMN, even when the edema and the epidermal thickness were less pronounced than in AA-treated ears.

Discussion

The formation of derivatives (**1a** and **1b**) by the introduction of new substituents into the structure of a lead flavanone **1** resulted in compounds with bioactive characteristics and different chemical properties. It also changed the shape as in **1c** and **1d**, which resulted in conformational restrictions that could affect the binding to the target site [42].

The evaluation of physical and biopharmaceutical properties of FF were possible because all the derivative flavanones were loaded in formulations in identical conditions. With regard to this, the flavanones **1**, **1a**, **1b**, **1c** and **1d** were successfully incorporated into FF. TEM images permitted the observation of the droplet structure, and confirmed the efficiency of the emulsion preparation method used [39]. In other studies, it has been observed that the molecular structure of emulsifiers had a great effect on the droplet size of the final emulsions [43]. The droplet size and stability of the emulsion is also affected by the type and concentration of the surfactant used [30].

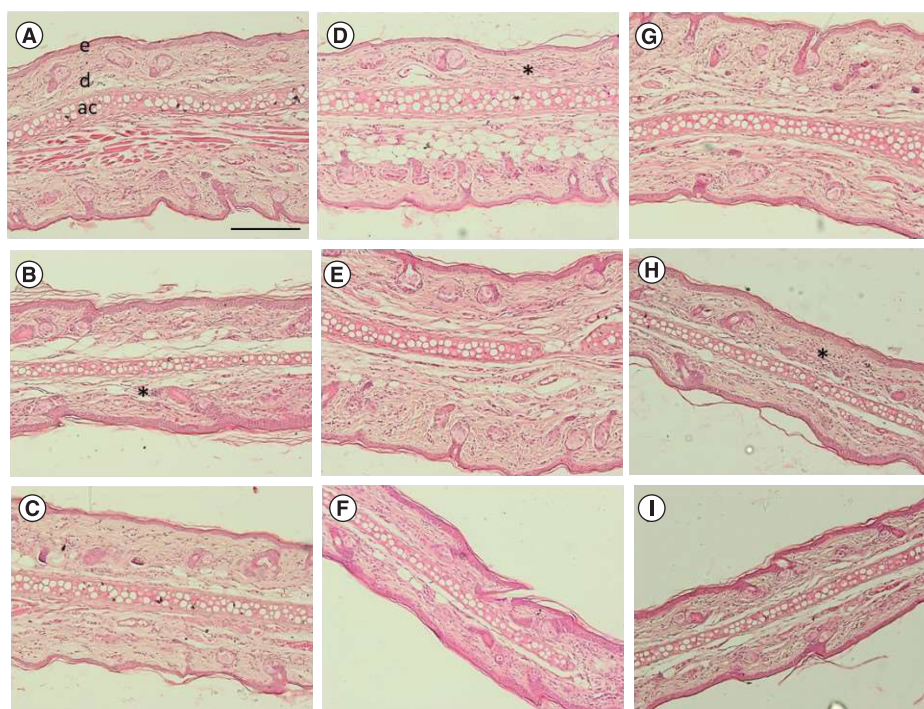


Figure 7. Histological sections of swollen ears stained with hematoxylin and eosin. (A) Control (-), (B) Control (+), (C) commercial gel, (D) nFF, (E) FF1, (F) FF1a, (G) FF1b, (H) FF1c and (I) FF1d.

*Leukocytes infiltrate. 100 × magnification. Scale bar = 200 μm.

ac: Auricular cartilage; e: Epidermis; d: Dermis.

Nevertheless, as shown in [Supplementary Table 2](#), the mean droplet size changed after the loading of flavanones. It could be hypothesized that the incorporated flavanones played an important role in the structure of the system and may affect it due to molecular interactions similar to the effect of the emulsifiers and the surfactants used to prepare them. Those molecular interactions could compress or expand the drop of emulsion and determine its magnitude.

Viscosity plays an important role in the texture perception of the FF when applied to inflamed skin. In line with this, the FF assayed exhibited a Newtonian behavior in that it showed characteristics suitable for topical flavanone delivery. In addition, these viscosity data can point to the option of dosing these formulations in a dispenser spray or roll on. In consequence, contamination of the formulation can be avoided, as well as it having the advantage of easy application. The viscosity data would allow us to use it as a quality control measure when the formulation is taken to an industrial level [44]. Further to this, the formulation extensibility measurements demonstrate the ease or difficulty in spreading the FF on damaged skin. With the results of the extensibility study set out in [Supplementary Figure 2](#), it is possible to ascertain that all the FF studied can be applied on skin effortlessly because with a low weight (200 g) the formulation has spread to the maximum possible.

In general, protection from physical and chemical degradation is one of the advantages in drug delivery of the majority of nanostructured systems [20]. From a practical viewpoint, it is important that formulations remain physically stable during storage. All the foregoing indicates the slow re-coalescence rate of FF drops because of continuous Brownian motion of the smaller droplets. However, the fact that nano-structured systems are transparent means that UV and visible light can penetrate into them, which may promote light-sensitive chemical degradation reactions to sensible components [45]. As shown by the data from FF1, FF1b, FF1c and FF1d, this is how it is possible that flavanones in these formulations interact in some way with the excipients that contain them, obtaining a kind of protection to degradation. On the other hand, the flavanone **1a** was unstable to chemical degradation when stored at 4°C in the formulation. The ester moiety in FF1a could suffer hydrolysis by the action of atmospheric water, therefore, the flavanone **1a** content was reduced [42]. Consequently, it may be necessary to improve the chemical stability of labile components by adding antioxidants or chelating agents [45]. The physicochemical origin of this effect is currently unknown and requires further study.

The aim of the *in vitro* studies was to assess the effect of formulation factors, to establish an *in vitro*–*in vivo* correlation-relationship and, to confirm that the flavanones are capable of releasing the formulations. Therefore, if the skin allows this, and regardless of whether the excipients help or not, the flavanones could pass through the skin. There is more than one factor involved in the release process, including the flavanones' physicochemical properties, structural characteristics of the material system, release environment and the possible interactions among these factors [38]. The increase of contact surface area with decreasing particle size offers a great potential of higher dissolution rates for molecules. Hence, particle size is crucial for realizing a better release profile. Thence it is possible that the drop size was the reason why FF1c released a greater quantity than the other FF. Nevertheless, not only is the size important, there are also other factors like the molecular polarizability, thus it may be that more polarizable molecules interact more strongly with the excipients so the quantity released may be lower. In addition, the π interactions and hydrogen bonds can also influence in the release [46]. In sum, the probable combination of all these interactions may have been the cause of the results in [Supplementary Table 6](#).

The *ex vivo* human skin permeation studies were carried out to define the permeation profile of flavanones formulations and their retained amounts in the tissue, which could be correlated to the efficacy of the treatment. The results for FF1a can be explained by the fact that ester moiety masks polar groups such as hydroxyl group (OH) contained in flavanone **1**, favoring passage through fatty cell membranes easily. In the case of methyl substituents, the molecule lipophilicity increased and was able to facilitate the absorption [42]. That may explain the reason why FF1b had Q_r higher than FF1. Although FF1a presented the highest Q_r , it is also the formulation that was able to reach the systemic system the most, and therefore that could exert its function into a local and systemic level. In addition, FF1a is the formulation with most chemical degradation, and it is not possible to guarantee the treatment without changes in the formulation. Therefore, the formulation should be enriched with an antioxidant and a desiccant to avoid degradation [45].

The *in vivo* study was carried out to evaluate the anti-inflammatory efficacy of the assayed FF. The results ([Figure 5](#)) can be put down to the fact that the excipients of formulations did not have any anti-inflammatory activity *per se*. Thus, the efficacy of the FF were intrinsically due to the flavanones. It might be assumed that the anti-inflammatory effect could be related to the amount of flavanone retained. Even though the flavanone **1d** in the *in vivo* assay turned out to be the most active while it was the least retained ($Q_r = 0.19 \text{ g/g}_{\text{skin}}/\text{cm}^2$). In several studies, the SARs of flavonoids revealed among other things that a planar ring system is essential in the flavonoid molecules to exhibit the activity and that hydroxyl groups at 5- and 7- position of A-ring seem to be favorable to structural features to the inhibition of AA-induced mouse ear edema [1,47,48]. Hence, the molecules **1c** and **1d** present a planar system and a higher rigidity and were able to support interaction more easily with the target of reducing the inflammation more than the other molecules in the *in vivo* assay. In the case of flavanone **1a**, it should be pointed that it was synthesized from the acetylation of flavanone **1**, thus the hydroxyl groups at 5- and 7- position were somehow eliminated, and which probably caused less *in vivo* activity compared with FF1. In addition, the fact is that the methylation of one of the functional hydroxyl groups moiety **1** yielded **1b**, and caused an increase in the anti-inflammatory activity compared with FF1 due to an increase in lipophilicity, as suggested by its higher skin retention. Probably, the introduction of the methyl group may improve the binding of the ligand to its receptor by filling a pocket on the target site [42]. That is why the presence of those structural conditions in flavanone **1** and **1b** was the cause of FF1 and FF1b reducing the epidermal thickness.

Finally, the SCH values after application of FF could indicate their hydration power due to the formation of an occlusive film on the skin thanks to the excipients. In the light of the foregoing, this permits the flavanones to penetrate easily through occluded hydrated skin and exert their action in the skin [49]. In addition, this hydration could reduce the physical discomfort associated with skin diseases like dryness and irritation [28].

Conclusion

According to the results of the physical characterization and stability studies, it can be concluded that the FF kept their appropriate properties during 180 days of storage except FF1a and FF1c. The formulations revealed sustained release behavior with a tendency to increased release inversely proportional to the formulation droplet size. This kind of evaluation can guarantee that the formulation releases the flavanones and cannot interfere in the flavanone permeation in human skin. In conclusion, the fact that natural flavanone **1** was chemically modified to obtain derivatives **1a**, **1b**, **1c** and **1d** allowed us to realize the variation of its physicochemical properties and to find out what resulted in the best biopharmaceutical behavior (**1b**). It also allowed us to realize whether these properties led to efficacy and/or effect. Based on *ex vivo* skin human permeation of the FF, the retained amount of flavanone in the

entire derivative FF (**1a–1d**) were higher than with natural FF**1**. Although, the *in vivo* experiments demonstrated that the molecule's action and intrinsic pharmacological potential is more important *per se* than the permeation profile. The entire FF showed anti-inflammatory efficacy values, being better with FF**1d** which has not been the one with the higher flavanone amount retained in the skin. For these reasons, *in vivo* and the histological study reflect that FF**1d** could and should attract considerable attention for skin inflammatory treatment. Also, the results suggest that the topical application of FF could be more effective in the treatment of inflamed skin's surface than the reference formulation used (diclofenac sodium gel).

Future perspective

Inflammatory diseases are becoming common in aging societies throughout the world. However, the overuse of synthetic drugs have the disadvantage of displaying side effects. An alternative to this is herbal drug therapy which offer safe remedies. Over the past decades, there has been an improvement in novel drug delivery systems for herbal drugs. Nevertheless, there are great possibilities of incorporating herbal drugs in different carrier systems or changing the structure of the drug at molecular level to improve its effectiveness before formulating it. Therefore, it is necessary to continue searching for lead molecules from natural products. In addition, the structure activity relationship necessarily has to be substantial that we can find predictions of biological activity from the modification of lead molecules.

Summary points

- A nanostructured formulation was used as carriers for the natural extracted flavanone **1** and derivatives (**1a**, **1b**, **1c** and **1d**) by structural modification of **1** for their topical application.
- The flavanone formulation FF (nFF, FF**1**, FF**1a**, FF**1b**, FF**1c** and FF**1d**) proved to have physical stability to storage (4°C) and, FF**1**, FF**1b** and FF**1c** resistance to chemical degradation for 6 months.
- The FF exhibited Newtonian behavior and provided a sustained release of drug according to the Weibull mathematical model.
- The FF skin permeation results demonstrate the possibility to use the flavanones (**1**, **1a**, **1b**, **1c** and **1d**) in a nano system formulation for topical purposes.
- The FF (**1**, **1a**, **1b**, **1c** and **1d**) showed a better anti-inflammatory efficacy on the animal model in comparison with the commercial gel of sodium diclofenac, obtaining the best effect when using FF**1d**.
- The *in vivo* anti-inflammatory results demonstrated the hydration of FF (**n**, **1**, **1a**, **1b**, **1c** and **1d**) without alterations of the skin structure.
- The chemical modification of lead molecule **1** improved its anti-inflammatory efficacy containing in the formulations.
- The FF can be proposed as a reasonable future treatment option of local inflammation for skin diseases.
- Results encourage further clinical investigation take advantage of the use of natural products containing in a nanosystem formulation for local anti-inflammatory treatments.

Supplementary data

To view the supplementary data that accompany this paper please visit the journal website at: www.futuremedicine.com/doi/suppl/10.2217/nnm-2020-0368

Author contributions

Substantial contributions to the conception or design of the work; or the acquisition, analysis or interpretation of data for the work have been provided by P Bustos-Salgado, B Andrade-Carrera, A Calpena-Campmany, MJ Rodríguez-Lagunas, V Domínguez-Villegas and ML Garduño-Ramírez. Drafting the work or revising it critically for important intellectual content has been contributed by P Bustos-Salgado, B Andrade-Carrera, A Calpena-Campmany, MJ Rodríguez-Lagunas, A Boix-Montañes, V Domínguez-Villegas and ML Garduño-Ramírez. Final approval of the version to be published has been contributed by P Bustos-Salgado, B Andrade-Carrera, A Calpena-Campmany, MJ Rodríguez-Lagunas, A Boix-Montañes, V Domínguez-Villegas and ML Garduño-Ramírez. Agreement to be accountable for all aspects of the work in ensuring that questions related to the accuracy or integrity of any part of the work are appropriately investigated and resolved has been provided by P Bustos-Salgado, B Andrade-Carrera, A Calpena-Campmany, MJ Rodríguez-Lagunas, A Boix-Montañes, V Domínguez-Villegas and ML Garduño-Ramírez.

Acknowledgments

The authors thanked L Gómez-Segura of the Bellvitge Hospital for her assistance in the management of the animals used in the experiments, also to L Delgado and L Halbaut for their excellent technical support. Moreover, they expressed their acknowledgement to Gattefossé for supplying the formulation components and skin samples in this study, to Hospital Barcelona-SCIAS (Barcelona, Spain) and to H Paul for his review of the use of the English language.

Financial & competing interests disclosure

This work was supported by a grant from CONACYT-México (grant number 709906). The authors have no other relevant affiliations or financial involvement with any organization or entity with a financial interest in or financial conflict with the subject matter or materials discussed in the manuscript apart from those disclosed.

No writing assistance was utilized in the production of this manuscript.

Ethical conduct of research

The authors state that they have obtained appropriate institutional review board approval or have followed the principles outlined in the Declaration of Helsinki for all human or animal experimental investigations. In addition, for investigations involving human subjects, informed consent has been obtained from the participants involved.

References

Papers of special note have been highlighted as: • of interest

- Gautam R, Jachak SM. Recent developments in anti-inflammatory natural products. *Harv. Bus. Rev.* 86(6), 84–92 (2008).
- **Describes anti-inflammatory natural products derived from plants. In addition, structure activity relationship studies carried out on the anti-inflammatory activity of flavonoid compounds are also discussed.**
- Yuan H, Ma Q, Ye L, Piao G. The traditional medicine and modern medicine from natural products. *Molecules* 21, 559 (2016).
- Nagula RL, Wairkar S. Recent advances in topical delivery of flavonoids: a review. *J. Control. Release* 296, 190–201 (2019).
- Chen X, Mukwaya E, Wong MS, Zhang Y. A systematic review on biological activities of prenylated flavonoids. *Pharm. Biol.* 52(5), 655–660 (2014).
- Brewer MS. Natural antioxidants: sources, compounds, mechanisms of action, and potential applications. *Compr. Rev. Food Sci. Food Saf.* 10(4), 221–247 (2011).
- Kamran M, Huma Z-E, Dangles O. A comprehensive review on flavanones, the major citrus polyphenols. *J. Food Compos. Anal.* 33(1), 85–104 (2014).
- Fowler ZL, Koffas MAG. Biosynthesis and biotechnological production of flavanones: current state and perspectives. *Appl. Microbiol. Biotechnol.* (83), 799–808 (2009).
- Narváez Mastache JM, Garduño-Ramírez ML, Alvarez L, Delgado G. Antihyperglycemic activity and chemical constituents of *Eysenhardtia platycarpa*. *J. Nat. Prod.* 69, 1687–1691 (2006).
- Domínguez-Villegas V, Domínguez-Villegas V, García ML, Calpena A, Clares-Naveros B, Garduño-Ramírez ML. Anti-inflammatory, antioxidant and cytotoxicity activities of methanolic extract and prenylated flavanones isolated from leaves of *Eysenhardtia platycarpa*. *Nat. Prod. Commun.* 8(2), 177–180 (2013).
- **Demonstrates the anti-inflammatory effect of the flavanones studied.**
- Piazzini V, Monteforte E, Luceri C et al. Nanoemulsion for improving solubility and permeability of *Vitex agnus-castus* extract: formulation and *in vitro* evaluation using PAMPA and Caco-2 approaches. *Drug Deliv.* 24(1), 380–390 (2017).
- Abdel-Mottaleb MM, Try C, Pellenquer Y, Lamprecht A. Nanomedicine strategies for targeting skin inflammation. *Nanomedicine (Lond.)* 9(11), 1–20 (2014).
- Martins Pinheiro I, Pereira Carvalho I, Sousa de Carvalho CE et al. Evaluation of the *in vivo* leishmanicidal activity of amphotericin B emulgel: an alternative for the treatment of skin leishmaniasis. *Exp. Parasitol.* 164, 49–55 (2016).
- Gopi S, Amalraj A, Haponiuk J, Thomas S. Introduction of nanotechnology in herbal drugs and nutraceutical: a review. *J. Nanomedicine Biotherapeutic Discov.* 6(2), 1–8 (2016).
- **Provides an overview of the introduction of nanotechnology into the field of herbal drugs and nutraceuticals.**
- Ahmad S, Ali MS, Alam MS, Alam MI, Alam N. Nanoemulsion as a novel carrier for drug delivery system: an overview. *Adv. Environmental Biol.* 10(10), 120–130 (2016).
- Espinoza LC, Silva-Abreu M, Clares B, Halbaut L, Cañas M, Calpena A-C. Formulation strategies to improve nose-to-brain delivery of donepezil. *Pharmaceutics* 11(64), 1–16 (2019).
- Qian C, Decker EA, Xiao H, McClements DJ. Physical and chemical stability of β -carotene-enriched nanoemulsions: influence of pH, ionic strength, temperature, and emulsifier type. *Food Chem.* 132(3), 1221–1229 (2012).

17. Rao J, McClements DJ. Lemon oil solubilization in mixed surfactant solutions: rationalizing microemulsion & nanoemulsion formation. *Food Hydrocoll.* 26(1), 268–276 (2012).
18. Chaiyana W, Anuchapreeda S, Leelapornpisid P, Phongpradist R, Viernstein H, Mueller M. Development of microemulsion delivery system of essential oil from *Zingiber cassumunar* Roxb. rhizome for improvement of stability and anti-inflammatory activity. *AAPS PharmSciTech* 18(4), 1332–1342 (2017).
19. Nimisha S, Fatima Z, Kaur C. A review on potential of novel vesicular carriers for carrying herbal drugs in the treatment of dermatological disorders. *J. Atoms Mol.* 6(3), 987–1003 (2016).
20. Saraf S. Applications of novel drug delivery system for herbal formulations. *Fitoterapia* 81(7), 680–689 (2010).
21. Domínguez-Villegas V, Clares-Naveros B, García-López ML, Calpena-Campmany AC, Bustos-Salgado P, Garduño-Ramírez ML. Development and characterization of two nano-structured systems for topical application of flavanones isolated from *Eysenhardtia platycarpa*. *Colloids Surf. B Biointerfaces* 116, 183–192 (2014).
22. Li S, Xiong Q, Lai X *et al.* Molecular modification of polysaccharides and resulting bioactivities. *Compr. Rev. Food Sci. Food Saf.* 15, 237–250 (2016).
23. Alalaiwe A, Lin C, Hsiao C, Chen E, Lin C. Development of flavanone and its derivatives as topical agents against psoriasis: the prediction of therapeutic efficiency through skin permeation evaluation and cell-based assay. *Int. J. Pharm.* 581, 119256 (2020).
24. Andrade-Carrera B, Clares B, Noé V *et al.* Cytotoxic evaluation of (2S)-5,7-Dihydroxy-6-prenylflavanone derivatives loaded PLGA nanoparticles against MiaPaCa-2 Cells. *Molecules* 22(9), 1553 (2017).
25. Benmeradi N, Payre B, Goodman SL. Easier and safer biological staining: high contrast uranylless staining of TEM grids using mPrep/g capsules. *Microsc. Microanal.* 21(S3), 721–722 (2015).
26. Suñer J, Calpena AC, Clares B, Cañadas C, Halbaut L. Development of clotrimazole multiple W/O/W emulsions as vehicles for drug delivery: effects of additives on emulsion stability. *AAPS PharmSciTech* 18(2), 539–550 (2017).
27. Provenza Bernal N, Calpena AC, Mallandrich M, Ruiz A, Clares B. Development, physical-chemical stability, and release studies of four alcohol-free spirinolactone suspensions for use in pediatrics. *Dissolution Technol.* 21(1), 19–30 (2014).
28. Carvajal-Vidal P, González-Pizarro R, Araya C *et al.* Nanostructured lipid carriers loaded with halobetasol propionate for topical treatment of inflammation: development, characterization, biopharmaceutical behavior and therapeutic efficacy of gel dosage forms. *Int. J. Pharm.* 585, 119480 (2020).
29. Suñer-Carbó J, Boix-Montañés A, Halbaut-Bellowa L *et al.* Skin permeation of econazole nitrate formulated in an enhanced hydrophilic multiple emulsion. *Mycoses* 60(3), 166–177 (2017).
30. Kumar N, Mandal A. Surfactant stabilized oil-in-water nanoemulsion: stability, interfacial tension, and rheology study for enhanced oil recovery application. *Energy and Fuels* 32(6), 6452–6466 (2018).
31. Rachmawati H, Budiputra DK, Mauludin R. Curcumin nanoemulsion for transdermal application: formulation and evaluation. *Drug Dev. Ind. Pharm.* 41(4), 560–566 (2015).
32. Mallandrich M, Fernández-Campos F, Clares B *et al.* Developing transdermal applications of ketorolac tromethamine entrapped in stimuli sensitive block copolymer hydrogels. *Pharm. Res.* 34(8), 1728–1740 (2017).
33. Bustos-Salgado P, Andrade-Carrera B, Garduño-Ramírez ML, Alvarado H, Calpena-Campmany A. Quantification of one prenylated flavanone from *Eysenhardtia platycarpa* and four derivatives in *ex vivo* human skin permeation samples applying a validated HPLC method. *Biomolecules* 10, 889 (2020).
34. Cañadas-Enrich C, Abrego G, Alvarado HL, Calpena-Campmany AC. Pranoprofen quantification in *ex vivo* corneal and scleral permeation samples: analytical validation. *J. Pharm. Biomed. Anal.* 160, 109–118 (2018).
35. Espinoza LC, Silva-Abreu M, Calpena AC *et al.* Nanoemulsion strategy of pioglitazone for the treatment of skin inflammatory diseases. *Nanomedicine* 19, 115–125 (2019).
36. Close B, Banister K, Baumans V *et al.* Recommendations for euthanasia of experimental animals: part 2. *Lab. Anim.* 31(1), 1–32 (1997).
37. Mostafa DM, Ammar NM, Basha M *et al.* Transdermal microemulsions of *Boswellia carterii* bird: formulation, characterization and *in vivo* evaluation of anti-inflammatory activity. *Drug Deliv.* 22(6), 748–756 (2015).
38. Souza SD. A review of *in vitro* drug release test methods for nano-sized dosage forms. *Adv. Pharm.* 2014, 12 (2014).
39. Fernández Campos F, Calpena Campmany AC, Rodríguez Delgado G, López Serrano O, Clares Naveros B. Development and characterization of a novel nystatin-loaded nanoemulsion for the buccal treatment of candidosis: ultrastructural effects and release studies. *J. Pharm. Sci.* 101(10), 3739–3752 (2012).
40. Alvarado HL, Abrego G, Souto EB *et al.* Nanoemulsions for dermal controlled release of oleanolic and ursolic acids: *in vitro*, *ex vivo* and *in vivo* characterization. *Colloids Surfaces B Biointerfaces* 130, 40–47 (2015).
41. Parra A, Clares B, Rosselló A *et al.* *Ex vivo* permeation of carprofen from nanoparticles: a comprehensive study through human, porcine and bovine skin as anti-inflammatory agent. *Int. J. Pharm.* 501(1–2), 10–17 (2016).
42. Gareth T. *Medicinal Chemistry An Introduction (2nd Edition)*. John Wiley & Sons, Chichester, England, 621 (2007).

43. Noor El-Din MR, El-Hamouly SH, Mohamed HM, Mishrif MR, Ragab AM. Water-in-diesel fuel nanoemulsions: preparation, stability and physical properties. *Egypt. J. Pet.* 22(4), 517–530 (2013).
44. Gasperlin M, Tusar L, Tusar M, Smid-Korbar J, Zupan J, Kristl J. Viscosity prediction of lipophilic semisolid emulsion systems by neural network modelling. *Int. J. Pharm.* 196, 37–50 (2000).
45. McClements DJ. Edible nanoemulsions: fabrication, properties, and functional performance. *Soft Matter* 7, 2297–2316 (2011).
46. Heng D, Cutler DJ, Chan HK, Yun J, Raper JA. What is a suitable dissolution method for drug nanoparticles? *Pharm. Res.* 25(7), 1696–1701 (2008).
47. Gomes A, Fernandes E, Lima J, Mira L, Corvo M. Molecular mechanisms of anti-inflammatory activity mediated by flavonoids. *Curr. Med. Chem.* 15(16), 1586–1605 (2008).
48. Jiang C, Liang L, Guo Y. Natural products possessing protein tyrosine phosphatase 1B (PTP1B) inhibitory activity found in the last decades. *Acta Pharmacol. Sin.* 33, 1217–1245 (2012).
49. Tanner T, Marks R. Delivering drugs by the transdermal route: review and comment. *Skin Res. Technol.* 14(3), 249–260 (2008).



“*Ex vivo* and *In vivo* Antiinflammatory Evaluations of Modulated Flavanones Solutions”

Paola Bustos-Salgado 1, María J. Rodríguez-Lagunas 2, Valeri Domínguez-Villegas 3, Berenice Andrade-Carrera 3, Ana Calpena-Campmany 1,* and María Luisa Garduño-Ramírez 4,*

1 Department of Pharmacy and Pharmaceutical Technology and Physical Chemistry, Faculty of Pharmacy and Food Science, University of Barcelona, Av. Joan XXIII 29-31, 08028 Barcelona, Spain; pbustosa19@alumnes.ub.edu

2 Department of Biochemistry and Physiology, Faculty of Pharmacy and Food Sciences, University of Barcelona, 08028 Barcelona, Spain; mjrodriguez@ub.edu

3 Facultad de Ciencias Químicas e Ingeniería, Universidad Autónoma del Estado de Morelos, Av. Universidad 1001, Cuernavaca, Morelos 62209, Mexico; valeri.dominguez@uaem.mx (V.D.-V.); bereniceac@uaem.mx (B.A.-C.)

4 Centro de Investigaciones Químicas, Instituto de Investigación en Ciencias Básicas y Aplicadas, Universidad Autónoma del Estado de Morelos, Av. Universidad 1001, Cuernavaca, Morelos 62209, Mexico

* Correspondence: anacalpena@ub.edu (A.C.-C.); lgarduno@uaem.mx (M.L.G.-R.);

Tel.: +34-93-402-4578 (A.C.-C.); +52-777-329-7997 (M.L.G.-R.)

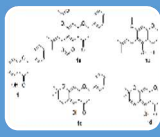
† Presented at the 1st International Electronic Conference on Pharmaceutics, 1–15 December 2020;

Available online: <https://iecp2020.sciforum.net/>. *Revista: Pharmaceutics* (MDPI) ISSN 1999-4923


Año de publicación: 2021

Resumen

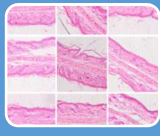
En el presente trabajo se investigó el efecto antiinflamatorio de las disoluciones hidroalcohólicas (FS) de las flavanonas **1** y **1a-1d**. El efecto antiinflamatorio dérmico de las flavanonas fue evaluado en modelos de edema de ratón inducido por TPA (13-acetato de 12-*O*-tetradecanoilforbol) y en modelos de edema de rata inducidos por ácido araquidónico (AA). Las FS causaron la inhibición del edema en ambos modelos evaluados. Los resultados de los ensayos *in vivo* e histológicos sugirieron que las flavanonas evaluadas son efectivas para ser usadas en el tratamiento de patología en la piel que cursan con inflamación favoreciendo el efecto de las flavanonas **1b** y **1d**.



Soluciones hidroalcohólicas de las flavanonas natural y derivadas.



Efecto anti-inflamatorio cutáneo
Modelos de edema de oreja de ratón inducido por TPA y edema de oreja de rata inducido por AA.



Ensayos histológicos

Ex Vivo and In Vivo Anti-inflammatory Evaluations of Modulated Flavanones Solutions [†]

Paola Bustos-Salgado ¹, María J. Rodríguez-Lagunas ², Valeri Domínguez-Villegas ³,
Berenice Andrade-Carrera ³, Ana Calpena-Campmany ^{1,*} and María Luisa Garduño-Ramírez ^{4,*}

¹ Department of Pharmacy and Pharmaceutical Technology and Physical Chemistry, Faculty of Pharmacy and Food Science, University of Barcelona, Av. Joan XXIII 29-31, 08028 Barcelona, Spain; pbustosa19@alumnes.ub.edu

² Department of Biochemistry and Physiology, Faculty of Pharmacy and Food Sciences, University of Barcelona, 08028 Barcelona, Spain; mjrodriguez@ub.edu

³ Facultad de Ciencias Químicas e Ingeniería, Universidad Autónoma del Estado de Morelos, Av. Universidad 1001, Cuernavaca, Morelos 62209, Mexico; valeri.dominguez@uaem.mx (V.D.-V.); bereniceac@uaem.mx (B.A.-C.)

⁴ Centro de Investigaciones Químicas, Instituto de Investigación en Ciencias Básicas y Aplicadas, Universidad Autónoma del Estado de Morelos, Av. Universidad 1001, Cuernavaca, Morelos 62209, Mexico

* Correspondence: anacalpena@ub.edu (A.C.-C.); lgarduno@uaem.mx (M.L.G.-R.); Tel.: +34-93-402-4578 (A.C.-C.); +52-777-329-7997 (M.L.G.-R.)

[†] Presented at the 1st International Electronic Conference on Pharmaceutics, 1–15 December 2020; Available online: <https://iecp2020.sciforum.net/>.

Abstract: Interest has developed in natural molecules due to their clinically proven effects on skin diseases. Flavanones display several biological activities, and recently have been the focus of studies due to their anti-inflammatory effect. To improve their pharmacological profile, four flavanones (**A**, **B**, **C**, and **D**) were synthesized by structural modification of one natural flavanone **1** (semi-systematic name: (2S)-5,7-dihydroxy-6-prenylflavanone) extracted from *Eysenhardtia platycarpa*. The hydroalcoholic flavanone solutions (FS) were assayed to investigate their anti-inflammatory effect on two in vivo cutaneous inflammation models. *Materials and methods:* the topical anti-inflammatory effects of FS were evaluated against models of 12-O-tetradecanoylphorbol acetate (TPA)-induced mouse ear edema and arachidonic acid (AA) in rat ear edema. *Results:* The vinylogous cyclized derivative (flavanone **D**) caused edema inhibition in the TPA-induced models with an inhibition of $96.27 \pm 1.93\%$; equally effective and potent in inhibiting the mouse ear edema as indomethacin had been. In addition, the AA-induced increase in ear thickness was reduced the most by the topical application of modulated ether (flavanone **B**). *Conclusions:* The in vivo and histology results suggest that flavanones **B** and **D** are effective as topical anti-inflammatory agents in inflammatory processes. Thus, this new compound represents a promising agent for the management of skin diseases with an inflammatory component.

Keywords: flavanones; *Eysenhardtia platycarpa*; anti-inflammatory activity

Citation: Bustos-Salgado, P.; Rodríguez-Lagunas, M.J.; Domínguez-Villegas, V.; Andrade-Carrera, B.; Calpena-Campmany, A.; Garduño-Ramírez, M.L. Ex Vivo and In Vivo Antiinflammatory Evaluations of Modulated Flavanones Solutions. *Proceedings* **2021**, *78*, 23. <https://doi.org/10.3390/IECP2020-08657>

Published: 1 December 2020

Publisher's Note: MDPI stays neutral with regard to jurisdictional claims in published maps and institutional affiliations.



Copyright: © 2020 by the authors. Licensee MDPI, Basel, Switzerland. This article is an open access article distributed under the terms and conditions of the Creative Commons Attribution (CC BY) license (<http://creativecommons.org/licenses/by/4.0/>).

1. Introduction

Skin inflammation is one of the most common skin problems. There are widespread dermatological diseases that include inflammatory responses in the skin and can present different ranges in severity. It is manifested by swelling, redness, heat, and pain in the affected tissue [1]. The most effective route of drug administration where higher concentration of the drug can be accomplished is the topical administration. Non-steroidal anti-inflammatory drugs (NSAIDs) are currently used to treat inflammation, but severe adverse effects make these drugs unsuitable for chronic therapies [2]. Natural products for human skin problems have been used since ancient times. Recently, they have gathered

considerable attention as new anti-inflammatory compounds because their long-established usage promises the development of safe and effective medicaments [3]. Flavanones have been the focus of much research and development due to their several biological activities, including anti-inflammatory effects [4]. They have been a potential source in the search for lead compounds and biologically active components [5]. In recent times, five flavanones were isolated from a methanolic extract of *Eysenhardtia platycarpa*, and they showed an anti-inflammatory effect during in vivo study [6–8]. Molecular modification represents one method used by medicinal chemistry for the rational variation of lead compounds with the aim of improving the efficacy and potency, and the reducing of undesirable side effects [9]. Based on the abovementioned interesting facts, the aim of this research was the in vivo anti-inflammatory evaluation of four flavanone derivatives in solution using one flavanone extracted from *E. platycarpa* as the starting material. The therapeutic efficacy of flavanones was checked by 12-*O*-tetradecanoylphorbol acetate (TPA) edema mouse and arachidonic acid (AA) edema rat models. In addition, the histopathology in rat ear was observed. We explored the relationship between chemical structure and the therapeutic efficiency of flavanones.

2. Experiments

2.1. Extraction and Isolation of Plant Material

E. platycarpa leaves were collected from the municipality of Tetipac, Guerrero State (Mexico), and they are kept in the Faculty Herbarium of Facultad de Ciencias de la Universidad Nacional Autónoma de México. The plant material was authenticated by Professor Ramiro Cruz (Register number 1325). Experimental procedures detailed for the extraction, isolation, purification, and structure elucidation of flavanone **1** (Figure 1), isolated from the methanolic extract of leaves of *E. platycarpa*, have been described previously [8]. Briefly, the dried leaves of *E. platycarpa* (100 g) were extracted with MeOH (1000 mL). Then, the extracts were merged and concentrated in vacuo, to obtain the crude extracts. Next, the flavanone **1** was isolated by silica gel column chromatography. Finally, it was purified by direct thin-layer chromatography (TLC). The yellow powder precipitate obtained was characterized by comparison with previously published melting point data and with ¹H-NMR results [10].

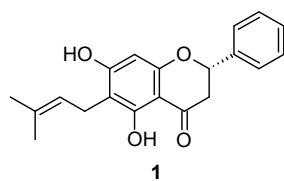


Figure 1. Natural flavanone **1** (2*S*)-5,7-dihydroxy-6-(3-methyl-2-buten-1-yl)-2-phenyl-2,3-dihydro-4*H*-1-Benzopyran-4-one) extracted from *Eysenhardtia platycarpa*.

2.2. Semi-synthesis from Natural Prenylated Flavanone

The flavanones **A–D** were obtained following the method previously reported [10] to yield the derivatives flavanones (2*S*)-5,7-bis(acetyloxy)-6-(3-methyl-2-buten-1-yl)-2-phenyl-2,3-dihydro-4*H*-1-Benzopyran-4-one **A**; (2*S*)-5-hydroxy-7-methoxy-6-(3-methyl-2-buten-1-yl)-2-phenyl-2,3-dihydro-4*H*-1-Benzopyran-4-one **B**; (8*S*)-5-hydroxy-2,2-dimethyl-8-phenyl-3,4,7,8-tetrahydro-2*H*,6*H*-Benzo[1,2-*b*:5,4-*b'*]dipyran-6-one **C**; and (8*S*)-5-hydroxy-2,2-dimethyl-8-phenyl-7,8-dihydro-2*H*,6*H*-Benzo[1,2-*b*:5,4-*b'*]dipyran-6-one **D** (Figure 2).

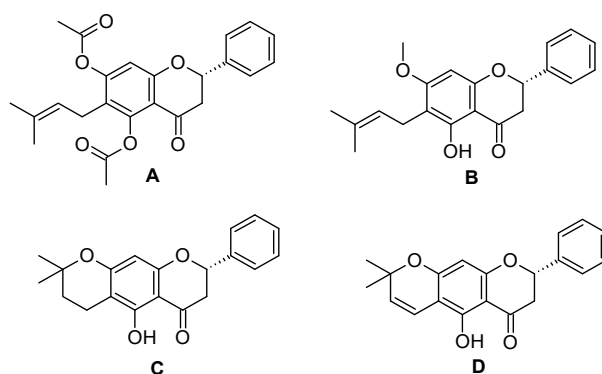


Figure 2. Derivative flavanones (2*S*)-5,7-bis(acetyloxy)-6-(3-methyl-2-buten-1-yl)-2-phenyl-2,3-dihydro-4*H*-1-Benzopyran-4-one (**A**); (2*S*)-5-hydroxy-7-methoxy-6-(3-methyl-2-buten-1-yl)-2-phenyl-2,3-dihydro-4*H*-1-Benzopyran-4-one (**B**); (8*S*)-5-hydroxy-2,2-dimethyl-8-phenyl-3,4,7,8-tetrahydro-2*H*,6*H*-Benzo[1,2-*b*:5,4-*b'*] dipyrans-6-one (**C**); and (8*S*)-5-hydroxy-2,2-dimethyl-8-phenyl-7,8-dihydro-2*H*,6*H*-Benzo[1,2-*b*:5,4-*b'*] dipyrans-6-one (**D**).

2.3. Anti-inflammatory Testing

TPA-induced mouse ear edema was carried out using male Wistar CD-1 mice ($n = 3$ for each of the flavanones **A–D**, 20 to 25 g) based on the protocol previously described. Edema was induced by the topical application of 2.5 μg per ear of TPA (12-*O*-tetradecanoylphorbol-13-acetate) dissolved in 20 μL ethanol (10 μL each ear side). The standard drug indomethacin was used as reference. It was dissolved in acetone and applied to both sides of the right ear (1 mg/ear) simultaneously with TPA. In the same way, 1 mg of each flavanone (**A–D**) was dissolved in acetone and applied on both sides of the right ear with TPA. Similarly, acetone was applied to both sides of the left ear. Four hours after the flavanone solutions were applied in one go, the animals were sacrificed by dislocating their neck. Subsequently, the left and right ears were perforated by punching bear (7 mm diameter), and the resulting tissues were accurately weighed. The edema weight and inhibition percentage were assessed according to the following equation:

$$\text{Inhibition (\%)} = \frac{\text{difference in weight of ear, control} - \text{difference in weight of ear, treated}}{\text{difference in weight of ear, control}} \times 100 \quad (1)$$

The studies were conducted under a protocol in accordance with Mexican Official Norm for Animal Care and Handling (NOM-062-ZOO-1999) and with the approval of the Academic Committee of Ethics of the Vivarium of the Autonomous University of the Morelos State of Mexico, with number 0122013.

2.4. Histological Analysis

The anti-inflammatory histological effect of the flavanones (**A–D**) was assessed using arachidonic acid (AA) in rat ear edema model [11]. Adult male Sprague Dawley[®] rats were used ($n = 5$ for each flavanone solution, 200–240 g). Firstly, 5 mg of AA was dissolved in 1 mL of phosphate-buffered saline solution. Then, 60 μL of AA solution was applied on both sides of the ears to induce the inflammatory process and left for 20 min of exposure. The animals in the positive control were treated only with AA solution. A solution of diclofenac sodium (5 mg/mL) in EtOH/H₂O (7:3) was used as reference drug (ref). One animal group was treated only with the mixture EtOH/H₂O (7:3), without any flavanone (nFS). The animals, except the negative and positive control, were treated with 50 μL of the respective flavanone solution (FS 1, FS **A**, FS **B**, FS **C**, and FS **D**) 20 min after AA exposition and the treatment was effected for 20 min. To finish, the animals were sacrificed using carbon dioxide, following the recommendations for euthanasia of experimental animals from the European Commission [12]. Then, the ears were cut off and the tissues were rinsed with PBS, pH 7.4, and left to stand overnight in 4% buffered formaldehyde and embedded in paraffin wax at the end. Transversal sections (5 μm) were stained with

hematoxylin and eosin. The ear inflammation was observed under a light microscope (Olympus BX41 and camera Olympus XC50) on blind coded samples. Ears from the non-treated animals were used as the control condition.

Additional to histology study, the stratum corneum hydration (SCH, arbitrary units AU) of rat ear was measured before and after the AA application and treatments with a Corneometer CM825 (Courage & Khazaka electronics GmbH, Köln, Germany). Similarly, ear thicknesses were verified before and after the AA and the different treatments with a digital micrometer (Wisamic Digital Thickness Gauge 0–12.7 mm). The edema reduction was calculated by the following equation [13]:

$$\Delta Edema\ reduction = thickness\ after\ treatment - thickness\ before\ treatment \tag{2}$$

3. Results

3.1. Model of Mice Ear Inflammation Induced with TPA

The anti-inflammatory study results of the flavanones are depicted in Table 1 as mean values ± the standard deviation (SD). The flavanone solutions showed good results of the anti-inflammatory efficacy studies. The flavanone natural **1** revealed a significant reduction of the dermal edema with inhibition percentage of 66.67 ± 1.55. However, only the flavanone modulated **D** showed an inhibition percentage of 96.27 ± 1.93 compared to the indomethacin of 91.35 ± 0.47.

Table 1. In vivo anti-inflammatory efficacy after TPA (12-O-tetradecanoylphorbol 13-acetate)-induced mouse edema. Mean ± SD (n = 3).

Solutions	FS 1	FS A	FS B	FS C	FS D	Indomethacin
% Inhibition	66.67 ± 1.55	10.27 ± 0.21	25.69 ± 0.52	40.61 ± 0.81	96.27 ± 1.93	91.35 ± 0.47
Human Skin Retention* (µg/g.cm ²)	50.22 ± 7.51	321.52 ± 45.23	381.75 ± 57.26	23.78 ± 5.46	116.14 ± 17.24	

* Results of the permeation studies expressed by mean and SD (n = 3) reported previously [14].

In previous studies [14], the solutions of the flavanone natural **1** and the derivative flavanones **A–D** were evaluated in ex vivo diffusional studies in Franz cells using human skin. This was to evaluate their intrinsic permeation and human skin retention (Table 1). The skin retention results of that study were correlated with the inhibition percentage of mouse edema induced by TPA. The function that best fitted to FS **1**, FS **C**, and FS **D** was the first order with a correlation coefficient (R²) equal to 1 (Figure 3).

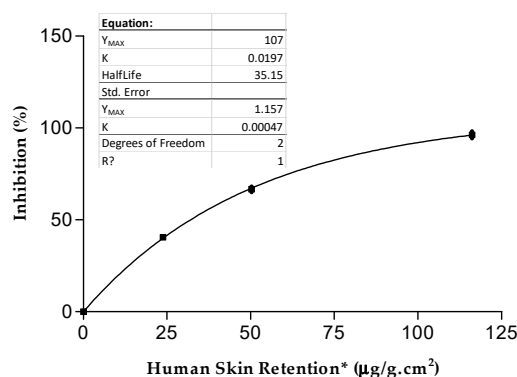


Figure 3. Correlated function inhibition vs. human skin retention.

3.2. In Vivo Rat Model and Anti-inflammatory Response after Flavanone Solutions Treatment

The edema reduction, associated with the flavanones solutions **A–D** treatment in an in vivo ear rat model of inflammation induced by arachidonic acid, was evaluated by the difference of thickness compared to initial ear measures. In the same way, the nFS and a

solution of diclofenac sodic were evaluated. The results are depicted in Figure 4. The reference solution of diclofenac sodic reduced the ear thickness compared with the FS D. This treatment was also used for the flavanone solution 1 and nFS, producing the same effect in the edema ear. Thereupon, the flavanone 1 had not contributed with any additional anti-inflammatory effect compared with the excipients. Similarly, the FS A with the FS C presented almost the same edema reduction. On the other hand, it was interesting to note that the FS B had a higher efficacy, since it reduced the thickness of the rat ears after 20 min of its application. It is important to point out that the ethanol, per se, can produce an effect of constriction and dehydration that could translate into an anti-inflammatory action.

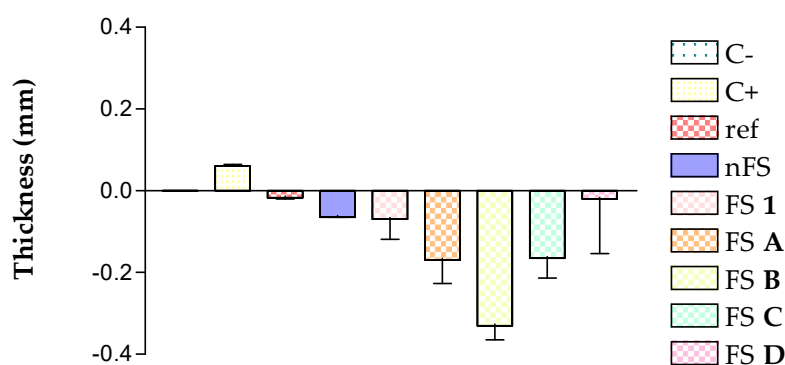


Figure 4. In vivo rat model anti-inflammatory response after FS (A–D) treatment in AA-induced edema model as the increment or decrement of thickness with respect to initial conditions. Results are expressed as mean ± SD ($n = 5$). C- = negative control, C+ = positive control, ref = reference drug, nFS = ethanol:water, FS = flavanone solution (A–D).

The skin hydration data may also reveal the importance of the treatment with FS. With regards to this, the skin hydration of rat ears was measured, and the results are shown in Figure 5 as the difference in stratum corneum hydration (SCH) after the formulation treatment on swelled ears and the basal SCH conditions as arbitrary units (AU). When the ears’ hydration was measured, it was found that the skin’s hydration changed with the application of all flavanone solutions. All of them reduced the skin’s hydration except in the case of FS B, which increased the hydration initial value.

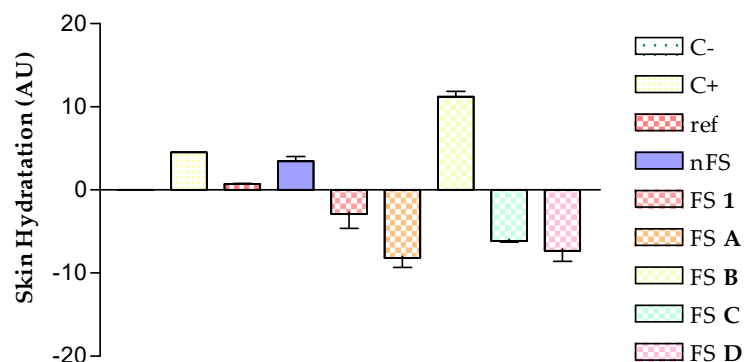


Figure 5. In vivo skin hydration after application of FS (A–D) in AA-induced rat ear edema as the difference in hydration compared to initial conditions. Results are expressed as mean ± SD ($n = 5$). C- = negative control, C+ = positive control, ref = reference drug, nFS = ethanol:water, FS = flavanone solution (A–D).

3.3. Histological Analysis

Histological analysis of ear sections was carried out for the assessment of the anti-inflammatory effect of the FS. Ears treated with AA (Figure 6) showed a mild inflammation characterized by edema, increased epidermal thickness, and infiltration of polymorphonuclear (PMN) leukocytes.

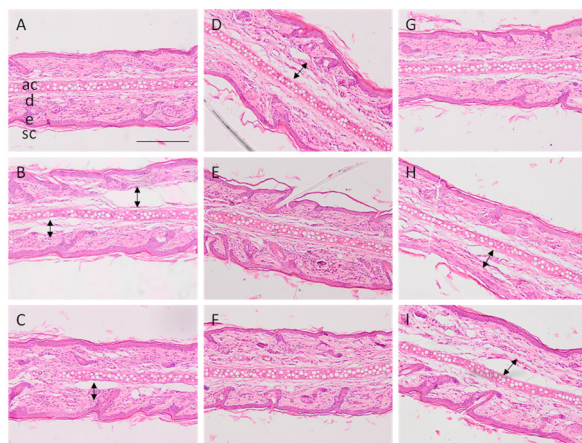


Figure 6. Representative micrographs of rat's ear ($\times 100$ magnification). (A): control-, (B): control+, (C): (nFS), (D): (ref), (E): (FS 1), (F): (FS A), (G): (FS B), (H): (FS C), (I): (FS D). e: epidermis, d: dermis, ac: auricular cartilage, sc: stratum corneum. Arrows indicate presence of edema. Scale bar = 200 μm .

4. Discussion

The results obtained in *in vivo* studies using different irritant agents (TPA and AA), in Table 1 and Figure 4, showed that the natural flavanone extracted **1** and the derivatives flavanones (A–D) have topical anti-inflammatory activity. All five FS were able to reduce the epidermal thickness present in the AA-treated ears. Furthermore, it is important to point out that the ethanol, per se, can produce constriction and dehydration effects that could translate into an anti-inflammatory action. Histological analysis of the ear of FS-treated animals confirmed the reduction of edema and stratum corneum swelling. Topical administration of reference drug slightly decreased these inflammatory indicators. The effect of the solutions diluent (EtOH:H₂O) was also assayed in order to observe its effect on inflammation, and this showed some reduction of the edema. FS B (Figure 6G) was the best solution in reducing the inflammation induced by AA, showing better results than the reference. Another matter is that FS 1 and FS A also showed less edema, although FS 1 showed greater presence of PMN. Furthermore, FS C and FS D were also able to reduce the edema, but to a lower degree than the previous solutions. The aforementioned show us that the chemical modification of flavanone **1** played an important role in exercising an anti-inflammatory activity. Some SARs studies of flavonoids revealed that a planar ring system is vital in the flavonoid molecules so that they exhibit the anti-inflammatory action and that hydroxyl groups at 5- and 7-position of A-ring seem to be favorable to structural features to the inhibition of AA-induced mouse ear edema [15–17]. These facts could be the reasons why the molecule structures of flavanones B that possess hydroxyl group at 5-position, and flavanone D with a more rigid structure, favored the anti-inflammatory effect in the models evaluated in this research. The natural flavanone **1** and derivative flavanones C and D showed a correlation of accumulation into the human skin with their local anti-inflammation effect evaluated in the TPA-induced model. This correlation could be owed to the fact that these three flavanones have similar physicochemical properties, such as area and molecular mass, as well as bond energy.

The working mechanisms of flavonoids as anti-inflammation agents are still not clearly defined. These kinds of compounds may act on several molecular targets simulta-

neously. Different mechanisms may also be involved in the activity of each flavanone assayed. The anti-inflammatory effect of some plants used in skin illnesses could be explained by their obstruction effect in the synthesis of inflammatory mediators such as leukotrienes and prostaglandins [18]. Although AA- and TPA-induced models are used to evaluate the anti-inflammatory effect, there are differences in the inflammation process that could help us to understand the inhibitory effects of the FS assayed on these models. It is known that AA produces only a modest increase in epidermal DNA synthesis, while TPA dramatically increases epidermal DNA synthesis and cell proliferation, producing a long-lasting hyperplasia [19]. The edema caused by TPA can be reduced by cyclooxygenase (COX) and 5-lipoxygenase (5-LOX) enzyme inhibition, and the blockage of LTB₄ receptors. In addition, the protein kinase C (PKC) and groups of enzymes such as the mitogen activated protein kinases (MAPKs) and phospholipase A2 could be involved. It is reported that dexamethasone is a phospholipase A2 (PLA2) inhibitor more active against TPA-induced than AA-induced ear edema [20]. According to our obtained results, FS **D** anti-inflammatory activity was greater against TPA-induced than AA-induced edema. Based on all these results, it can be suggested that FS **D** has a similar activity profile to PLA2 inhibitors. On the other hand, the ear edema caused by topical application of AA has been widely used to evaluate COX and 5-LOX inhibitors [21]. Considering that BW755C is a dual COX/LOX inhibitor and zileuton is a 5-LOX inhibitor, they showed a higher anti-inflammatory activity against AA-induced than TPA-induced edema in previous studies [20]. We hypothesize a dual COX/LOX inhibitory activity for FS **B**. However, this would need to be confirmed by additional studies.

5. Conclusions

Based on obtained results, it can be concluded that the derivatization of natural flavanone **1** to yield flavanones **A**, **B**, **C**, and **D** allowed us to comprehend the importance of molecular structure to derive an anti-inflammatory action on skin. The FS **B** and FS **D** showed better anti-inflammatory efficacy values. For these reasons, data obtained reflected that FS **B** and FS **D** could, and should, attract considerable attention for skin inflammatory treatment. Future studies can add to current findings, leading to better understanding of these flavanones with the potential to develop dermatological treatments and skin care products using these compounds. Moreover, the probable mechanism of action through which flavanones exert their effects could involve several targets, resulting in the reduction of important inflammatory mediators in the cutaneous tissue. Investigations into the mechanism of action of the anti-inflammatory activity and into the compounds responsible for the activity of flavanones must be completed.

Author Contributions: M.L.G.-R. and A.C.-C. conceived and designed the experiments; P.B.-S., V.D.-V., B.A.-C., and M.J.R.-L. performed the experiments; P.B.-S., A.C.-C., and M.J.R.-L. analyzed the data; M.L.G.-R. contributed reagents/materials/analysis tools; P.B.-S. wrote the paper. All authors have read and agreed to the published version of the manuscript.

Institutional Review Board Statement: The studies were conducted under a protocol in accordance with Mexican Official Norm for Animal Care and Handling (NOM-062-ZOO-1999) and with the approval of the Academic Committee of Ethics of the Vivarium of the Autonomous University of the Morelos State of Mexico, with number 0122013. Furthermore, the studies were conducted according to the guidelines stated in the protocol "Principles of Laboratory Animal Care" (publication 214/97 of 30 July).

Informed Consent Statement: Not applicable.

Data Availability Statement: Not applicable.

Acknowledgments: This work was supported by a grant from CONACyT-México (grant number 709906). The authors would like to thank Lidia Gómez-Segura of the Bellvitge Hospital for her assistance in the management of the animals used in the experiments. Moreover, we express our acknowledgement to Harry Paul for his review of the use of the English language.

Conflicts of Interest: The authors declare no conflicts of interest. The founding sponsors had no role in the design of the study; in the collection, analyses, or interpretation of data; in the writing of the manuscript, and in the decision to publish the results.

Abbreviations

The following abbreviations are used in this manuscript:

AA	Arachidonic acid
TPA	12- <i>O</i> -tetradecanoylphorbol-13-acetate
FS	Flavanone solution
nFS	Solution without any flavanone
TLC	Thin-layer chromatography
NSAID	Non-steroidal anti-inflammatory drugs
MeOH	Methanol
¹ H-NMR	Proton nuclear magnetic resonance
ref	Reference drug
EtOH	Ethanol
H ₂ O	Water
PBS	Phosphate buffered saline
SCH	Stratum corneum hydration
AU	Arbitrary units
PMN	Polymorphonuclear
COX	Cyclooxygenase
LOX	Lipoxygenase
SAR	Structure activity relationship
DNA	Deoxyribonucleic Acid
PCK	protein kinase C
MAPKs	mitogen activated protein kinases
PLA2	phospholipase A2

References

1. Abdel-Mottaleb, M.M.; Try, C.; Pellequer, Y.; Lamprecht, A. Nanomedicine strategies for targeting skin inflammation. *Nanomedicine* **2014**, *9*, 1727–1743, doi:10.2217/nnm.14.74.
2. Paoletti, T.; Fallarini, S.; Gugliesi, F.; Minassi, A.; Appendino, G.; Lombardi, G. Anti-inflammatory and vascularprotective properties of 8-prenylapigenin. *Eur. J. Pharmacol.* **2009**, *620*, 120–130, doi:10.1016/j.ejphar.2009.08.015.
3. Singh, M.R.; Nag, M.K.; Patel, S.; Daharwal, S.J. Novel Approaches for Dermal and Transdermal Delivery of Herbal Drugs. *Res. J. Pharmacogn. Phytochem.* **2013**, *5*, 271–279.
4. Alalaiwe, A.; Lin, C.-F.; Hsiao, C.-Y.; Chen, E.-L.; Lin, C.-Y.; Lien, W.-C.; Fang, J.-Y. Development of flavanone and its derivatives as topical agents against psoriasis: The prediction of therapeutic efficiency through skin permeation evaluation and cell-based assay. *Int. J. Pharm.* **2020**, *581*, 119256, doi:10.1016/j.ijpharm.2020.119256.
5. Shi, L.; Feng, X.E.; Cui, J.R.; Fang, L.; Du, G.H.; Li, Q.S. Synthesis and biological activity of flavanone derivatives. *Bioorganic Med. Chem. Lett.* **2010**, *20*, 5466–5468, doi:10.1016/j.bmcl.2010.07.090.
6. Narváez-Mastache, J.M.; Soto, C.; Delgado, G. Antioxidant Evaluation of Eysenhardtia Species (Fabaceae): Relay Synthesis of 3-*O*-Acetyl-11 α ,12 α -epoxy-oleanan-28,13 β -olide Isolated from *E. platycarpa* and Its Protective Effect in Experimental Diabetes. *Biol. Pharm. Bull.* **2007**, *30*, 1503–1510, doi:10.1248/bpb.30.1503.
7. Gutierrez, R.M.P.; Baez, E.G. Evaluation of antidiabetic, antioxidant and antiglycating activities of the *Eysenhardtia polystachya*. *Pharmacogn. Mag.* **2014**, *10*, 404–18, doi:10.4103/0973-1296.133295.
8. Domínguez-Villegas, V.; Domínguez-Villegas, V.; García, M.L.; Calpena, A.; Clares-Naveros, B.; Garduño-Ramírez, M.L. Anti-Inflammatory, Antioxidant and Cytotoxicity Activities of Methanolic Extract and Prenylated Flavanones Isolated from Leaves of *Eysenhardtia platycarpa*. *Nat. Prod. Commun.* **2013**, *8*, 177–180, doi:10.1177/1934578 × 1300800211.
9. Li, S.; Xiong, Q.; Lai, X.; Li, X.; Wan, M.; Zhang, J.; Yan, Y.; Cao, M.; Lu, L.; Guan, J.; et al. Molecular Modification of Polysaccharides and Resulting Bioactivities. *Compr. Rev. Food Sci. Food Saf.* **2015**, *15*, 237–250, doi:10.1111/1541-4337.12161.
10. Andrade-Carrera, B.; Clares, B.; Noé, V.; Mallandrich, M.; Calpena, A.; García, M.L.; Garduño-Ramírez, M. Cytotoxic Evaluation of (2S)-5,7-Dihydroxy-6-prenylflavanone Derivatives Loaded PLGA Nanoparticles against MiaPaCa-2 Cells. *Molecules* **2017**, *22*, 1553, doi:10.3390/molecules22091553.
11. Espinoza, L.C.; Silva-Abreu, M.; Calpena, A.C.; Rodríguez-Lagunas, M.J.; Fábrega, M.-J.; Garduño-Ramírez, M.L.; Clares, B. Nanoemulsion strategy of pioglitazone for the treatment of skin inflammatory diseases. *Nanomed. Nanotechnol. Biol. Med.* **2019**, *19*, 115–125, doi:10.1016/j.nano.2019.03.017.

12. Close, B.; Banister, K.; Baumans, V.; Bernoth, E.-M.; Bromage, N.; Bunyan, J.; Erhardt, W.; Flecknell, P.; Gregory, N.; Hackbarth, H.; et al. Recommendations for euthanasia of experimental animals: Part 2. *Lab. Anim.* **1997**, *31*, 1–32, doi:10.1258/002367797780600297.
13. Domínguez-Villegas, V.; Clares, B.; García-López, M.; Calpena-Campmany, A.C.; Bustos-Zagal, P.; Garduño-Ramirez, M. Development and characterization of two nano-structured systems for topical application of flavanones isolated from *Eysenhardtia platycarpa*. *Colloids Surf. B Biointerfaces* **2014**, *116*, 183–192, doi:10.1016/j.colsurfb.2013.12.009.
14. Bustos-Salgado, P.; Andrade-Carrera, B.; Garduño-Ramírez, M.L.; Alvarado, H.L.; Calpena, A. Quantification of one Prenylated Flavanone from *Eysenhardtia platycarpa* and four derivatives in Ex Vivo Human Skin Permeation Samples Applying a Validated HPLC Method. *Biomolecules* **2020**, *10*, 889, doi:10.3390/biom10060889.
15. Gomes, A.; Fernandes, E.; Lima, J.L.F.C.; Mira, L.; Corvo, M.L. Molecular Mechanisms of Anti-Inflammatory Activity Mediated by Flavonoids. *Curr. Med. Chem.* **2008**, *15*, 1586–1605, doi:10.2174/092986708784911579.
16. Gautam, R.; Jachak, S.M. Recent developments in anti-inflammatory natural products. *Med. Res. Rev.* **2009**, *29*, 767–820, doi:10.1002/med.20156.
17. Jiang, C.-S.; Liang, L.-F.; Guo, Y.-W. Natural products possessing protein tyrosine phosphatase 1B (PTP1B) inhibitory activity found in the last decades. *Acta Pharmacol. Sin.* **2012**, *33*, 1217–1245, doi:10.1038/aps.2012.90.
18. Rauh, L.K.; Horinouchi, C.D.; Loddi, A.M.; Pietrovski, E.F.; Neris, R.; Souza-Fonseca-Guimaraes, F.; Buchi, D.F.; Biavatti, M.W.; Otuki, M.F.; Cabrini, D.A. Effectiveness of *Vernonia scorpioides* Ethanolic extract against skin inflammatory processes. *J. Ethnopharmacol.* **2011**, *138*, 390–397, doi:10.1016/j.jep.2011.09.012.
19. Young, J.M.; Spires, D.A.; Bedord, C.J.; Wagner, B.; Ballaron, S.J.; De Young, L.M. The Mouse Ear Inflammatory Response to Topical Arachidonic Acid. *J. Investig. Dermatol.* **1984**, *82*, 367–371, doi:10.1111/1523-1747.ep12260709.
20. Escribano-Ferrer, E.; Regué, J.Q.; Garcia-Sala, X.; Montañés, A.B.; Lamuela-Raventos, R.M. In Vivo Anti-inflammatory and Anti-allergic Activity of Pure Naringenin, Naringenin Chalcone, and Quercetin in Mice. *J. Nat. Prod.* **2019**, *82*, 177–182, doi:10.1021/acs.jnatprod.8b00366.
21. Sanaki, T.; Kasai-Yamamoto, E.; Yoshioka, T.; Sakai, S.; Yuyama, K.; Fujiwara, T.; Numata, Y.; Igarashi, Y. Direct Involvement of Arachidonic Acid in the Development of Ear Edema via TRPV3. *J. Oleo Sci.* **2017**, *66*, 591–599, doi:10.5650/jos.ess16227.